

Chapter 6

Finite element method: d -dimensions

6.1. Introduction

In this chapter we generalize the formulation, construction, implementation, and error analysis of the finite element method introduced in Chapter 4 for one-dimensional problems to PDEs over domains in $\Omega \subset \mathbb{R}^d$ ($d \geq 1$) using the variational formalism introduced in Chapter 5. For simplicity, we restrict attention to linear, second-order, scalar-valued PDEs. The extension to nonlinear, systems of PDEs will be addressed in Chapters 7–8; we will not have time to consider higher order PDEs. As we will see, most of the details of the construction are unchanged in the more complex setting (nonlinear, systems of PDEs), which makes this a reasonable and highly relevant starting point.

6.2. H^1 -conforming finite elements

In this section we provide a formal definition of a finite element and construct the most widely used finite elements: H^1 conforming (nodal) elements.

Definition 6.2.1 (Finite element). Let

- (i) $K \subset \mathbb{R}^d$ be a compact set with non-empty interior and piecewise smooth boundary (element domain),
- (ii) \mathcal{Y} be a finite-dimensional function space on K ($M := \dim \mathcal{Y}$) (space of shape functions), and
- (iii) $\mathcal{D} := \{D_1, \dots, D_M\}$ is a basis for \mathcal{Y}' (dual space of \mathcal{Y}) (degrees of freedom).

Then $(K, \mathcal{Y}, \mathcal{D})$ is called a *finite element*.

In this course we will only consider *nodal* elements. Let $\mathcal{N} \subset K$ be a set of $N_{\text{nd}}^{\text{el}}$ ordered *nodes* denoted $\hat{\xi}_1, \dots, \hat{\xi}_{N_{\text{nd}}^{\text{el}}}$ with the j th coordinate ($j = 1, \dots, d$) of node i ($i = 1, \dots, N_{\text{nd}}^{\text{el}}$) denoted $\hat{\xi}_{ji}$. For now, we only allow for a single degree of freedom per node ($M = N_{\text{nd}}^{\text{el}}$) because we are considering scalar-valued variational problems, i.e., u in (6.151) is a scalar-valued function; this will be generalized in Chapter 8 when considering vector-valued variational problems. In this setting, let $(K, \mathcal{Y}, \mathcal{D})$ be a nodal finite element with associated node set \mathcal{N}_h^K , then the degrees of freedom of any $v \in \mathcal{Y}$ are

$$D_i(v) := v(\hat{\xi}_i). \quad (6.1)$$

In the remainder, we use the notation $\hat{v}_i := v(\hat{\xi}_i)$. Furthermore, let $\{\psi_1, \dots, \psi_{N_{\text{nd}}^{\text{el}}}\}$ be a basis of \mathcal{Y} that possesses the *nodal* property, i.e.,

$$\psi_i(\hat{\xi}_j) = \delta_{ij}. \quad (6.2)$$

Recall this property guarantees the basis functions are linearly independent. In this setting, any $v \in \mathcal{Y}$ can be expressed in terms of the degrees of freedom and basis functions as

$$v = \sum_{i=1}^M D_i(v) \psi_i = \sum_{i=1}^M \hat{v}_i \psi_i, \quad (6.3)$$

i.e., the coefficients that expand v in the basis $\{\psi_1, \dots, \psi_{N_{\text{nd}}^{\text{el}}}\}$ are equal to the *value* of the function at the nodes.

Example 6.1: Linear finite element in one dimension

The linear, one-dimensional finite element used in Chapter 4 is a finite element $(K, \mathcal{Y}, \mathcal{D})$. The element domain is simply a closed interval $K := [a, b]$ for $a, b \in \mathbb{R}$ and the local function space is $\mathcal{Y} := \mathcal{P}^1(K)$. The nodes of the element are located at the endpoints of K , i.e., $\mathcal{N} := \{\hat{\xi}_1, \hat{\xi}_2\}$ where $\hat{\xi}_1 = a$ and $\hat{\xi}_2 = b$, and $\mathcal{D} = \{D_1, D_2\}$ are the nodal degrees of freedom associated with these nodes, i.e., $D_i(v) := \hat{v}_i := v(\hat{\xi}_i)$ for $i = 1, 2$ and any $v \in \mathcal{Y}$. The finite element $(K, \mathcal{Y}, \mathcal{D})$ is summarized as

$$K := [a, b], \quad \mathcal{Y} := \mathcal{P}^1(K), \quad \mathcal{N} := \{a, b\}, \quad \mathcal{D} := \{v(a), v(b)\}. \quad (6.4)$$

The (unique) nodal basis $\{\psi_1, \psi_2\}$ of \mathcal{Y} associated with the node set \mathcal{N} is

$$\psi_1(\xi) := \frac{b - \xi}{b - a}, \quad \psi_2(\xi) := \frac{\xi - a}{b - a}. \quad (6.5)$$

An illustration of this finite element and its nodal basis functions in the special case where $a = -1$, $b = 1$ is provided in Figure 6.2.

Example 6.2: Bilinear quadrilateral finite element in two dimensions

As another example we construct the bilinear, one-dimensional finite element used in Homework 2. The element domain is simply a closed quadrilateral $K := [a_1, b_1] \times [a_2, b_2]$ for $a_1, a_2, b_1, b_2 \in \mathbb{R}$ and the local function space is $\mathcal{Y} := \mathcal{Q}^1(K)$. The nodes of the element are located at the corners of K , i.e., $\mathcal{N}_h = \{\hat{\xi}_1, \dots, \hat{\xi}_4\}$, where

$$\hat{\xi}_1 = \begin{bmatrix} a_1 \\ a_2 \end{bmatrix}, \quad \hat{\xi}_2 = \begin{bmatrix} b_1 \\ a_2 \end{bmatrix}, \quad \hat{\xi}_3 = \begin{bmatrix} a_1 \\ b_2 \end{bmatrix}, \quad \hat{\xi}_4 = \begin{bmatrix} b_1 \\ b_2 \end{bmatrix} \quad (6.6)$$

and $\mathcal{D} = \{D_1, D_2, D_3, D_4\}$ are the nodal degrees of freedom associated with these nodes, i.e., $D_i(v) := \hat{v}_i := v(\hat{\xi}_i)$ for $i = 1, 2, 3, 4$ and any $v \in \mathcal{Y}$. The bilinear quadrilateral finite element $(K, \mathcal{Y}, \mathcal{D})$ is summarized as

$$\begin{aligned} K &:= [a_1, b_1] \times [a_2, b_2], \quad \mathcal{Y} := \mathcal{Q}^1(K), \quad \mathcal{N} := \left\{ \begin{bmatrix} a_1 \\ a_2 \end{bmatrix}, \begin{bmatrix} b_1 \\ a_2 \end{bmatrix}, \begin{bmatrix} a_1 \\ b_2 \end{bmatrix}, \begin{bmatrix} b_1 \\ b_2 \end{bmatrix} \right\}, \\ \mathcal{D} &:= \left\{ v \left(\begin{bmatrix} a_1 \\ a_2 \end{bmatrix} \right), v \left(\begin{bmatrix} b_1 \\ a_2 \end{bmatrix} \right), v \left(\begin{bmatrix} a_1 \\ b_2 \end{bmatrix} \right), v \left(\begin{bmatrix} b_1 \\ b_2 \end{bmatrix} \right) \right\}. \end{aligned} \quad (6.7)$$

The (unique) nodal basis $\{\psi_1, \psi_2, \psi_3, \psi_4\}$ of \mathcal{Y} associated with the node set \mathcal{N} is

$$\begin{aligned} \psi_1(r, s) &:= \frac{b_1 - r}{b_1 - a_1} \frac{b_2 - s}{b_2 - a_2}, & \psi_2(r, s) &:= \frac{r - a_1}{b_1 - a_1} \frac{b_2 - s}{b_2 - a_2}, \\ \psi_3(r, s) &:= \frac{b_1 - r}{b_1 - a_1} \frac{s - a_2}{b_2 - a_2}, & \psi_4(r, s) &:= \frac{r - a_1}{b_1 - a_1} \frac{s - a_2}{b_2 - a_2}. \end{aligned} \quad (6.8)$$

An illustration of this finite element and its nodal basis functions in the special case where $a_1 = a_2 = -1$, $b_1 = b_2 = 1$ are provided in Figure 6.3, 6.4.

In the remainder of this section we introduce various classes of H^1 -conforming finite elements that we will use in this class, namely, polynomial simplex and hypercube elements. For now, we will not worry about the configuration of the element in the domain. Rather we will define them on a idealized, *reference* domain, denoted $\Omega_{\square} \subset \mathbb{R}^d$. In the next section, we will introduce a mapping to push them to their appropriate configuration/orientation in the domain Ω . Since these ideal elements will be used to generate all of the physical elements in a mesh, we call them *master* elements. Since we have committed to nodal elements, we no longer need to discuss the degrees of freedom \mathcal{D} since they will be given uniquely from the nodes. Therefore, a *master finite element* is completely defined by $(\Omega_{\square}, \mathcal{Y}_{\square}, \mathcal{N}_{\square})$, where $\Omega_{\square} \subset \mathbb{R}^d$ is the master element

geometry, \mathcal{Y}_\square is the function space associated with the master element, and $\mathcal{N}_\square \subset \Omega_\square$ is the collection of N_{nd}^{el} nodes that define the element degrees of freedom. In the remainder of this section, we define a number of useful master finite elements in $d = 1, 2$ and higher dimensions. In particular, we define the element geometry Ω_\square , the distribution of nodes and their numbering \mathcal{N}_\square , and the associated (usually polynomial) function space \mathcal{Y}_\square .

6.2.1 Polynomial spaces

In Chapter 2 we introduced the polynomial space $\mathcal{P}^p(\Omega)$ for $\Omega \subset \mathbb{R}$. In higher dimensions $\Omega \subset \mathbb{R}^d$ ($d > 1$) there are many relevant polynomial spaces; however, we will consider the two most common ones $\mathcal{P}^k(\Omega)$ and $\mathcal{Q}^k(\Omega)$ defined as

$$\begin{aligned}\mathcal{P}^k(\Omega) &:= \left\{ p \in \mathcal{F}_{\Omega \rightarrow \mathbb{R}} \mid p(\boldsymbol{\xi}) = \sum_{\substack{\alpha \in \mathbb{N}_0^d \\ \|\alpha\|_1 \leq k}} a_\alpha \boldsymbol{\xi}^\alpha, \boldsymbol{\xi} \in \Omega, a_\alpha \in \mathbb{R} \right\} \\ \mathcal{Q}^k(\Omega) &:= \left\{ p \in \mathcal{F}_{\Omega \rightarrow \mathbb{R}} \mid p(\boldsymbol{\xi}) = \sum_{\substack{\alpha \in \mathbb{N}_0^d \\ \|\alpha\|_\infty \leq k}} a_\alpha \boldsymbol{\xi}^\alpha, \boldsymbol{\xi} \in \Omega, a_\alpha \in \mathbb{R} \right\}. \end{aligned} \quad (6.9)$$

It can be shown that these are linear spaces of dimension

$$\dim \mathcal{P}^k(\Omega) = \binom{k+d}{d}, \quad \dim \mathcal{Q}^k(\Omega) = (k+1)^d. \quad (6.10)$$

Example 6.3: Polynomial spaces in $d = 1$ dimension

In $d = 1$ dimension, both the $\mathcal{P}^k(\Omega)$ and $\mathcal{Q}^k(\Omega)$ polynomial spaces are identical and equal to

$$\mathcal{P}^k(\Omega) = \mathcal{Q}^k(\Omega) = \left\{ p \in \mathcal{F}_{\Omega \rightarrow \mathbb{R}} \mid p(\xi) = \sum_{n=0}^k a_n \xi^n, \xi \in \Omega, a_n \in \mathbb{R} \right\} \quad (6.11)$$

and have dimension $\dim \mathcal{P}^k(\Omega) = \dim \mathcal{Q}^k(\Omega) = k + 1$.

Example 6.4: Polynomial spaces in $d = 2$ dimension

In $d = 2$ dimensions, the polynomial spaces are

$$\begin{aligned}\mathcal{P}^k(\Omega) &:= \left\{ p \in \mathcal{F}_{\Omega \rightarrow \mathbb{R}} \mid p(\boldsymbol{\xi}) = \sum_{\alpha_1 + \alpha_2 \leq k} a_{\alpha_1 \alpha_2} \xi_1^{\alpha_1} \xi_2^{\alpha_2}, \boldsymbol{\xi} \in \Omega, a_{\alpha_1 \alpha_2} \in \mathbb{R} \right\} \\ \mathcal{Q}^k(\Omega) &:= \left\{ p \in \mathcal{F}_{\Omega \rightarrow \mathbb{R}} \mid p(\boldsymbol{\xi}) = \sum_{1 \leq \alpha_1, \alpha_2 \leq k} a_{\alpha_1 \alpha_2} \xi_1^{\alpha_1} \xi_2^{\alpha_2}, \boldsymbol{\xi} \in \Omega, a_{\alpha_1 \alpha_2} \in \mathbb{R} \right\} \end{aligned} \quad (6.12)$$

and have dimension $\dim \mathcal{P}^k(\Omega) = (k+1)(k+2)/2$ and $\dim \mathcal{Q}^k(\Omega) = (k+1)^2$. Now we state the monomial basis of $\mathcal{P}^k(\Omega)$ and $\mathcal{Q}^k(\Omega)$ for the special case of $k = 0, 1, 2$

$$\begin{aligned}\mathcal{P}^0(\Omega) &= \text{span}\{1\}, & \mathcal{Q}^0(\Omega) &= \text{span}\{1\} \\ \mathcal{P}^1(\Omega) &= \text{span}\{1, \xi_1, \xi_2\}, & \mathcal{Q}^1(\Omega) &= \text{span}\{1, \xi_1, \xi_2, \xi_1 \xi_2\} \\ \mathcal{P}^2(\Omega) &= \text{span}\{1, \xi_1, \xi_2, \xi_1^2, \xi_1 \xi_2, \xi_2^2\}, & \mathcal{Q}^2(\Omega) &= \text{span}\{1, \xi_1, \xi_2, \xi_1^2, \xi_1 \xi_2, \xi_2^2, \xi_1 \xi_2^2, \xi_1^2 \xi_2, \xi_1^2 \xi_2^2\} \end{aligned} \quad (6.13)$$

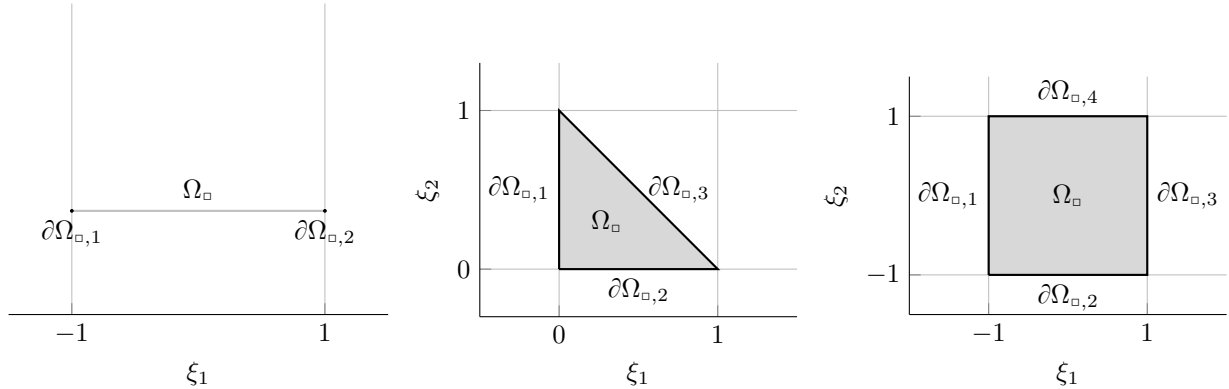


Figure 6.1: Master element geometry and boundary numbering for line ($d = 1$ hypercube) (left), triangle ($d = 2$ simplex) (middle), and quadrilateral ($d = 2$ hypercube) (right).

from which we can see the dimensions are

$$\begin{aligned} \dim \mathcal{P}^0(\Omega) &= 1, & \dim \mathcal{Q}^0(\Omega) &= 1 \\ \dim \mathcal{P}^1(\Omega) &= 3, & \dim \mathcal{Q}^1(\Omega) &= 4 \\ \dim \mathcal{P}^2(\Omega) &= 6, & \dim \mathcal{Q}^2(\Omega) &= 9 \end{aligned} \quad (6.14)$$

in agreement with the preceding general formula.

6.2.2 $d = 1$ dimension: $\mathcal{P}^p = \mathcal{Q}^p$ master line element

Element domain

In $d = 1$ dimension the only possible element geometry is a line segment. For convenience, we take the master element domain to be the bi-unit interval centered at zero

$$\Omega_{\square} := [-1, 1]. \quad (6.15)$$

Then the boundary of the master element is $\partial\Omega_{\square} = \{-1, 1\}$. We separate these into an ordered set of *faces* $\mathcal{F}_{\square} = \{\partial\Omega_{\square,1}, \partial\Omega_{\square,2}\}$, where $\partial\Omega_{\square,1} = \{-1\}$ with associated unit outward normal $N_{\square,1} = \{-1\}$ and $\partial\Omega_{\square,2} = \{1\}$ with associated unit outward normal $N_{\square,2} = \{1\}$. The complete geometry of the master line element is illustrated in Figure 6.1.

Local function space

We take the local function space to be the space of polynomials up to (and including) degree p , i.e., $\mathcal{Y}_{\square} := \mathcal{P}^p(\Omega_{\square}) = \mathcal{Q}^p(\Omega_{\square})$ (recall in $d = 1$ these polynomial spaces are the same). Therefore, the local function space has dimension $\dim \mathcal{Y}_{\square} = p + 1$.

Distribution and numbering of nodes

Before we can construct a nodal basis of \mathcal{Y}_{\square} , we must distribute $N_{\text{nd}}^{\text{el}} = p + 1$ nodes throughout the element geometry. To ensure the nodal basis functions are linearly independent, the nodes must not overlap (and should not be too close to prevent ill-conditioning). Furthermore we insist that a node lies on each face as this makes enforcing global continuity straightforward. For simplicity, we uniformly distribute nodes through Ω_{\square} , i.e., $\mathcal{N}_h = \{\hat{\xi}_1, \dots, \hat{\xi}_{p+1}\}$ where

$$\hat{\xi}_i = -1 + 2 \frac{i-1}{p} \quad (6.16)$$

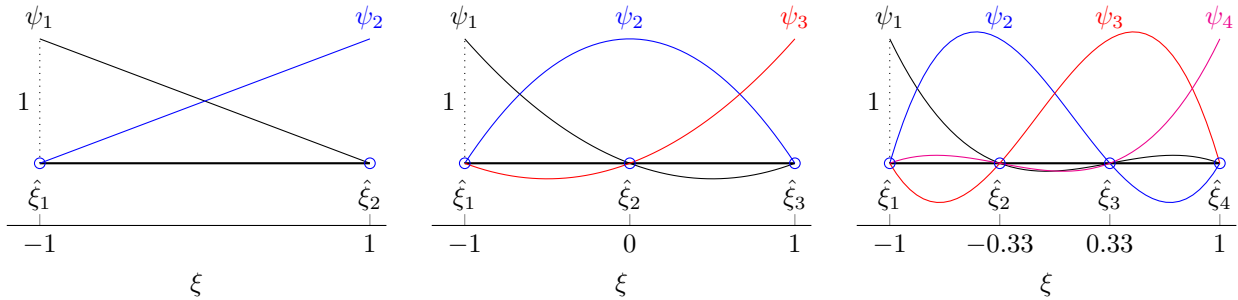


Figure 6.2: Master \mathcal{P}^p line element including nodal positions/numbering and nodal basis functions for $p = 1, 2, 3$ (left-to-right).

for $i = 1, \dots, p+1$ (Figure 6.2). It is well-known that uniform placement of nodes can lead to ill-conditioned systems for high p ; this can be remedied using non-uniform points such the Chebyshev or Gauss-Legendre-Lobatto nodes.

Construction of nodal element basis functions

Finally, we turn to a construction of basis functions of $\mathcal{Y}_{\square} := \mathcal{P}^p(\Omega_{\square})$ that satisfy the nodal property: $\psi_i(\hat{\xi}_j) = \delta_{ij}$ for $i, j = 1, \dots, p+1$. Notice that the nodal property constrains the value of each basis function at $p+1$ (unique) locations; since the basis functions are polynomials of degree p , these constraints uniquely define them. From this observation, we set out to construct the basis functions *by inspection*.

To begin, we consider the special case of $p = 1$ and observe that ψ_1 must go to zero at $\hat{\xi}_2$ from which we postulate it takes the form $\psi_1(\xi) = \alpha(\xi - \hat{\xi}_2)$ for some $\alpha \in \mathbb{R}$. Similarly, we postulate $\psi_2(\xi) = \beta(\xi - \hat{\xi}_1)$ for some $\beta \in \mathbb{R}$. It can readily be seen that these are linear functions that satisfy $\psi_1(\hat{\xi}_2) = \psi_2(\hat{\xi}_1) = 0$, which makes them valid candidates for a nodal basis of $\mathcal{P}^1(\Omega_{\square})$. The only conditions that remain are the normalization conditions $\psi_1(\hat{\xi}_1) = \psi_2(\hat{\xi}_2) = 1$, which leads to the following expressions for the coefficients

$$\alpha = \frac{1}{\hat{\xi}_1 - \hat{\xi}_2}, \quad \beta = \frac{1}{\hat{\xi}_2 - \hat{\xi}_1} \quad (6.17)$$

to yield the nodal basis

$$\psi_1(\xi) = \frac{\hat{\xi}_2 - \xi}{\hat{\xi}_2 - \hat{\xi}_1} = \frac{1 - \xi}{2}, \quad \psi_2(\xi) = \frac{\xi - \hat{\xi}_1}{\hat{\xi}_2 - \hat{\xi}_1} = \frac{\xi + 1}{2}, \quad (6.18)$$

where we have used that $\hat{\xi}_1 = -1$ and $\hat{\xi}_2 = 1$.

We follow a similar procedure for the $p = 2$ case and postulate that

$$\psi_1(\xi) = \alpha(\xi - \hat{\xi}_2)(\xi - \hat{\xi}_3), \quad \psi_2(\xi) = \beta(\xi - \hat{\xi}_1)(\xi - \hat{\xi}_3), \quad \psi_3(\xi) = \gamma(\xi - \hat{\xi}_1)(\xi - \hat{\xi}_2), \quad (6.19)$$

where $\alpha, \beta, \gamma \in \mathbb{R}$ are constants that must be determined. It is easy to verify that $\psi_i(\hat{\xi}_j) = 0$ for $i \neq j$. The constants are determined to be

$$\alpha = \frac{1}{(\hat{\xi}_1 - \hat{\xi}_2)(\hat{\xi}_1 - \hat{\xi}_3)}, \quad \beta = \frac{1}{(\hat{\xi}_2 - \hat{\xi}_1)(\hat{\xi}_2 - \hat{\xi}_3)}, \quad \gamma = \frac{1}{(\hat{\xi}_3 - \hat{\xi}_1)(\hat{\xi}_3 - \hat{\xi}_2)}, \quad (6.20)$$

from the normalization conditions $\psi_i(\hat{\xi}_i) = 1$ (no summation on i), which leads to the nodal basis functions

$$\begin{aligned} \psi_1(\xi) &= \frac{(\xi - \hat{\xi}_2)(\xi - \hat{\xi}_3)}{(\hat{\xi}_1 - \hat{\xi}_2)(\hat{\xi}_1 - \hat{\xi}_3)} = \frac{\xi(\xi - 1)}{2} \\ \psi_2(\xi) &= \frac{(\xi - \hat{\xi}_1)(\xi - \hat{\xi}_3)}{(\hat{\xi}_2 - \hat{\xi}_1)(\hat{\xi}_2 - \hat{\xi}_3)} = (\xi + 1)(1 - \xi) \\ \psi_3(\xi) &= \frac{(\xi - \hat{\xi}_1)(\xi - \hat{\xi}_2)}{(\hat{\xi}_3 - \hat{\xi}_1)(\hat{\xi}_3 - \hat{\xi}_2)} = \frac{\xi(\xi + 1)}{2} \end{aligned} \quad (6.21)$$

because the nodes are $\hat{\xi}_1 = -1$, $\hat{\xi}_2 = 0$, and $\hat{\xi}_3 = 1$ from (6.16). We follow the same procedure precisely to obtain an expression for the nodal basis functions of $\mathcal{P}^p(\Omega_\square)$ associated with the nodes $\mathcal{N}_\square = \{\hat{\xi}_1, \dots, \hat{\xi}_{p+1}\}$

$$\psi_i(\xi) = \prod_{\substack{j=1 \\ j \neq i}}^{p+1} \frac{\xi - \hat{\xi}_j}{\hat{\xi}_i - \hat{\xi}_j} = \frac{\xi - \hat{\xi}_1}{\hat{\xi}_i - \hat{\xi}_1} \cdots \frac{\xi - \hat{\xi}_{i-1}}{\hat{\xi}_i - \hat{\xi}_{i-1}} \frac{\xi - \hat{\xi}_{i+1}}{\hat{\xi}_i - \hat{\xi}_{i+1}} \cdots \frac{\xi - \hat{\xi}_{p+1}}{\hat{\xi}_i - \hat{\xi}_{p+1}}, \quad (6.22)$$

see Figure 6.2 for an illustration of the basis functions up to $p = 3$. It is a simple exercise to verify that this collection of functions satisfies the nodal property.

6.2.3 $d = 2$ dimensions: \mathcal{Q}^p master quadrilateral element

Unlike in $d = 1$ dimension, there are infinitely many possible element geometries in $d > 1$ dimensions; we will only consider a small, but extremely useful subset of these possibilities. We begin with the \mathcal{Q}^p quadrilateral element.

Element domain

The reference domain of the master quadrilateral element is taken to be the bi-unit interval centered at zero for consistency with the line element

$$\Omega_\square := [-1, 1] \times [-1, 1]. \quad (6.23)$$

Notice that the master quadrilateral element is a Cartesian product of the master line element with itself. The boundary of the master element is $\partial\Omega_\square = \bigcup_{i=1}^4 \partial\Omega_{\square,i}$, where

$$\partial\Omega_{\square,1} := \{-1\} \times [-1, 1], \quad \partial\Omega_{\square,2} := [-1, 1] \times \{-1\}, \quad \partial\Omega_{\square,3} := \{1\} \times [-1, 1], \quad \partial\Omega_{\square,4} := [-1, 1] \times \{1\} \quad (6.24)$$

and the corresponding unit outward normals are

$$\mathbf{N}_{\square,1} := \begin{bmatrix} -1 \\ 0 \end{bmatrix}, \quad \mathbf{N}_{\square,2} := \begin{bmatrix} 0 \\ -1 \end{bmatrix}, \quad \mathbf{N}_{\square,3} := \begin{bmatrix} 1 \\ 0 \end{bmatrix}, \quad \mathbf{N}_{\square,4} := \begin{bmatrix} 0 \\ 1 \end{bmatrix}. \quad (6.25)$$

The complete geometry of the master quadrilateral element is illustrated in Figure 6.1.

Local function space

We take the local function space to be the space $\mathcal{Y}_\square := \mathcal{Q}^p(\Omega_\square)$, i.e., polynomial functions where the largest exponent is p . The dimension of the local function space is $\dim \mathcal{Y}_\square = (p+1)^2$. An important property of this function space is that any function $v \in \mathcal{Q}^p(\Omega_\square)$ is a one-dimensional polynomial of degree p when restricted to any face $\partial\Omega_{\square,k}$, $k = 1, \dots, 4$. To see this we introduce a parametrization of boundary 2 (chosen arbitrarily), $\gamma : [-1, 1] \rightarrow \partial\Omega_{\square,2}$ defined as $\gamma(s) := (s, -1) \in \partial\Omega_{\square,2}$. Then, for any $v \in \mathcal{Q}^p(\Omega_\square)$, we expand it as

$$v(\xi) = \sum_{\alpha_1 \leq p, \alpha_2 \leq p} a_{\alpha_1 \alpha_2} \xi_1^{\alpha_1} \xi_2^{\alpha_2}, \quad (6.26)$$

where $a_{ij} \in \mathbb{R}$ for $i, j = 1, \dots, p+1$. We then restrict v to $\partial\Omega_{\square,2}$ by composing with the face parametrization γ

$$f(s) := v(\gamma(s)) = \sum_{\alpha_1 \leq p, \alpha_2 \leq p} a_{\alpha_1 \alpha_2} \gamma_1(s)^{\alpha_1} \gamma_2(s)^{\alpha_2} = \sum_{\alpha_2 \leq p} \left(\sum_{\alpha_1 \leq p} (-1)^{\alpha_1} a_{\alpha_1 \alpha_2} \right) s^{\alpha_2}, \quad (6.27)$$

which is clearly a polynomial of degree at most p , i.e., $f \in \mathcal{P}^p([-1, 1])$.

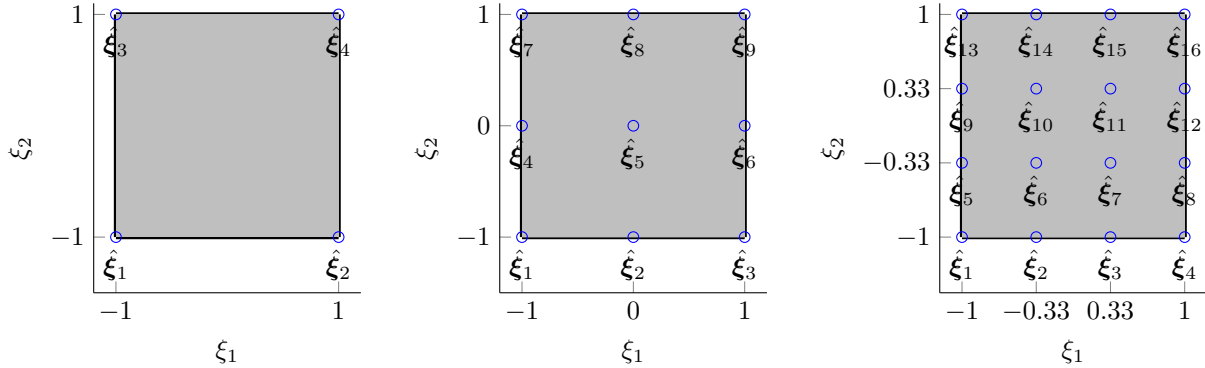


Figure 6.3: Master \mathcal{Q}^p quadrilateral element including nodal positions and numbering for $p = 1, 2, 3$ (left-to-right).

Distribution and numbering of nodes

Before we construct a nodal basis of \mathcal{Y}_{\square} , we must distribute $N_{\text{nd}}^{\text{el}} = (p + 1)^2$ nodes throughout the element domain Ω_{\square} . To ensure all basis functions are linearly independent, the nodes must not overlap (or be too close to prevent ill-conditioning). We also require that $p + 1$ nodes lie on each of the four faces of the quadrilateral Ω_{\square} . Recall from the previous section that functions of $\mathcal{Q}^p(\Omega_{\square})$ are one-dimensional polynomials of degree p when restricted to faces $\partial\Omega_{\square}$ and are therefore uniquely determined by $p + 1$ nodal values. This gives a convenient way to enforce global continuity between elements: if the nodal values of two abutting elements match at the $p + 1$ nodes on their common face, then the functions will match everywhere on that face since they will define the same one-dimensional polynomial.

To satisfy these requirements, we define the nodes of the \mathcal{Q}^p master quadrilateral to be the Cartesian product of the nodes of the \mathcal{Q}^p master line element, numbered first in the ξ_1 -direction then in the ξ_2 -direction (Figure 6.3 for $p = 1, 2, 3$). To make this precise, let $\{\hat{s}_1, \dots, \hat{s}_{p+1}\} \subset [-1, 1]$ be the nodes of the master line element and introduce two mappings

$$\mathcal{I} : \{1, \dots, (p + 1)^2\} \rightarrow \{1, \dots, p + 1\}, \quad \mathcal{J} : \{1, \dots, (p + 1)^2\} \rightarrow \{1, \dots, p + 1\}, \quad (6.28)$$

where \mathcal{I} maps the quadrilateral node number to the node number along the ξ_1 -axis and \mathcal{J} maps to the node number along the ξ_2 -axis, i.e., the i th quadrilateral node is the $\mathcal{I}(i)$ th node in the ξ_1 -direction and the $\mathcal{J}(i)$ th node in the ξ_2 -direction. To agree with the node numbering in Figure 6.3, we have

$$\mathcal{I}(k) := 1 + [(k - 1)\%(p + 1)], \quad \mathcal{J}(k) := 1 + \left\lfloor \frac{k - 1}{p + 1} \right\rfloor \quad (6.29)$$

for $k = 1, \dots, (p + 1)^2$, where $\%$ is the modulus operator (remainder after division) and $\lfloor \cdot \rfloor$ is the floor operator. With this notation, the k th quadrilateral node is defined in terms of the line element nodes as

$$\hat{\xi}_k := \begin{bmatrix} \hat{\xi}_{1k} \\ \hat{\xi}_{2k} \end{bmatrix} := \begin{bmatrix} \hat{s}_{\mathcal{I}(k)} \\ \hat{s}_{\mathcal{J}(k)} \end{bmatrix}. \quad (6.30)$$

Example 6.5: Nodes of bilinear \mathcal{Q}^1 quadrilateral

To define the nodes of \mathcal{Q}^1 master quadrilateral element, recall the nodes of the \mathcal{Q}^1 master line element $\hat{s}_1 = -1$, $\hat{s}_2 = 1$ and, in the special case of $p = 1$, the quadrilateral-to-line mappings (6.28)-(6.29) are

$$\mathcal{I} = \{1, 2, 1, 2\}, \quad \mathcal{J} = \{1, 1, 2, 2\}. \quad (6.31)$$

From this and (6.30), the nodes of the master \mathcal{Q}^1 quadrilateral element are

$$\begin{aligned}\hat{\boldsymbol{\xi}}_1 &= \begin{bmatrix} \hat{\xi}_{11} \\ \hat{\xi}_{21} \end{bmatrix} = \begin{bmatrix} \hat{s}_{\mathcal{I}(1)} \\ \hat{s}_{\mathcal{J}(1)} \end{bmatrix} = \begin{bmatrix} \hat{s}_1 \\ \hat{s}_1 \end{bmatrix} = \begin{bmatrix} -1 \\ -1 \end{bmatrix}, & \hat{\boldsymbol{\xi}}_2 &= \begin{bmatrix} \hat{\xi}_{12} \\ \hat{\xi}_{22} \end{bmatrix} = \begin{bmatrix} \hat{s}_{\mathcal{I}(2)} \\ \hat{s}_{\mathcal{J}(2)} \end{bmatrix} = \begin{bmatrix} \hat{s}_2 \\ \hat{s}_1 \end{bmatrix} = \begin{bmatrix} 1 \\ -1 \end{bmatrix}, \\ \hat{\boldsymbol{\xi}}_3 &= \begin{bmatrix} \hat{\xi}_{13} \\ \hat{\xi}_{23} \end{bmatrix} = \begin{bmatrix} \hat{s}_{\mathcal{I}(3)} \\ \hat{s}_{\mathcal{J}(3)} \end{bmatrix} = \begin{bmatrix} \hat{s}_1 \\ \hat{s}_2 \end{bmatrix} = \begin{bmatrix} -1 \\ 1 \end{bmatrix}, & \hat{\boldsymbol{\xi}}_4 &= \begin{bmatrix} \hat{\xi}_{14} \\ \hat{\xi}_{24} \end{bmatrix} = \begin{bmatrix} \hat{s}_{\mathcal{I}(4)} \\ \hat{s}_{\mathcal{J}(4)} \end{bmatrix} = \begin{bmatrix} \hat{s}_2 \\ \hat{s}_2 \end{bmatrix} = \begin{bmatrix} 1 \\ 1 \end{bmatrix},\end{aligned}\quad (6.32)$$

which clearly agrees with Figure 6.3.

Example 6.6: Nodes of biquadratic \mathcal{Q}^2 quadrilateral

To define the nodes of \mathcal{Q}^2 master quadrilateral element, recall the nodes of the \mathcal{Q}^2 master line element $\hat{s}_1 = -1, \hat{s}_2 = 0, \hat{s}_3 = 1$ and, in the special case of $p = 2$, the quadrilateral-to-line mappings (6.28)-(6.29) are

$$\mathcal{I} = \{1, 2, 3, 1, 2, 3, 1, 2, 3\}, \quad \mathcal{J} = \{1, 1, 1, 2, 2, 2, 3, 3, 3\}. \quad (6.33)$$

From this and (6.30), the nodes of the master \mathcal{Q}^2 quadrilateral element are

$$\begin{aligned}\hat{\boldsymbol{\xi}}_1 &= \begin{bmatrix} \hat{\xi}_{11} \\ \hat{\xi}_{21} \\ \hat{\xi}_{31} \end{bmatrix} = \begin{bmatrix} \hat{s}_{\mathcal{I}(1)} \\ \hat{s}_{\mathcal{J}(1)} \\ \hat{s}_{\mathcal{I}(3)} \end{bmatrix} = \begin{bmatrix} \hat{s}_1 \\ \hat{s}_1 \\ \hat{s}_3 \end{bmatrix} = \begin{bmatrix} -1 \\ -1 \\ 1 \end{bmatrix}, & \hat{\boldsymbol{\xi}}_2 &= \begin{bmatrix} \hat{\xi}_{12} \\ \hat{\xi}_{22} \\ \hat{\xi}_{32} \end{bmatrix} = \begin{bmatrix} \hat{s}_{\mathcal{I}(2)} \\ \hat{s}_{\mathcal{J}(2)} \\ \hat{s}_{\mathcal{I}(5)} \end{bmatrix} = \begin{bmatrix} \hat{s}_2 \\ \hat{s}_1 \\ \hat{s}_2 \end{bmatrix} = \begin{bmatrix} 1 \\ -1 \\ 0 \end{bmatrix}, \\ \hat{\boldsymbol{\xi}}_3 &= \begin{bmatrix} \hat{\xi}_{13} \\ \hat{\xi}_{23} \\ \hat{\xi}_{33} \end{bmatrix} = \begin{bmatrix} \hat{s}_{\mathcal{I}(3)} \\ \hat{s}_{\mathcal{J}(3)} \\ \hat{s}_{\mathcal{I}(7)} \end{bmatrix} = \begin{bmatrix} \hat{s}_3 \\ \hat{s}_1 \\ \hat{s}_3 \end{bmatrix} = \begin{bmatrix} 1 \\ -1 \\ 1 \end{bmatrix}, & \hat{\boldsymbol{\xi}}_4 &= \begin{bmatrix} \hat{\xi}_{14} \\ \hat{\xi}_{24} \\ \hat{\xi}_{34} \end{bmatrix} = \begin{bmatrix} \hat{s}_{\mathcal{I}(4)} \\ \hat{s}_{\mathcal{J}(4)} \\ \hat{s}_{\mathcal{I}(8)} \end{bmatrix} = \begin{bmatrix} \hat{s}_1 \\ \hat{s}_2 \\ \hat{s}_3 \end{bmatrix} = \begin{bmatrix} -1 \\ 0 \\ 1 \end{bmatrix}, \\ \hat{\boldsymbol{\xi}}_5 &= \begin{bmatrix} \hat{\xi}_{15} \\ \hat{\xi}_{25} \\ \hat{\xi}_{35} \end{bmatrix} = \begin{bmatrix} \hat{s}_{\mathcal{I}(5)} \\ \hat{s}_{\mathcal{J}(5)} \\ \hat{s}_{\mathcal{I}(9)} \end{bmatrix} = \begin{bmatrix} \hat{s}_2 \\ \hat{s}_2 \\ \hat{s}_3 \end{bmatrix} = \begin{bmatrix} 0 \\ 0 \\ 1 \end{bmatrix}, & \hat{\boldsymbol{\xi}}_6 &= \begin{bmatrix} \hat{\xi}_{16} \\ \hat{\xi}_{26} \\ \hat{\xi}_{36} \end{bmatrix} = \begin{bmatrix} \hat{s}_{\mathcal{I}(6)} \\ \hat{s}_{\mathcal{J}(6)} \\ \hat{s}_{\mathcal{I}(10)} \end{bmatrix} = \begin{bmatrix} \hat{s}_3 \\ \hat{s}_2 \\ \hat{s}_3 \end{bmatrix} = \begin{bmatrix} 1 \\ 0 \\ 1 \end{bmatrix}, \\ \hat{\boldsymbol{\xi}}_7 &= \begin{bmatrix} \hat{\xi}_{17} \\ \hat{\xi}_{27} \\ \hat{\xi}_{37} \end{bmatrix} = \begin{bmatrix} \hat{s}_{\mathcal{I}(7)} \\ \hat{s}_{\mathcal{J}(7)} \\ \hat{s}_{\mathcal{I}(11)} \end{bmatrix} = \begin{bmatrix} \hat{s}_1 \\ \hat{s}_3 \\ \hat{s}_3 \end{bmatrix} = \begin{bmatrix} -1 \\ 1 \\ 1 \end{bmatrix}, & \hat{\boldsymbol{\xi}}_8 &= \begin{bmatrix} \hat{\xi}_{18} \\ \hat{\xi}_{28} \\ \hat{\xi}_{38} \end{bmatrix} = \begin{bmatrix} \hat{s}_{\mathcal{I}(8)} \\ \hat{s}_{\mathcal{J}(8)} \\ \hat{s}_{\mathcal{I}(12)} \end{bmatrix} = \begin{bmatrix} \hat{s}_2 \\ \hat{s}_3 \\ \hat{s}_3 \end{bmatrix} = \begin{bmatrix} 0 \\ 1 \\ 1 \end{bmatrix}, \\ \hat{\boldsymbol{\xi}}_9 &= \begin{bmatrix} \hat{\xi}_{19} \\ \hat{\xi}_{29} \\ \hat{\xi}_{39} \end{bmatrix} = \begin{bmatrix} \hat{s}_{\mathcal{I}(9)} \\ \hat{s}_{\mathcal{J}(9)} \\ \hat{s}_{\mathcal{I}(13)} \end{bmatrix} = \begin{bmatrix} \hat{s}_3 \\ \hat{s}_3 \\ \hat{s}_3 \end{bmatrix} = \begin{bmatrix} 1 \\ 1 \\ 1 \end{bmatrix},\end{aligned}\quad (6.34)$$

which clearly agrees with Figure 6.3.

Construction of element basis functions

Lastly we turn to a construction of the nodal basis of $\mathcal{Y}_\square := \mathcal{Q}^p(\Omega_\square)$. Given the *tensor product structure* of the master quadrilateral domain and its nodes, we construct the nodal basis via a Cartesian product of the nodal basis functions of the master line element. Again, let $\{\hat{s}_1, \dots, \hat{s}_{p+1}\}$ be the nodes of the \mathcal{P}^p master line element, \mathcal{I} and \mathcal{J} be the quadrilateral-to-line nodal mapping from the previous section, and $\{\tilde{\psi}_1, \dots, \tilde{\psi}_{p+1}\}$ be the corresponding nodal basis, i.e., $\tilde{\psi}_i(\hat{s}_j) = \delta_{ij}$ for $i, j = 1, \dots, p + 1$. Then we define the nodal basis functions $\{\psi_1, \dots, \psi_{N_{\text{nd}}^{\text{el}}}\}$ of the \mathcal{Q}^p quadrilateral to be

$$\psi_i(\boldsymbol{\xi}) := \tilde{\psi}_{\mathcal{I}(i)}(\xi_1) \tilde{\psi}_{\mathcal{J}(i)}(\xi_2). \quad (6.35)$$

Using the expression in (6.22) for the one-dimensional nodal basis, this becomes

$$\psi_i(\boldsymbol{\xi}) = \left(\prod_{\substack{j=1 \\ j \neq \mathcal{I}(i)}}^{p+1} \frac{\xi_1 - \hat{s}_j}{\hat{s}_{\mathcal{I}(i)} - \hat{s}_j} \right) \left(\prod_{\substack{k=1 \\ k \neq \mathcal{J}(i)}}^{p+1} \frac{\xi_2 - \hat{s}_k}{\hat{s}_{\mathcal{J}(i)} - \hat{s}_k} \right) \quad (6.36)$$

To verify this choice of basis has the nodal property, we evaluate ψ_i at node $\hat{\boldsymbol{\xi}}_j$

$$\psi_i(\hat{\boldsymbol{\xi}}_j) = \tilde{\psi}_{\mathcal{I}(i)}(\hat{\xi}_{1j}) \tilde{\psi}_{\mathcal{J}(i)}(\hat{\xi}_{2j}) = \tilde{\psi}_{\mathcal{I}(i)}(\hat{s}_{\mathcal{I}(j)}) \tilde{\psi}_{\mathcal{J}(i)}(\hat{s}_{\mathcal{J}(j)}) = \delta_{\mathcal{I}(i)\mathcal{I}(j)} \delta_{\mathcal{J}(i)\mathcal{J}(j)} = \delta_{ij}, \quad (6.37)$$

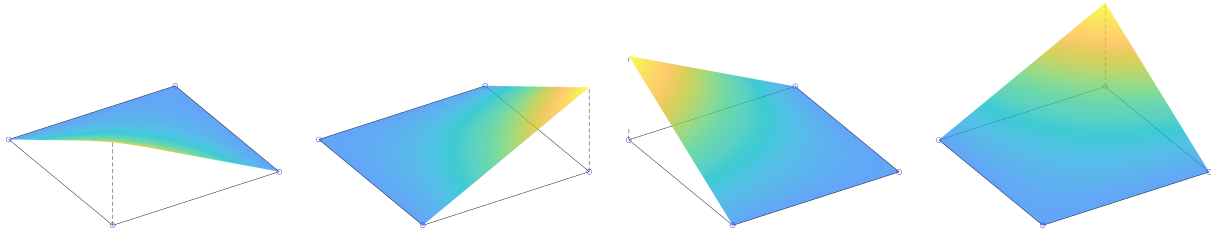


Figure 6.4: Nodal basis functions of \mathcal{Q}^1 master quadrilateral element.

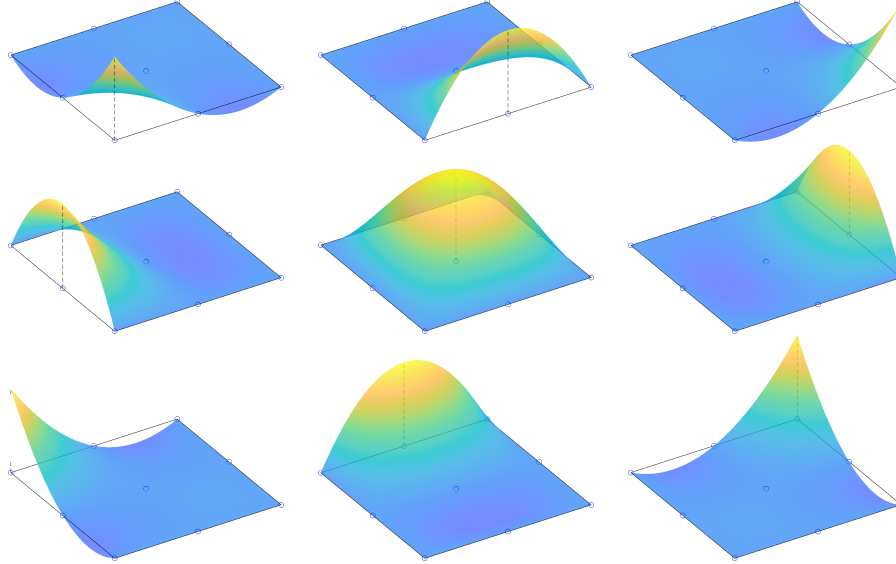


Figure 6.5: Nodal basis functions of \mathcal{Q}^2 master quadrilateral element.

where the last equality follows because the product $\delta_{\mathcal{I}(i)\mathcal{I}(j)}\delta_{\mathcal{J}(i)\mathcal{J}(j)}$ only survives if $\mathcal{I}(i) = \mathcal{I}(j)$ (the ξ_1 index of nodes i and j must match) and $\mathcal{J}(i) = \mathcal{J}(j)$ (the ξ_2 index of nodes i and j must match), which can only happen if $i = j$. The nodal basis functions for the \mathcal{Q}^1 , \mathcal{Q}^2 , and \mathcal{Q}^3 master quadrilateral are shown in Figures 6.4-6.6.

Example 6.7: Bilinear \mathcal{Q}^1 quadrilateral nodal basis

Recall the quadrilateral-to-line mappings for the bilinear quadrilateral (6.28)-(6.29). Then the nodal basis functions of the \mathcal{Q}^1 quadrilateral (Figure 6.4) using the tensor product formula in (6.36) are

$$\begin{aligned}
 \psi_1(\xi) &= \tilde{\psi}_1(\xi_1)\tilde{\psi}_1(\xi_2) &= \frac{\xi_1 - \hat{s}_2}{\hat{s}_1 - \hat{s}_2} \frac{\xi_2 - \hat{s}_2}{\hat{s}_2 - \hat{s}_1} &= \frac{1}{4}(1 - \xi_1)(1 - \xi_2) \\
 \psi_2(\xi) &= \tilde{\psi}_2(\xi_1)\tilde{\psi}_1(\xi_2) &= \frac{\xi_1 - \hat{s}_1}{\hat{s}_2 - \hat{s}_1} \frac{\xi_2 - \hat{s}_2}{\hat{s}_1 - \hat{s}_2} &= \frac{1}{4}(\xi_1 + 1)(1 - \xi_2) \\
 \psi_3(\xi) &= \tilde{\psi}_1(\xi_1)\tilde{\psi}_2(\xi_2) &= \frac{\xi_1 - \hat{s}_1}{\hat{s}_2 - \hat{s}_1} \frac{\xi_2 - \hat{s}_2}{\hat{s}_1 - \hat{s}_2} &= \frac{1}{4}(1 - \xi_1)(\xi_2 + 1) \\
 \psi_4(\xi) &= \tilde{\psi}_2(\xi_1)\tilde{\psi}_2(\xi_2) &= \frac{\xi_1 - \hat{s}_1}{\hat{s}_2 - \hat{s}_1} \frac{\xi_2 - \hat{s}_1}{\hat{s}_2 - \hat{s}_1} &= \frac{1}{4}(\xi_1 + 1)(\xi_2 + 1),
 \end{aligned} \tag{6.38}$$

where the last equality used that the nodes of the \mathcal{P}^1 master element are $\hat{s}_1 = -1$ and $\hat{s}_2 = 1$.

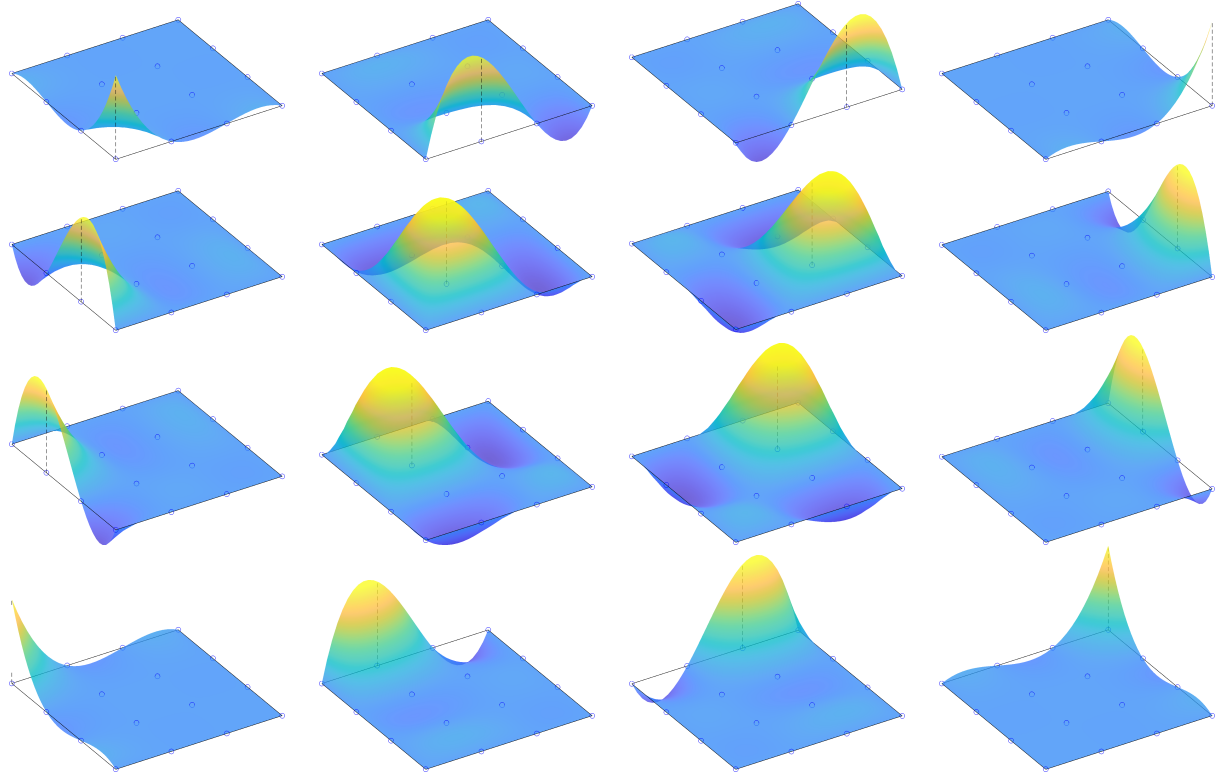


Figure 6.6: Nodal basis functions of \mathcal{Q}^3 master quadrilateral element.

Example 6.8: Biquadratic \mathcal{Q}^2 quadrilateral nodal basis

Recall the quadrilateral-to-line mappings for the biquadratic quadrilateral (6.28)-(6.29). Then the nodal basis functions of the \mathcal{Q}^2 quadrilateral (Figure 6.5) using the tensor product formula in (6.36) are

$$\begin{aligned}
 \psi_1(\xi) &= \tilde{\psi}_1(\xi_1)\tilde{\psi}_1(\xi_2) & = \frac{\xi_1 - \hat{s}_2}{\hat{s}_1 - \hat{s}_2} \frac{\xi_1 - \hat{s}_3}{\hat{s}_1 - \hat{s}_3} \frac{\xi_2 - \hat{s}_2}{\hat{s}_1 - \hat{s}_2} \frac{\xi_2 - \hat{s}_3}{\hat{s}_1 - \hat{s}_3} & = \frac{\xi_1(\xi_1 - 1)\xi_2(\xi_2 - 1)}{4} \\
 \psi_2(\xi) &= \tilde{\psi}_2(\xi_1)\tilde{\psi}_1(\xi_2) & = \frac{\xi_1 - \hat{s}_1}{\hat{s}_2 - \hat{s}_1} \frac{\xi_1 - \hat{s}_3}{\hat{s}_2 - \hat{s}_3} \frac{\xi_2 - \hat{s}_2}{\hat{s}_1 - \hat{s}_2} \frac{\xi_2 - \hat{s}_3}{\hat{s}_1 - \hat{s}_3} & = \frac{(\xi_1 + 1)(1 - \xi_1)\xi_2(\xi_2 - 1)}{2} \\
 \psi_3(\xi) &= \tilde{\psi}_3(\xi_1)\tilde{\psi}_1(\xi_2) & = \frac{\xi_1 - \hat{s}_1}{\hat{s}_3 - \hat{s}_1} \frac{\xi_1 - \hat{s}_2}{\hat{s}_3 - \hat{s}_2} \frac{\xi_2 - \hat{s}_2}{\hat{s}_1 - \hat{s}_2} \frac{\xi_2 - \hat{s}_3}{\hat{s}_1 - \hat{s}_3} & = \frac{\xi_1(\xi_1 + 1)\xi_2(\xi_2 - 1)}{4} \\
 \psi_4(\xi) &= \tilde{\psi}_1(\xi_1)\tilde{\psi}_2(\xi_2) & = \frac{\xi_1 - \hat{s}_2}{\hat{s}_1 - \hat{s}_2} \frac{\xi_1 - \hat{s}_3}{\hat{s}_1 - \hat{s}_3} \frac{\xi_2 - \hat{s}_1}{\hat{s}_2 - \hat{s}_1} \frac{\xi_2 - \hat{s}_3}{\hat{s}_2 - \hat{s}_3} & = \frac{\xi_1(\xi_1 - 1)(\xi_2 + 1)(1 - \xi_2)}{2} \\
 \psi_5(\xi) &= \tilde{\psi}_2(\xi_1)\tilde{\psi}_2(\xi_2) & = \frac{\xi_1 - \hat{s}_1}{\hat{s}_2 - \hat{s}_1} \frac{\xi_1 - \hat{s}_3}{\hat{s}_2 - \hat{s}_3} \frac{\xi_2 - \hat{s}_1}{\hat{s}_2 - \hat{s}_1} \frac{\xi_2 - \hat{s}_3}{\hat{s}_2 - \hat{s}_3} & = (\xi_1 + 1)(1 - \xi_1)(\xi_2 + 1)(1 - \xi_2) \quad (6.39) \\
 \psi_6(\xi) &= \tilde{\psi}_3(\xi_1)\tilde{\psi}_2(\xi_2) & = \frac{\xi_1 - \hat{s}_1}{\hat{s}_3 - \hat{s}_1} \frac{\xi_1 - \hat{s}_2}{\hat{s}_3 - \hat{s}_2} \frac{\xi_2 - \hat{s}_1}{\hat{s}_2 - \hat{s}_1} \frac{\xi_2 - \hat{s}_3}{\hat{s}_2 - \hat{s}_3} & = \frac{\xi_1(\xi_1 + 1)(\xi_2 + 1)(1 - \xi_2)}{2} \\
 \psi_7(\xi) &= \tilde{\psi}_1(\xi_1)\tilde{\psi}_3(\xi_2) & = \frac{\xi_1 - \hat{s}_2}{\hat{s}_1 - \hat{s}_2} \frac{\xi_1 - \hat{s}_3}{\hat{s}_1 - \hat{s}_3} \frac{\xi_2 - \hat{s}_1}{\hat{s}_3 - \hat{s}_1} \frac{\xi_2 - \hat{s}_2}{\hat{s}_3 - \hat{s}_2} & = \frac{\xi_1(\xi_1 - 1)\xi_2(\xi_2 + 1)}{4} \\
 \psi_8(\xi) &= \tilde{\psi}_2(\xi_1)\tilde{\psi}_3(\xi_2) & = \frac{\xi_1 - \hat{s}_1}{\hat{s}_2 - \hat{s}_1} \frac{\xi_1 - \hat{s}_3}{\hat{s}_2 - \hat{s}_3} \frac{\xi_2 - \hat{s}_1}{\hat{s}_3 - \hat{s}_1} \frac{\xi_2 - \hat{s}_2}{\hat{s}_3 - \hat{s}_2} & = \frac{(\xi_1 + 1)(1 - \xi_1)\xi_2(\xi_2 + 1)}{2} \\
 \psi_9(\xi) &= \tilde{\psi}_3(\xi_1)\tilde{\psi}_3(\xi_2) & = \frac{\xi_1 - \hat{s}_1}{\hat{s}_3 - \hat{s}_1} \frac{\xi_1 - \hat{s}_2}{\hat{s}_3 - \hat{s}_2} \frac{\xi_2 - \hat{s}_1}{\hat{s}_3 - \hat{s}_1} \frac{\xi_2 - \hat{s}_2}{\hat{s}_3 - \hat{s}_2} & = \frac{\xi_1(\xi_1 + 1)\xi_2(\xi_2 + 1)}{4}
 \end{aligned}$$

where the last equality used that the nodes of the \mathcal{P}^2 master element are $\hat{s}_1 = -1$, $\hat{s}_2 = 0$, and $\hat{s}_3 = 1$.

6.2.4 $d = 2$ dimensions: \mathcal{P}^p triangle elements

Next we introduce the most common, versatile two-dimensional finite element, the triangle.

Element domain

The reference domain of the master triangle element is taken to be the unit right triangle

$$\Omega_{\square} := \{\boldsymbol{\xi} \in \mathbb{R}^d \mid \xi_1 \geq 0, \xi_2 \geq 0, \xi_1 + \xi_2 \leq 1\}. \quad (6.40)$$

The boundary of the master triangle consists of three faces $\partial\Omega_{\square} = \bigcup_{i=1}^3 \partial\Omega_{\square,i}$, where

$$\partial\Omega_{\square,1} := \{0\} \times [0, 1], \quad \partial\Omega_{\square,2} := [0, 1] \times \{0\}, \quad \partial\Omega_{\square,3} := \{(s, 1-s) \mid s \in [0, 1]\} \quad (6.41)$$

and the corresponding unit outward normals are

$$\mathbf{N}_{\square,1} := \begin{bmatrix} -1 \\ 0 \end{bmatrix}, \quad \mathbf{N}_{\square,2} := \begin{bmatrix} 0 \\ -1 \end{bmatrix}, \quad \mathbf{N}_{\square,3} := \frac{1}{\sqrt{2}} \begin{bmatrix} 1 \\ 1 \end{bmatrix}. \quad (6.42)$$

The complete geometry of the master triangle element is illustrated in Figure 6.1.

Local function space

We take the local function space to be $\mathcal{Y}_{\square} := \mathcal{P}^p(\Omega_{\square})$. The dimension of the local function space is

$$\dim \mathcal{Y}_{\square} = \frac{(p+1)(p+2)}{2}. \quad (6.43)$$

An important property of this function space is every $v \in \mathcal{P}^p(\Omega_{\square})$ is a one-dimensional polynomial of degree p when restricted to any line $\Gamma = \{(a_1 + b_1 s, a_2 + b_2 s) \mid s \in \mathbb{R}\}$ for any $a_1, a_2, b_1, b_2 \in \mathbb{R}^2$. To see this, let $\gamma : \mathbb{R} \rightarrow \Gamma$ be a parametrization of Γ defined as $\gamma(s) := (a_1 + b_1 s, a_2 + b_2 s)$. Then, for any $v \in \mathcal{P}^p(\Omega_{\square})$, we expand in a monomial basis as

$$v(\boldsymbol{\xi}) = \sum_{\alpha_1 + \alpha_2 \leq p} a_{\alpha_1 \alpha_2} \xi_1^{\alpha_1} \xi_2^{\alpha_2}. \quad (6.44)$$

We restrict v to Γ by composing with the parametrization γ to obtain

$$f(s) := v(\gamma(s)) = \sum_{\alpha_1 + \alpha_2 \leq p} a_{\alpha_1 \alpha_2} \gamma_1(s)^{\alpha_1} \gamma_2^{\alpha_2} = \sum_{\alpha_1 + \alpha_2 \leq p} a_{\alpha_1 \alpha_2} (a_1 + b_1 s)^{\alpha_1} (a_2 + b_2 s)^{\alpha_2}, \quad (6.45)$$

where clearly the largest monomial term is $s^{\alpha_1 + \alpha_2}$ and since $\alpha_1 + \alpha_2 \leq p$, this is a polynomial of degree at most p . Since all boundaries of the master triangular element are straight lines, this implies that functions of $\mathcal{P}^p(\Omega_{\square})$ restricted to the faces of the master element are one-dimensional polynomials of degree at most p .

Distribution and numbering of nodes

Before we construct a nodal basis of \mathcal{Y} , we must distribute $N_{\text{nd}}^{\text{el}} = (p+1)(p+2)/2$ nodes throughout the element domain Ω_{\square} . To ensure all basis functions are linearly independent, the nodes must not overlap (or be too close to prevent ill-conditioning). Similar to the quadrilateral element, we require that $p+1$ nodes lie on each of the three faces of the triangle Ω_{\square} . Again, this comes from the fact that functions of $\mathcal{P}^p(\Omega_{\square})$ are one-dimensional polynomials of degree p when restricted to faces $\partial\Omega_{\square}$ and are therefore uniquely determined by $p+1$ nodal values, which gives a convenient way to enforce global continuity (ensure the nodal values of abutting elements agree at the $p+1$ nodes). A convenient and systematic way to populate the master triangle with nodes is to:

- (1) uniformly distribute $p+1$ nodes $\{\hat{s}_1, \dots, \hat{s}_{p+1}\}$ throughout the unit interval $[0, 1]$, i.e., $\hat{s}_i = (i-1)/p$,
- (2) form their tensor product following the procedure in Section 6.2.3 to yield $(p+1)^2$ nodes $\{\zeta_1, \dots, \zeta_{(p+1)^2}\}$ in the unit square $[0, 1]^2$, and

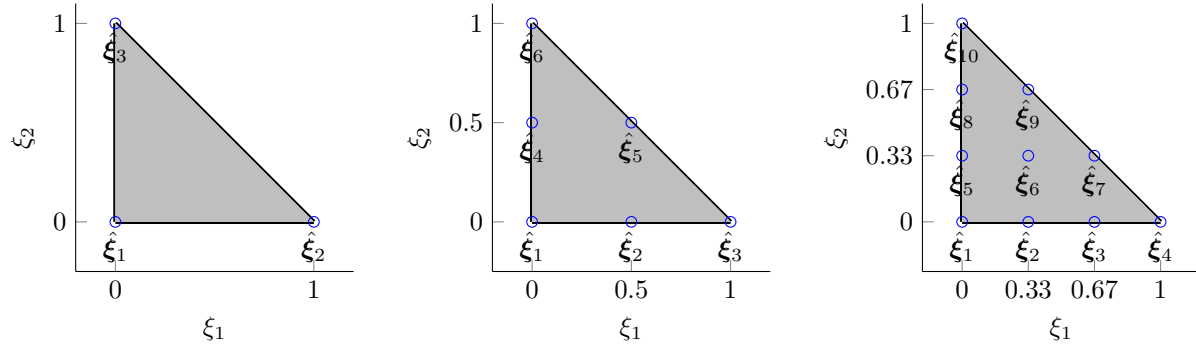


Figure 6.7: Master \mathcal{P}^p triangle element including nodal positions and numbering for $p = 1, 2, 3$ (left-to-right).

- (3) retain only the nodes that lie in the master triangle domain Ω_\square and re-number sequentially (preserve ordering) to obtain the nodes $\{\hat{\xi}_1, \dots, \hat{\xi}_{N_{\text{nd}}^{\text{el}}}\}$.

This procedure will generate nodes in the master triangle that are uniformly spaced with $p+1$ nodes lying on each boundary (Figure 6.7 for $p = 1, 2, 3$).

Example 6.9: Nodes of linear \mathcal{P}^1 triangle

From (6.43) with $p = 1$, there are 3 nodes associated with the \mathcal{P}^1 master triangle. The only locations we can place these nodes to ensure each face has 2 nodes is at the triangle vertices

$$\hat{\xi}_1 = \begin{bmatrix} 0 \\ 0 \end{bmatrix}, \quad \hat{\xi}_2 = \begin{bmatrix} 1 \\ 0 \end{bmatrix}, \quad \hat{\xi}_3 = \begin{bmatrix} 0 \\ 1 \end{bmatrix}, \quad (6.46)$$

which clearly agrees with Figure 6.7.

Example 6.10: Nodes of quadratic \mathcal{P}^2 triangle

From (6.43) with $p = 2$, there are 6 nodes associated with the \mathcal{P}^2 master triangle and each face must contain $p+1 = 3$ nodes. Following the procedure outlined in this section, we define equally spaced nodes in the unit interval $\hat{s}_1 = 0$, $\hat{s}_2 = 0.5$, $\hat{s}_3 = 1$, which leads to the following nodes in the unit square (following the procedure in Section 6.2.3 to construct nodes in \mathbb{R}^2 as tensor products of those in \mathbb{R}):

$$\begin{aligned} \zeta_1 &= \begin{bmatrix} 0 \\ 0 \end{bmatrix}, & \zeta_2 &= \begin{bmatrix} 0.5 \\ 0 \end{bmatrix}, & \zeta_3 &= \begin{bmatrix} 1 \\ 0 \end{bmatrix}, \\ \zeta_4 &= \begin{bmatrix} 0 \\ 0.5 \end{bmatrix}, & \zeta_5 &= \begin{bmatrix} 0.5 \\ 0.5 \end{bmatrix}, & \zeta_6 &= \begin{bmatrix} 1 \\ 0.5 \end{bmatrix}, \\ \zeta_7 &= \begin{bmatrix} 0 \\ 1 \end{bmatrix}, & \zeta_8 &= \begin{bmatrix} 0.5 \\ 1 \end{bmatrix}, & \zeta_9 &= \begin{bmatrix} 1 \\ 1 \end{bmatrix}. \end{aligned} \quad (6.47)$$

The only nodes that lie in the master triangle domain are ζ_i for $i \in \{1, 2, 3, 4, 5, 7\}$, so we re-number these nodes sequentially (retaining their original ordering) as the nodes of the master triangle

$$\begin{aligned} \xi_1 &= \begin{bmatrix} 0 \\ 0 \end{bmatrix}, & \xi_2 &= \begin{bmatrix} 0.5 \\ 0 \end{bmatrix}, & \xi_3 &= \begin{bmatrix} 1 \\ 0 \end{bmatrix}, \\ \xi_4 &= \begin{bmatrix} 0 \\ 0.5 \end{bmatrix}, & \xi_5 &= \begin{bmatrix} 0.5 \\ 0.5 \end{bmatrix}, & \xi_6 &= \begin{bmatrix} 0 \\ 1 \end{bmatrix}, \end{aligned} \quad (6.48)$$

which clearly agrees with Figure 6.7.

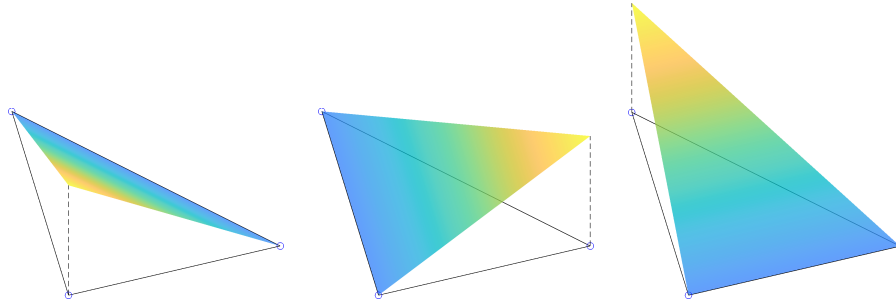


Figure 6.8: Nodal basis functions of \mathcal{P}^1 master triangle element.

Construction of element basis functions

Unfortunately the triangle does not possess the Cartesian product structure that we utilized to build up the nodal basis functions of the \mathcal{Q}^p quadrilateral from the nodal basis of the \mathcal{P}^p line elements. Instead, we introduce a systematic procedure, known as Vandermonde's method, to construct the nodal basis. Let $\{\psi_1, \dots, \psi_{N_{\text{nd}}^{\text{el}}}\}$ denote the nodal basis of the local function space \mathcal{Y}_{\square} of the master triangle Ω_{\square} . Since each $\psi_i \in \mathcal{P}^p(\Omega_{\square})$, it can be expanded in a monomial basis that includes all terms up to those with exponents that sum to p , i.e., $\{\xi_1^\alpha \xi_2^\beta \mid \alpha + \beta \leq p\}$, so we can write our $N_{\text{nd}}^{\text{el}}$ basis functions as

$$\psi_i(\boldsymbol{\xi}) = \sum_{k=1}^{N_{\text{nd}}^{\text{el}}} \hat{C}_{ik} \xi_1^{\alpha_k} \xi_2^{\beta_k} \quad (6.49)$$

where $\boldsymbol{\alpha}, \boldsymbol{\beta} \in \mathbb{N}_0^{N_{\text{nd}}^{\text{el}}}$ are vectors of natural numbers such that $\alpha_i + \beta_i \leq p$ for $i = 1, \dots, N_{\text{nd}}^{\text{el}}$ that are used to sweep over all $N_{\text{nd}}^{\text{el}}$ permissible exponents.

Denote the $N_{\text{nd}}^{\text{el}}$ nodes of the p th order simplex element as $\{\hat{\boldsymbol{\xi}}_i\}_{i=1}^{N_{\text{nd}}^{\text{el}}}$, where $\hat{\boldsymbol{\xi}}_i = (\hat{\xi}_{1i}, \hat{\xi}_{2i})^T$. The nodal property is

$$\psi_i(\hat{\boldsymbol{\xi}}_j) = \delta_{ij},$$

for $i, j = 1, \dots, N_{\text{nd}}^{\text{el}}$, which leads to

$$\sum_{k=1}^{N_{\text{nd}}^{\text{el}}} \hat{C}_{ik} \hat{\xi}_{1j}^{\alpha_k} \hat{\xi}_{2j}^{\beta_k} = \delta_{ij}$$

once the expression for $\psi_i(\boldsymbol{\xi})$ is used from (6.81). Let $\hat{V}_{ij} = \hat{\xi}_{1i}^{\alpha_j} \hat{\xi}_{2i}^{\beta_j}$ be the Vandermonde matrix corresponding to the d -dimensional, p th order simplex evaluated at $\{\hat{\boldsymbol{\xi}}_i\}_{i=1}^{N_{\text{nd}}^{\text{el}}}$, then the above constraints can be written in matrix form as $\hat{\mathbf{V}} \hat{\mathbf{C}}^T = \mathbf{I}_{N_{\text{nd}}^{\text{el}}}$, where $\hat{\mathbf{V}}$, $\hat{\mathbf{C}}$ are the matrices with indices \hat{V}_{ij} , \hat{C}_{ij} , respectively, and $\mathbf{I}_{N_{\text{nd}}^{\text{el}}}$ is the $N_{\text{nd}}^{\text{el}} \times N_{\text{nd}}^{\text{el}}$ identity matrix. Once we compute the coefficients, $\hat{\mathbf{C}} = \hat{\mathbf{V}}^{-T}$, we substitute this expression into (6.49) to give the final expression for

$$\psi_i(\boldsymbol{\xi}) = \sum_{k=1}^{N_{\text{nd}}^{\text{el}}} \hat{C}_{ik} \xi_1^{\alpha_k} \xi_2^{\beta_k} = \sum_{k=1}^{N_{\text{nd}}^{\text{el}}} \left(\hat{\mathbf{V}}^{-1} \right)_{ki} \xi_1^{\alpha_k} \xi_2^{\beta_k}. \quad (6.50)$$

The nodal basis functions for the \mathcal{P}^1 , \mathcal{P}^2 , and \mathcal{P}^3 master triangle are shown in Figures 6.8-6.10.

Example 6.11: Linear \mathcal{P}^1 triangle nodal basis

To provide a concrete example, we consider the \mathcal{P}^1 master triangle. The vectors used to sweep over the admissible monomials are

$$\boldsymbol{\alpha} = (0, 1, 0), \quad \boldsymbol{\beta} = (0, 0, 1), \quad (6.51)$$

which leads to the following monomial expansion of the basis functions

$$\psi_i(\boldsymbol{\xi}) = \hat{C}_{i1} \xi_1^{\alpha_1} \xi_2^{\beta_1} + \hat{C}_{i2} \xi_1^{\alpha_2} \xi_2^{\beta_2} + \hat{C}_{i3} \xi_1^{\alpha_3} \xi_2^{\beta_3} = \hat{C}_{i1} \xi_1^0 \xi_2^0 + \hat{C}_{i2} \xi_1^1 \xi_2^0 + \hat{C}_{i3} \xi_1^0 \xi_2^1 = \hat{C}_{i1} + \hat{C}_{i2} \xi_1 + \hat{C}_{i3} \xi_2, \quad (6.52)$$

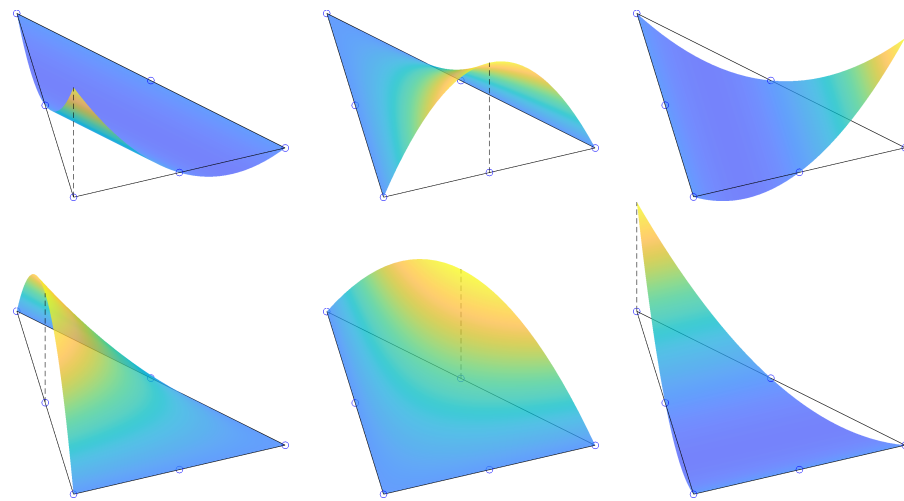


Figure 6.9: Nodal basis functions of \mathcal{P}^2 master triangle element.

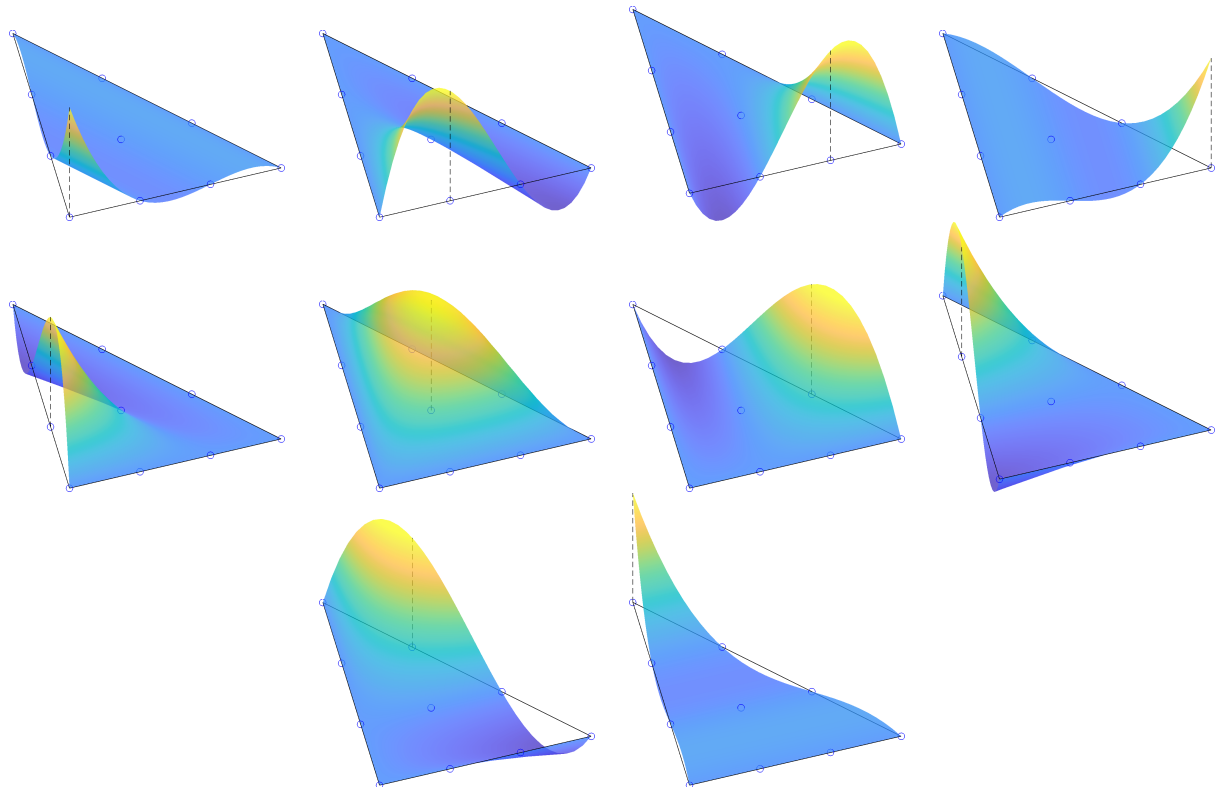


Figure 6.10: Nodal basis functions of \mathcal{P}^3 master triangle element.

which clearly lies in $\mathcal{P}^1(\Omega_\square)$. The corresponding Vandermonde matrix is

$$\mathbf{V} = \begin{bmatrix} 1 & 0 & 0 \\ 1 & 1 & 0 \\ 1 & 0 & 1 \end{bmatrix}, \quad (6.53)$$

which leads to the following matrix of coefficients

$$\hat{\mathbf{C}} = \begin{bmatrix} 1 & -1 & -1 \\ 0 & 1 & 0 \\ 0 & 0 & 1 \end{bmatrix}. \quad (6.54)$$

Combining these coefficients with the expansion in (6.49) we have

$$\begin{aligned} \psi_1(\xi) &= 1 - \xi_1 - \xi_2 \\ \psi_2(\xi) &= \xi_1 \\ \psi_3(\xi) &= \xi_2. \end{aligned} \quad (6.55)$$

It is a simple exercise to show these possess the nodal property with respect to the nodes of the \mathcal{P}^1 master triangle defined in Example 6.9. These nodal basis functions are shown in Figure 6.8.

Example 6.12: Quadratic \mathcal{P}^2 triangle nodal basis

Next we consider the \mathcal{P}^2 master triangle. The vectors used to sweep over the admissible monomials are

$$\boldsymbol{\alpha} = (0, 1, 0, 2, 1, 0), \quad \boldsymbol{\beta} = (0, 0, 1, 0, 1, 2), \quad (6.56)$$

which leads to the following monomial expansion of the basis functions

$$\begin{aligned} \psi_i(\xi) &= \hat{C}_{i1}\xi_1^{\alpha_1}\xi_2^{\beta_1} + \hat{C}_{i2}\xi_1^{\alpha_2}\xi_2^{\beta_2} + \hat{C}_{i3}\xi_1^{\alpha_3}\xi_2^{\beta_3} + \hat{C}_{i4}\xi_1^{\alpha_4}\xi_2^{\beta_4} + \hat{C}_{i5}\xi_1^{\alpha_5}\xi_2^{\beta_5} + \hat{C}_{i6}\xi_1^{\alpha_6}\xi_2^{\beta_6} \\ &= \hat{C}_{i1}\xi_1^0\xi_2^0 + \hat{C}_{i2}\xi_1^1\xi_2^0 + \hat{C}_{i3}\xi_1^0\xi_2^1 + \hat{C}_{i4}\xi_1^2\xi_2^0 + \hat{C}_{i5}\xi_1^1\xi_2^1 + \hat{C}_{i6}\xi_1^0\xi_2^2 \\ &= \hat{C}_{i1} + \hat{C}_{i2}\xi_1 + \hat{C}_{i3}\xi_2 + \hat{C}_{i4}\xi_1^2 + \hat{C}_{i5}\xi_1\xi_2 + \hat{C}_{i6}\xi_2^2, \end{aligned} \quad (6.57)$$

which clearly lies in $\mathcal{P}^1(\Omega_\square)$. The corresponding Vandermonde matrix is

$$\mathbf{V} = \begin{bmatrix} 1 & 0 & 0 & 0 & 0 & 0 \\ 1 & 0.5 & 0 & 0.25 & 0 & 0 \\ 1 & 1 & 0 & 1 & 0 & 0 \\ 1 & 0 & 0.5 & 0 & 0 & 0.25 \\ 1 & 0.5 & 0.5 & 0.25 & 0.25 & 0.25 \\ 1 & 0 & 1 & 0 & 0 & 1 \end{bmatrix}, \quad (6.58)$$

which leads to the following matrix of coefficients

$$\hat{\mathbf{C}} = \begin{bmatrix} 1 & -3 & -3 & 2 & 4 & 2 \\ 0 & 4 & 0 & -4 & -4 & 0 \\ 0 & -1 & 0 & 2 & 0 & 0 \\ 0 & 0 & 4 & 0 & -4 & -4 \\ 0 & 0 & 0 & 0 & 4 & 0 \\ 0 & 0 & -1 & 0 & 0 & 2 \end{bmatrix}. \quad (6.59)$$

Combining these coefficients with the expansion in (6.49) we have

$$\begin{aligned}\psi_1(\xi) &= 1 - 3(\xi_1 + \xi_2) + 2(\xi_1 + \xi_2)^2 \\ \psi_2(\xi) &= 4\xi_1(1 - \xi_1 - \xi_2) \\ \psi_3(\xi) &= \xi_1(-1 + 2\xi_1) \\ \psi_4(\xi) &= 4\xi_2(1 - \xi_1 - \xi_2) \\ \psi_5(\xi) &= 4\xi_1\xi_2 \\ \psi_6(\xi) &= \xi_2(-1 + 2\xi_2).\end{aligned}\tag{6.60}$$

It is a simple exercise to show these possess the nodal property with respect to the nodes of the \mathcal{P}^2 master triangle defined in Example 6.10. These nodal basis functions are shown in Figure 6.9.

6.2.5 d dimensions: \mathcal{Q}^p hypercube elements

In $d > 2$ dimensions, the number of possible geometries explodes, i.e., in $d = 3$ could have tetrahedra, cubes, prisms, pyramids. Unfortunately we do not have time to develop all these elements; instead, we focus on elements that generalize to any number of dimensions. We introduce a systematic procedure to define the element domain, local function space, nodes, and construct nodal basis functions. We begin with the hypercube element, the d -dimensional generalization of a quadrilateral.

Element domain

The reference domain of the master hypercube element is taken to be the bi-unit interval centered at zero

$$\Omega_{\square} := \{\boldsymbol{\xi} \in \mathbb{R}^d \mid -1 \leq \xi_i \leq 1, i = 1, \dots, d\}.\tag{6.61}$$

The master hypercube element is the Cartesian product of the master line element with itself d times. The boundary of the master element is $\partial\Omega_{\square} = \bigcup_{i=1}^{2d} \partial\Omega_{\square,i}$, where

$$\begin{aligned}\partial\Omega_{\square,i} &:= \{\boldsymbol{\xi} \in \mathbb{R}^d \mid \xi_i = -1, -1 \leq \xi_j \leq 1, j \neq i\} \\ \partial\Omega_{\square,d+i} &:= \{\boldsymbol{\xi} \in \mathbb{R}^d \mid \xi_i = 1, -1 \leq \xi_j \leq 1, j \neq i\}\end{aligned}\tag{6.62}$$

and the corresponding unit outward normals are

$$\mathbf{N}_{\square,i} := -\mathbf{e}_i, \quad \mathbf{N}_{\square,d+i} := \mathbf{e}_i.\tag{6.63}$$

for $i = 1, \dots, d$. Notice that this definition coincides with the master line element for $d = 1$ and quadrilateral element for $d = 2$. The complete geometry of the master hypercube element is illustrated in Figure 6.1 ($d = 1, 2$) and Figure 6.11 ($d = 3$).

Local function space

We take the local function space to be the space $\mathcal{Y}_{\square} := \mathcal{Q}^p(\Omega_{\square})$, i.e., polynomial functions where the largest exponent is p . The dimension of the local function space is $\dim \mathcal{Y}_{\square} = (p+1)^d$. Similar to the $d = 2$ case, functions that belong to $\mathcal{Q}^p(\Omega_{\square})$ are polynomials in $d-1$ dimension where the largest exponent is p when restricted to any face of Ω_{\square} . To see this we introduce a parametrization of boundary 1 (chosen arbitrarily), $\gamma : [-1, 1]^{d-1} \rightarrow \partial\Omega_{\square,1}$ defined as $\gamma(s_1, \dots, s_{d-1}) := (-1, s_1, \dots, s_{d-1}) \in \partial\Omega_{\square,1}$. Then, for any $v \in \mathcal{Q}^p(\Omega_{\square})$, we expand it in a monomial basis as

$$v(\boldsymbol{\xi}) = \sum_{\substack{\alpha \in \mathbb{N}^d \\ \max \alpha \leq p}} a_{\alpha} \xi_1^{\alpha_1} \cdots \xi_d^{\alpha_d},\tag{6.64}$$

where $a_{\alpha} \in \mathbb{R}$ for $\alpha \in \mathbb{N}^d$, $\max \alpha \leq p$. We restrict v to $\partial\Omega_{\square,1}$ by composing with the face parametrization γ

$$f(s) = v(\gamma(s)) = \sum_{\substack{\alpha \in \mathbb{N}^d \\ \max \alpha \leq p}} a_{\alpha} \gamma_1(s)^{\alpha_1} \cdots \gamma_d(s)^{\alpha_d} = \sum_{\alpha_2, \dots, \alpha_d \leq p} \left(\sum_{\alpha_1 \leq p} a_{\alpha} (-1)^{\alpha_1} \right) s_1^{\alpha_2} \cdots s_{d-1}^{\alpha_{d-1}},\tag{6.65}$$

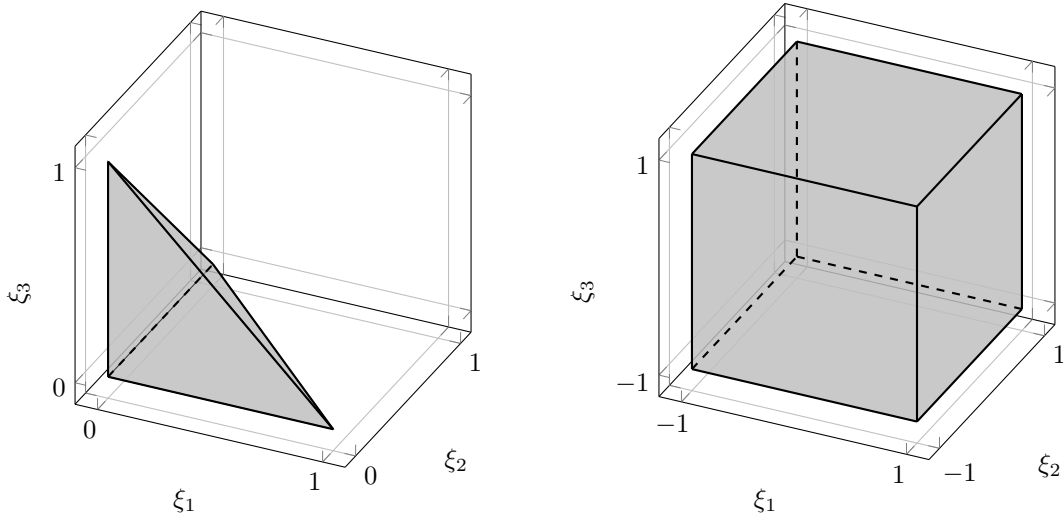


Figure 6.11: Master element geometry for $d = 3$ simplex (tetrahedra) (left) and $d = 3$ hypercube (hexahedron) (right).

which is clearly a polynomial of degree at most p in $d - 1$ dimensions, i.e., $f \in \mathcal{Q}^p([-1, 1]^{d-1})$.

Distribution and numbering of nodes

Before we construct a nodal basis of \mathcal{Y}_\square , we must distribute $N_{\text{nd}}^{\text{el}} = (p + 1)^d$ nodes throughout the element domain Ω_\square . To ensure all basis functions are linearly independent, the nodes must not overlap (or be too close to prevent ill-conditioning). We also require that $(p + 1)^{d-1}$ nodes lie on each of the $2d$ faces of the hypercube Ω_\square . Again, this is because any element of $\mathcal{Q}^p(\Omega_\square)$ restricted to a face will be uniquely determined by its value at $(p + 1)^{d-1}$ nodes, which gives a straightforward way to enforce global continuity.

Mimicing the construction of the nodes for the \mathcal{Q}^p quadrilateral, we define the nodes of the \mathcal{Q}^p master hypercube as the Cartesian product of the nodes of the \mathcal{Q}^p master line element with itself d times, numbered first in the ξ_1 -direction, then ξ_2 , etc (Figure 6.13). To make this precise, let $\{\hat{s}_1, \dots, \hat{s}_{p+1}\} \subset [-1, 1]$ be the nodes of the master line element and introduce

$$\mathcal{I}_i : \{1, \dots, (p + 1)^d\} \rightarrow \{1, \dots, p + 1\}, \quad i = 1, \dots, d, \quad (6.66)$$

where \mathcal{I}_i maps the hypercube node number to the node number along the ξ_i -axis, i.e., the i th hypercube node is the $\mathcal{I}_j(i)$ th node in the ξ_j -direction (in the $d = 2$ case, \mathcal{I}_1 and \mathcal{I}_2 are precisely \mathcal{I} and \mathcal{J} , respectively, in (6.28)). For our node numbering that varies first in the ξ_1 -direction, then ξ_2 , etc., these mappings are

$$\mathcal{I}_i(k) := 1 + \left\lfloor \frac{k - 1 - \sum_{j=i+1}^d (\mathcal{I}_j(k) - 1)(p + 1)^{j-1}}{(p + 1)^{i-1}} \right\rfloor, \quad (6.67)$$

$i = 2, \dots, d$. With this notation, the k th hypercube node is defined in terms of the line element nodes as

$$\hat{\boldsymbol{\xi}}_k = \begin{bmatrix} \hat{\xi}_{1k} \\ \vdots \\ \hat{\xi}_{dk} \end{bmatrix} = \begin{bmatrix} \hat{s}_{\mathcal{I}_1(k)} \\ \vdots \\ \hat{s}_{\mathcal{I}_d(k)} \end{bmatrix}. \quad (6.68)$$

Example 6.13: Nodes of trilinear \mathcal{Q}^1 hexahedral

To define the nodes of \mathcal{Q}^1 master hexahedral element, recall the nodes of the \mathcal{Q}^1 master line element $\hat{s}_1 = -1$, $\hat{s}_2 = 1$ and, in the special case of $p = 1$, the hypercube-to-line mappings (6.66)-(6.67) are

$$\mathcal{I}_1 = \{1, 2, 1, 2, 1, 2, 1, 2\}, \quad \mathcal{I}_2 = \{1, 1, 2, 2, 1, 1, 2, 2\}, \quad \mathcal{I}_3 = \{1, 1, 1, 1, 2, 2, 2, 2\}. \quad (6.69)$$

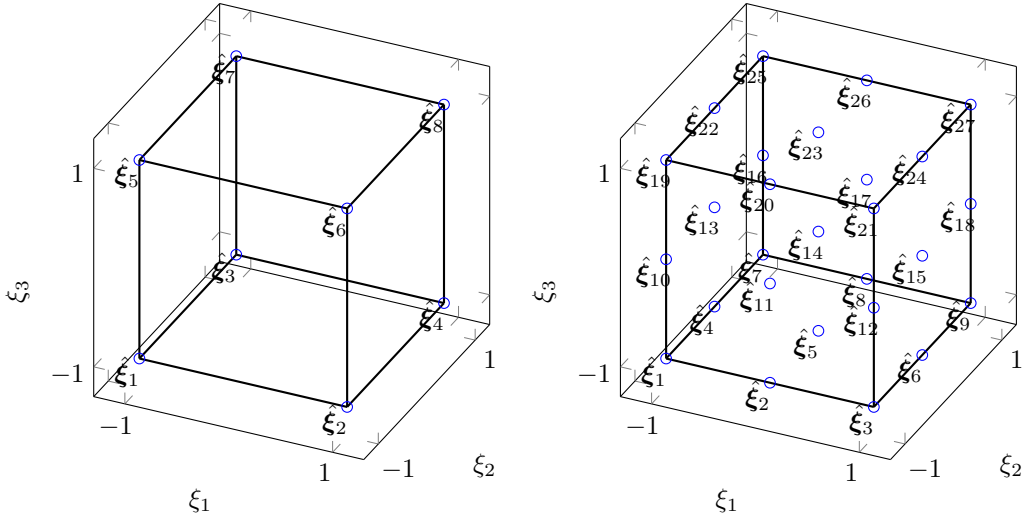


Figure 6.12: Master \mathcal{Q}^p hexahedra element including nodal positions and numbering for $p = 1, 2, 3$ (left-to-right).

From this and (6.68), the nodes of the master \mathcal{Q}^1 hexahedral element are

$$\begin{aligned}\hat{\xi}_1 &= \begin{bmatrix} \hat{\xi}_{11} \\ \hat{\xi}_{21} \\ \hat{\xi}_{31} \end{bmatrix} = \begin{bmatrix} \hat{s}_{\mathcal{I}_1(1)} \\ \hat{s}_{\mathcal{I}_2(1)} \\ \hat{s}_{\mathcal{I}_3(1)} \end{bmatrix} = \begin{bmatrix} \hat{s}_1 \\ \hat{s}_1 \\ \hat{s}_1 \end{bmatrix} = \begin{bmatrix} -1 \\ -1 \\ -1 \end{bmatrix}, & \hat{\xi}_2 &= \begin{bmatrix} \hat{\xi}_{12} \\ \hat{\xi}_{22} \\ \hat{\xi}_{32} \end{bmatrix} = \begin{bmatrix} \hat{s}_{\mathcal{I}_1(2)} \\ \hat{s}_{\mathcal{I}_2(2)} \\ \hat{s}_{\mathcal{I}_3(2)} \end{bmatrix} = \begin{bmatrix} \hat{s}_2 \\ \hat{s}_1 \\ \hat{s}_1 \end{bmatrix} = \begin{bmatrix} 1 \\ -1 \\ -1 \end{bmatrix} \\ \hat{\xi}_3 &= \begin{bmatrix} \hat{\xi}_{13} \\ \hat{\xi}_{23} \\ \hat{\xi}_{33} \end{bmatrix} = \begin{bmatrix} \hat{s}_{\mathcal{I}_1(3)} \\ \hat{s}_{\mathcal{I}_2(3)} \\ \hat{s}_{\mathcal{I}_3(3)} \end{bmatrix} = \begin{bmatrix} \hat{s}_1 \\ \hat{s}_2 \\ \hat{s}_1 \end{bmatrix} = \begin{bmatrix} -1 \\ 1 \\ -1 \end{bmatrix}, & \hat{\xi}_4 &= \begin{bmatrix} \hat{\xi}_{14} \\ \hat{\xi}_{24} \\ \hat{\xi}_{34} \end{bmatrix} = \begin{bmatrix} \hat{s}_{\mathcal{I}_1(4)} \\ \hat{s}_{\mathcal{I}_2(4)} \\ \hat{s}_{\mathcal{I}_3(4)} \end{bmatrix} = \begin{bmatrix} \hat{s}_2 \\ \hat{s}_2 \\ \hat{s}_1 \end{bmatrix} = \begin{bmatrix} 1 \\ 1 \\ -1 \end{bmatrix}, \\ \hat{\xi}_5 &= \begin{bmatrix} \hat{\xi}_{15} \\ \hat{\xi}_{25} \\ \hat{\xi}_{35} \end{bmatrix} = \begin{bmatrix} \hat{s}_{\mathcal{I}_1(5)} \\ \hat{s}_{\mathcal{I}_2(5)} \\ \hat{s}_{\mathcal{I}_3(5)} \end{bmatrix} = \begin{bmatrix} \hat{s}_1 \\ \hat{s}_1 \\ \hat{s}_2 \end{bmatrix} = \begin{bmatrix} -1 \\ -1 \\ 1 \end{bmatrix}, & \hat{\xi}_6 &= \begin{bmatrix} \hat{\xi}_{16} \\ \hat{\xi}_{26} \\ \hat{\xi}_{36} \end{bmatrix} = \begin{bmatrix} \hat{s}_{\mathcal{I}_1(6)} \\ \hat{s}_{\mathcal{I}_2(6)} \\ \hat{s}_{\mathcal{I}_3(6)} \end{bmatrix} = \begin{bmatrix} \hat{s}_2 \\ \hat{s}_1 \\ \hat{s}_2 \end{bmatrix} = \begin{bmatrix} 1 \\ -1 \\ 1 \end{bmatrix} \\ \hat{\xi}_7 &= \begin{bmatrix} \hat{\xi}_{17} \\ \hat{\xi}_{27} \\ \hat{\xi}_{37} \end{bmatrix} = \begin{bmatrix} \hat{s}_{\mathcal{I}_1(7)} \\ \hat{s}_{\mathcal{I}_2(7)} \\ \hat{s}_{\mathcal{I}_3(7)} \end{bmatrix} = \begin{bmatrix} \hat{s}_1 \\ \hat{s}_2 \\ \hat{s}_2 \end{bmatrix} = \begin{bmatrix} -1 \\ 1 \\ 1 \end{bmatrix}, & \hat{\xi}_8 &= \begin{bmatrix} \hat{\xi}_{18} \\ \hat{\xi}_{28} \\ \hat{\xi}_{38} \end{bmatrix} = \begin{bmatrix} \hat{s}_{\mathcal{I}_1(8)} \\ \hat{s}_{\mathcal{I}_2(8)} \\ \hat{s}_{\mathcal{I}_3(8)} \end{bmatrix} = \begin{bmatrix} \hat{s}_2 \\ \hat{s}_2 \\ \hat{s}_2 \end{bmatrix} = \begin{bmatrix} 1 \\ 1 \\ 1 \end{bmatrix},\end{aligned}\tag{6.70}$$

which clearly agrees with Figure 6.12.

Construction of element basis functions

Finally we construct the nodal basis of $\mathcal{Y}_\square = \mathcal{Q}^p(\Omega_\square)$ using the tensor product structure of the master hypercube element. Let $\{\hat{s}_1, \dots, \hat{s}_{p+1}\}$ be the nodes of the \mathcal{P}^p master line element, $\mathcal{I}_1, \dots, \mathcal{I}_d$ be the hypercube-to-line nodal mapping from the previous section, and $\{\tilde{\psi}_1, \dots, \tilde{\psi}_d\}$ be the corresponding nodal basis, i.e., $\tilde{\psi}_i(\hat{s}_j) = \delta_{ij}$ for $i, j = 1, \dots, p + 1$. Then we define the nodal basis functions $\{\psi_1, \dots, \psi_{N_{\text{nd}}^{\text{el}}}\}$ of the \mathcal{Q}^p hypercube element to be

$$\psi_i(\boldsymbol{\xi}) := \prod_{j=1}^d \tilde{\psi}_{\mathcal{I}_j(i)}(\xi_j).\tag{6.71}$$

Using the expression in (6.22) for the one-dimensional nodal basis, this becomes

$$\psi_i(\boldsymbol{\xi}) = \prod_{k=1}^d \left(\prod_{\substack{j=1 \\ j \neq \mathcal{I}_k(i)}}^{p+1} \frac{\xi_k - \hat{s}_j}{\hat{s}_{\mathcal{I}_k(i)} - \hat{s}_j} \right).\tag{6.72}$$

To verify this choice of basis has the nodal property, we evaluate ψ_i at node $\hat{\xi}_j$

$$\psi_i(\hat{\xi}_j) = \prod_{k=1}^d \tilde{\psi}_{\mathcal{I}_k(i)}(\hat{\xi}_{kj}) = \prod_{k=1}^d \tilde{\psi}_{\mathcal{I}_k(i)}(\hat{s}_{\mathcal{I}_k(j)}) = \prod_{k=1}^d \delta_{\mathcal{I}_k(i)\mathcal{I}_k(j)} = \delta_{ij}, \quad (6.73)$$

where the last equality follows because the product $\prod_{k=1}^d \delta_{\mathcal{I}_k(i)\mathcal{I}_k(j)}$ only survives if $\mathcal{I}_k(i) = \mathcal{I}_k(j)$ for $i = 1, \dots, d$, which can only happen if $i = j$.

Example 6.14: Trilinear \mathcal{Q}^1 hexahedral nodal basis

Recall the hypercube-to-line mappings for the trilinear hexahedral element (6.66)-(6.67). Then the nodal basis functions of the \mathcal{Q}^1 hexahedral element using the tensor product formula in (6.73) are

$$\begin{aligned} \psi_1(\xi) &= \tilde{\psi}_1(\xi_1)\tilde{\psi}_1(\xi_2)\tilde{\psi}_1(\xi_3) &= \frac{\xi_1 - \hat{s}_2}{\hat{s}_1 - \hat{s}_2} \frac{\xi_2 - \hat{s}_2}{\hat{s}_1 - \hat{s}_2} \frac{\xi_3 - \hat{s}_2}{\hat{s}_1 - \hat{s}_2} &= \frac{1}{8}(1 - \xi_1)(1 - \xi_2)(1 - \xi_3) \\ \psi_2(\xi) &= \tilde{\psi}_2(\xi_1)\tilde{\psi}_1(\xi_2)\tilde{\psi}_1(\xi_3) &= \frac{\xi_1 - \hat{s}_1}{\hat{s}_2 - \hat{s}_1} \frac{\xi_2 - \hat{s}_2}{\hat{s}_1 - \hat{s}_2} \frac{\xi_3 - \hat{s}_2}{\hat{s}_1 - \hat{s}_2} &= \frac{1}{8}(1 + \xi_1)(1 - \xi_2)(1 - \xi_3) \\ \psi_3(\xi) &= \tilde{\psi}_1(\xi_1)\tilde{\psi}_2(\xi_2)\tilde{\psi}_1(\xi_3) &= \frac{\xi_1 - \hat{s}_2}{\hat{s}_1 - \hat{s}_2} \frac{\xi_2 - \hat{s}_1}{\hat{s}_2 - \hat{s}_1} \frac{\xi_3 - \hat{s}_2}{\hat{s}_1 - \hat{s}_2} &= \frac{1}{8}(1 - \xi_1)(1 + \xi_2)(1 - \xi_3) \\ \psi_4(\xi) &= \tilde{\psi}_2(\xi_1)\tilde{\psi}_2(\xi_2)\tilde{\psi}_1(\xi_3) &= \frac{\xi_1 - \hat{s}_1}{\hat{s}_2 - \hat{s}_1} \frac{\xi_2 - \hat{s}_1}{\hat{s}_2 - \hat{s}_1} \frac{\xi_3 - \hat{s}_2}{\hat{s}_1 - \hat{s}_2} &= \frac{1}{8}(1 + \xi_1)(1 + \xi_2)(1 - \xi_3) \\ \psi_5(\xi) &= \tilde{\psi}_1(\xi_1)\tilde{\psi}_1(\xi_2)\tilde{\psi}_2(\xi_3) &= \frac{\xi_1 - \hat{s}_2}{\hat{s}_1 - \hat{s}_2} \frac{\xi_2 - \hat{s}_2}{\hat{s}_1 - \hat{s}_2} \frac{\xi_3 - \hat{s}_1}{\hat{s}_2 - \hat{s}_1} &= \frac{1}{8}(1 - \xi_1)(1 - \xi_2)(1 + \xi_3) \\ \psi_6(\xi) &= \tilde{\psi}_2(\xi_1)\tilde{\psi}_1(\xi_2)\tilde{\psi}_2(\xi_3) &= \frac{\xi_1 - \hat{s}_1}{\hat{s}_2 - \hat{s}_1} \frac{\xi_2 - \hat{s}_2}{\hat{s}_1 - \hat{s}_2} \frac{\xi_3 - \hat{s}_1}{\hat{s}_2 - \hat{s}_1} &= \frac{1}{8}(1 + \xi_1)(1 - \xi_2)(1 + \xi_3) \\ \psi_7(\xi) &= \tilde{\psi}_1(\xi_1)\tilde{\psi}_2(\xi_2)\tilde{\psi}_2(\xi_3) &= \frac{\xi_1 - \hat{s}_2}{\hat{s}_1 - \hat{s}_2} \frac{\xi_2 - \hat{s}_1}{\hat{s}_2 - \hat{s}_1} \frac{\xi_3 - \hat{s}_1}{\hat{s}_2 - \hat{s}_1} &= \frac{1}{8}(1 - \xi_1)(1 + \xi_2)(1 + \xi_3) \\ \psi_8(\xi) &= \tilde{\psi}_2(\xi_1)\tilde{\psi}_2(\xi_2)\tilde{\psi}_2(\xi_3) &= \frac{\xi_1 - \hat{s}_1}{\hat{s}_2 - \hat{s}_1} \frac{\xi_2 - \hat{s}_1}{\hat{s}_2 - \hat{s}_1} \frac{\xi_3 - \hat{s}_1}{\hat{s}_2 - \hat{s}_1} &= \frac{1}{8}(1 + \xi_1)(1 + \xi_2)(1 + \xi_3). \end{aligned} \quad (6.74)$$

where the last equality used that the nodes of the \mathcal{P}^1 master element are $\hat{s}_1 = -1$ and $\hat{s}_2 = 1$.

6.2.6 d dimensions: \mathcal{P}^p simplex elements

Finally, we turn to the most versatile class of elements, simplices, the d -dimensional generalization of a triangle.

Element domain

The reference domain of the master simplex element is taken to be

$$\Omega_\square := \left\{ \xi \in \mathbb{R}^d \mid \sum_{i=1}^d \xi_i \leq 1, \xi_i \geq 0, i = 1, \dots, d \right\}. \quad (6.75)$$

The boundary of the master element is $\partial\Omega_\square = \bigcup_{i=1}^{d+1} \partial\Omega_{\square,i}$, where

$$\begin{aligned} \partial\Omega_{\square,i} &:= \left\{ \xi \in \mathbb{R}^d \mid \xi_i = 0, 0 \leq \xi_j \leq 1, j \neq i \right\} \\ \partial\Omega_{\square,d+1} &:= \left\{ \xi \in \mathbb{R}^d \mid \sum_{j=1}^d \xi_j = 1, 0 \leq \xi_j \leq 1, j = 1, \dots, d \right\}. \end{aligned} \quad (6.76)$$

and the corresponding unit outward normals are

$$\mathbf{N}_{\square,i} := -\mathbf{e}^{(i)}, \quad \mathbf{N}_{\square,d+1} := \sum_{i=1}^d \frac{1}{\sqrt{d}} \mathbf{e}^{(i)} \quad (6.77)$$

for $i = 1, \dots, d$. Notice that even though a $d = 1$ dimensional simplex is a line ($\Omega_\square = [0, 1]$), it does not coincide with the master line element introduced in Section 6.2.2. The complete geometry of the master simplex element is illustrated in Figure 6.1 ($d = 2$ triangle) and Figure 6.11 ($d = 3$ tetrahedra).

Local function space

We take the local function space to be $\mathcal{Y}_\square := \mathcal{P}^p(\Omega_\square)$. The dimension of the local function space is

$$\dim \mathcal{Y}_\square = \binom{p+d}{d}. \quad (6.78)$$

Similar to the $d = 2$ case, functions that belong to $\mathcal{P}^p(\Omega_\square)$ are polynomials of degree p in $d - 1$ dimensions when restricted to any plane.

Distribution and numbering of nodes

Before we construct a nodal basis of \mathcal{Y}_\square , we must distribute

$$N_{\text{nd}}^{\text{el}} = \binom{p+d}{d} \quad (6.79)$$

nodes throughout the element domain Ω_\square . To ensure all basis functions are linearly independent, the nodes must not overlap (or be too close to prevent ill-conditioning). We also require that $\binom{p+d-1}{d-1}$ nodes lie on each of the faces of the simplex Ω_\square . Again, this is because any element of $\mathcal{P}^p(\Omega_\square)$ restricted to a face will be uniquely determined by its value at $\binom{p+d-1}{d-1}$ nodes, which gives a straightforward way to enforce global continuity. A systematic procedure to populate the master simplex with nodes is the straightforward generalization of the procedure in Section 6.2.4 to populate the master triangle with nodes:

- (1) uniformly distribute $p + 1$ nodes $\{\hat{s}_1, \dots, \hat{s}_{p+1}\}$ throughout the unit interval $[0, 1]$,
- (2) form their tensor product following the procedure in Section 6.2.5 to yield $(p+1)^d$ nodes $\{\zeta_1, \dots, \zeta_{(p+1)^d}\}$ nodes in the unit hypercube $[0, 1]^d$, and
- (3) retain only the nodes that lie in the master simplex domain Ω_\square and re-number sequentially (preserving order) to obtain the nodes $\{\xi_1, \dots, \xi_{N_{\text{nd}}^{\text{el}}}\}$.

This procedure will generate nodes in the master simplex that are uniformly spaced with $\binom{p+d-1}{d-1}$ on each boundary (Figure 6.13 for $p = 1, 2, 3$).

Example 6.15: Nodes of linear \mathcal{P}^1 tetrahedra

From (6.78) with $p = 1$, there are $\binom{p+d}{d} = \binom{4}{1} = 4$ nodes associated with the \mathcal{P}^1 master tetrahedra.

The only locations we can place them to ensure each face has $\binom{p+d-1}{d-1} = \binom{3}{2} = 3$ nodes is at the tetrahedra vertices

$$\hat{\xi}_1 = \begin{bmatrix} 0 \\ 0 \\ 0 \end{bmatrix}, \quad \hat{\xi}_2 = \begin{bmatrix} 1 \\ 0 \\ 0 \end{bmatrix}, \quad \hat{\xi}_3 = \begin{bmatrix} 0 \\ 1 \\ 0 \end{bmatrix}, \quad \hat{\xi}_4 = \begin{bmatrix} 0 \\ 0 \\ 1 \end{bmatrix}, \quad (6.80)$$

which clearly agrees with Figure 6.13.

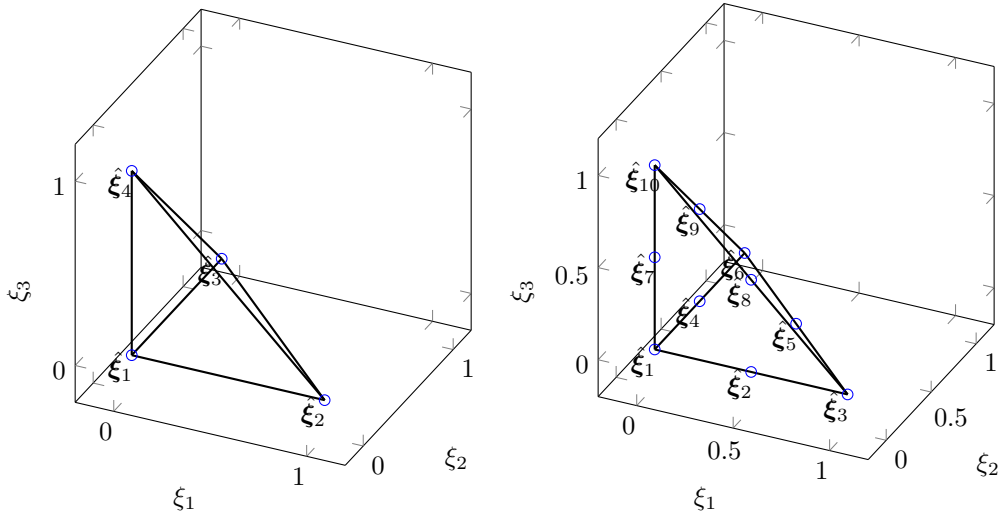


Figure 6.13: Master \mathcal{P}^p tetrahedra element including nodal positions and numbering for $p = 1, 2, 3$ (left-to-right).

Construction of element basis functions

Finally we generalize Vandermonde's method introduced in Section 6.2.4 to define a nodal basis of $\mathcal{P}^p(\Omega_\square)$ ($\Omega_\square \subset \mathbb{R}^d$), which we denote $\{\psi_1, \dots, \psi_{N_{\text{nd}}^{\text{el}}}\}$. Since each $\psi_i \in \mathcal{P}^p(\Omega_\square)$, it can be expanded in a monomial basis that includes all terms up to those with exponents that sum to p , i.e., $\{\xi_1^{\alpha_1} \cdots \xi_d^{\alpha_d} \mid \sum_{i=1}^d \alpha_i \leq p\}$, so we can write our $N_{\text{nd}}^{\text{el}}$ basis functions as

$$\psi_i(\boldsymbol{\xi}) = \sum_{k=1}^{N_{\text{nd}}^{\text{el}}} \hat{C}_{ik} \prod_{j=1}^d \xi_j^{\Upsilon_{jk}} \quad (6.81)$$

where $\Upsilon \in \mathbb{N}_0^{d \times N_{\text{nd}}^{\text{el}}}$ is a matrix of natural numbers such that $\sum_{i=1}^d \Upsilon_{ij} \leq p$ for each $j = 1, \dots, N_{\text{nd}}^{\text{el}}$ that is used to sweep over all $N_{\text{nd}}^{\text{el}}$ permissible exponents. For convenience, we introduce the function $\omega_i(\boldsymbol{\xi})$, $i = 1, \dots, N_{\text{nd}}^{\text{el}}$

$$\omega_i(\boldsymbol{\xi}) = \prod_{s=1}^d \xi_s^{\Upsilon_{si}},$$

so the basis functions can conveniently be expressed as $\psi_i(\boldsymbol{\xi}) = \sum_{k=1}^{N_{\text{nd}}^{\text{el}}} \hat{C}_{ik} \omega_k(\boldsymbol{\xi})$.

Example 6.16: Monomial expansion in $\mathcal{P}^1(\mathbb{R}^2)$

To demonstrate the general monomial expansion in (6.81) agrees with known special cases we consider $p = 1$, $d = 2$ (\mathcal{P}^1 triangle). In this case, we take

$$\Upsilon = \begin{bmatrix} 0 & 1 & 0 \\ 0 & 0 & 1 \end{bmatrix}, \quad (6.82)$$

which leads to the following monomial expansion of the basis functions

$$\psi_i(\boldsymbol{\xi}) = \hat{C}_{i1} \xi_1^{\Upsilon_{11}} \xi_2^{\Upsilon_{21}} + \hat{C}_{i2} \xi_1^{\Upsilon_{12}} \xi_2^{\Upsilon_{22}} + \hat{C}_{i3} \xi_1^{\Upsilon_{13}} \xi_2^{\Upsilon_{23}} = \hat{C}_{i1} \xi_1^0 \xi_2^0 + \hat{C}_{i2} \xi_1^1 \xi_2^0 + \hat{C}_{i3} \xi_1^0 \xi_2^1 = \hat{C}_{i1} + \hat{C}_{i2} \xi_1 + \hat{C}_{i3} \xi_2, \quad (6.83)$$

where the monomial terms are

$$\omega_1(\boldsymbol{\xi}) = 1, \quad \omega_2(\boldsymbol{\xi}) = \xi_1, \quad \omega_3(\boldsymbol{\xi}) = \xi_2. \quad (6.84)$$

Example 6.17: Monomial expansion in $\mathcal{P}^2(\mathbb{R}^2)$

Next we consider the special case $p = 2$, $d = 2$ (\mathcal{P}^2 triangle). In this case, we take

$$\Upsilon = \begin{bmatrix} 0 & 1 & 0 & 2 & 1 & 0 \\ 0 & 0 & 1 & 0 & 1 & 2 \end{bmatrix}, \quad (6.85)$$

which leads to the following monomial expansion of the basis functions

$$\begin{aligned} \psi_i(\xi) &= \hat{C}_{i1}\xi_1^{\Upsilon_{11}}\xi_2^{\Upsilon_{21}} + \hat{C}_{i2}\xi_1^{\Upsilon_{12}}\xi_2^{\Upsilon_{22}} + \hat{C}_{i3}\xi_1^{\Upsilon_{13}}\xi_2^{\Upsilon_{23}} + \hat{C}_{i4}\xi_1^{\Upsilon_{14}}\xi_2^{\Upsilon_{24}} + \hat{C}_{i5}\xi_1^{\Upsilon_{15}}\xi_2^{\Upsilon_{25}} + \hat{C}_{i6}\xi_1^{\Upsilon_{16}}\xi_2^{\Upsilon_{26}} \\ &= \hat{C}_{i1}\xi_1^0\xi_2^0 + \hat{C}_{i2}\xi_1^1\xi_2^0 + \hat{C}_{i3}\xi_1^0\xi_2^1 + \hat{C}_{i4}\xi_1^2\xi_2^0 + \hat{C}_{i5}\xi_1^1\xi_2^1 + \hat{C}_{i6}\xi_1^0\xi_2^2 \\ &= \hat{C}_{i1} + \hat{C}_{i2}\xi_1 + \hat{C}_{i3}\xi_2 + \hat{C}_{i4}\xi_1^2 + \hat{C}_{i5}\xi_1\xi_2 + \hat{C}_{i6}\xi_2^2, \end{aligned} \quad (6.86)$$

where the monomial terms are

$$\omega_1(\xi) = 1, \quad \omega_2(\xi) = \xi_1, \quad \omega_3(\xi) = \xi_2, \quad \omega_4(\xi) = \xi_1^2, \quad \omega_5(\xi) = \xi_1\xi_2, \quad \omega_6(\xi) = \xi_2^2. \quad (6.87)$$

Example 6.18: Monomial expansion in $\mathcal{P}^1(\mathbb{R}^3)$

Finally we consider the special case $p = 1$, $d = 3$ (\mathcal{P}^1 tetrahedra). In this case, we take

$$\Upsilon = \begin{bmatrix} 0 & 1 & 0 & 0 \\ 0 & 0 & 1 & 0 \\ 0 & 0 & 0 & 1 \end{bmatrix}, \quad (6.88)$$

which leads to the following monomial expansion of the basis functions

$$\begin{aligned} \psi_i(\xi) &= \hat{C}_{i1}\xi_1^{\Upsilon_{11}}\xi_2^{\Upsilon_{21}}\xi_3^{\Upsilon_{31}} + \hat{C}_{i2}\xi_1^{\Upsilon_{12}}\xi_2^{\Upsilon_{22}}\xi_3^{\Upsilon_{32}} + \hat{C}_{i3}\xi_1^{\Upsilon_{13}}\xi_2^{\Upsilon_{23}}\xi_3^{\Upsilon_{33}} + \hat{C}_{i4}\xi_1^{\Upsilon_{14}}\xi_2^{\Upsilon_{24}}\xi_3^{\Upsilon_{34}} \\ &= \hat{C}_{i1}\xi_1^0\xi_2^0\xi_3^0 + \hat{C}_{i2}\xi_1^1\xi_2^0\xi_3^0 + \hat{C}_{i3}\xi_1^0\xi_2^1\xi_3^0 + \hat{C}_{i4}\xi_1^0\xi_2^0\xi_3^1 \\ &= \hat{C}_{i1} + \hat{C}_{i2}\xi_1 + \hat{C}_{i3}\xi_2 + \hat{C}_{i4}\xi_3, \end{aligned} \quad (6.89)$$

where the monomial terms are

$$\omega_1(\xi) = 1, \quad \omega_2(\xi) = \xi_1, \quad \omega_3(\xi) = \xi_2, \quad \omega_4(\xi) = \xi_3. \quad (6.90)$$

Denote the N_{nd}^{el} nodes of the p th order simplex element as $\{\hat{\xi}_i\}_{i=1}^{N_{nd}^{el}}$, where $\hat{\xi}_i = (\hat{\xi}_{1i}, \dots, \hat{\xi}_{di})^T$. The nodal property is

$$\psi_i(\hat{\xi}_j) = \delta_{ij},$$

for $i, j = 1, \dots, N_{nd}^{el}$, which leads to

$$\sum_{k=1}^{N_{nd}^{el}} \hat{C}_{ik} \omega_k(\hat{\xi}_j) = \delta_{ij}$$

once the expression for $\psi_i(\xi)$ is used from (6.81). Let $\hat{V}_{ij} = \omega_j(\hat{\xi}_i) = \prod_{s=1}^d \hat{\xi}_{si}^{\Upsilon_{sj}}$ be the Vandermonde matrix corresponding to the d -dimensional, p th order simplex evaluated at $\{\hat{\xi}_i\}_{i=1}^{N_{nd}^{el}}$, then the above constraints can be written in matrix form as $\hat{V} \hat{C}^T = \mathbf{I}_{N_{nd}^{el}}$, where \hat{V} , \hat{C} are the matrices with indices \hat{V}_{ij} , \hat{C}_{ij} , respectively, and $\mathbf{I}_{N_{nd}^{el}}$ is the $N_{nd}^{el} \times N_{nd}^{el}$ identity matrix. Once we compute the coefficients, $\hat{C} = \hat{V}^{-T}$, we substitute this expression into (6.81) to give the final expression for

$$\psi_i(\xi) = \sum_{k=1}^{N_{nd}^{el}} \hat{C}_{ik} \omega_k(\xi) = \sum_{k=1}^{N_{nd}^{el}} (\hat{V}^{-1})_{ki} \omega_k(\xi). \quad (6.91)$$

Example 6.19: Linear \mathcal{P}^1 tetrahedra nodal basis

To provide a concrete example, we consider the \mathcal{P}^1 master tetrahedron ($d = 3$). In Example 6.18, we provided a concrete expression for the monomial terms ω_i , $i = 1, \dots, 4$, which we use to construct the Vandermonde matrix as

$$\mathbf{V} = \begin{bmatrix} 1 & 0 & 0 & 0 \\ 1 & 1 & 0 & 0 \\ 1 & 0 & 1 & 0 \\ 1 & 0 & 0 & 1 \end{bmatrix}, \quad (6.92)$$

which leads to the following matrix of coefficients

$$\hat{\mathbf{C}} = \begin{bmatrix} 1 & -1 & -1 & -1 \\ 0 & 1 & 0 & 0 \\ 0 & 0 & 1 & 0 \\ 0 & 0 & 0 & 1 \end{bmatrix}. \quad (6.93)$$

Combining these coefficients with the expansion in (6.81) we have

$$\psi_1(\xi) = 1 - \xi_1 - \xi_2 - \xi_3, \quad \psi_2(\xi) = \xi_1, \quad \psi_3(\xi) = \xi_2, \quad \psi_4(\xi) = \xi_3. \quad (6.94)$$

It is a simple exercise to show these possess the nodal property with respect to the nodes of the \mathcal{P}^1 master tetrahedra defined in Example 6.15.

Remark 6.1. We have used Vandermonde's procedure to derive the analytical form of the nodal basis functions; however, it is much more useful (and efficient) as a numerical procedure to (numerically) evaluate the nodal basis functions at points throughout the element domain Ω_\square as we will see.

Remark 6.2. The Vandermonde matrix becomes ill-conditioned for high polynomial degrees p since the monomial basis becomes linearly dependent (numerically). To improve the conditioning of the final system, we could expand the basis functions ψ_i in an orthogonal basis of \mathcal{P}^p (replacing step (6.81)) and repeat the procedure.

6.3. Physical finite element via domain mapping

Now that we have introduced several master elements, we must address the question of how to use these to define the actual *physical* finite elements that will define our discretization. The approach is to introduce a *bijection* from a master element domain to the physical element domain and use properties of the mapping and master element to completely define the physical (mapped) element.

6.3.1 Mapped finite element

Now that we have introduced several master elements, we must address We begin with a definition of a physical (mapped) finite element.

Definition 6.3.1 (Mapped finite element). Let $(\Omega_\square, \mathcal{Y}_\square, \mathcal{D}_\square)$ ($\dim \mathcal{Y}_\square = M$) be a master nodal finite element with nodes $\mathcal{N}_\square = \{\hat{\xi}_1, \dots, \hat{\xi}_M\}$ and let $\mathcal{G} : \Omega_\square \rightarrow K$ map (bijection) the master element domain $\Omega_\square \subset \mathbb{R}^d$ to the physical element domain $K \subset \mathbb{R}^d$. Then, $(K, \mathcal{Y}, \mathcal{D})$ is the mapped (physical) finite element, where

- (1) the element domain $K \subset \mathbb{R}^d$ is defined by mapping the master element domain

$$K := \mathcal{G}(\Omega_\square), \quad (6.95)$$

- (2) the local function space \mathcal{Y} is defined in terms of \mathcal{Y}_\square and the mapping \mathcal{G} as

$$\mathcal{Y} := \mathcal{Y}_\square \circ \mathcal{G}^{-1} := \{f \in \mathcal{F}_{K \rightarrow \mathbb{R}} \mid \exists h \in \mathcal{Y}_\square \text{ such that } f(\mathbf{x}) = h(\mathcal{G}^{-1}(\mathbf{x})) \ \forall \mathbf{x} \in K\}, \quad (6.96)$$

(3) \mathcal{D} are the nodal degrees of freedom associated with the node set

$$\mathcal{N} := \mathcal{G}(\mathcal{N}_\square) := \{\mathcal{G}(\hat{\xi}_1), \dots, \mathcal{G}(\hat{\xi}_M)\}. \quad (6.97)$$

Let $\mathcal{B}_\square := \{\psi_1, \dots, \psi_M\} \subset \mathcal{Y}_\square$ be the *nodal* basis of the local function space \mathcal{Y}_\square associated with the node set \mathcal{N}_\square . Then define the following collection of vectors $\mathcal{B} := \{\phi_1, \dots, \phi_M\} \subset \mathcal{Y}$, where

$$\phi_i(\mathbf{x}) := \psi_i(\mathcal{G}^{-1}(\mathbf{x})) \quad \mathbf{x} \in K. \quad (6.98)$$

The dimension of the local function space of the physical element is the same as that of the master element ($\dim \mathcal{Y} = \dim \mathcal{Y}_\square = M$). Furthermore, \mathcal{B} is a nodal basis of \mathcal{Y} associated with the node set \mathcal{N} (Proposition 6.1). For convenience, define

$$\hat{\mathbf{x}}_i := \mathcal{G}(\hat{\xi}_i) \quad (6.99)$$

for $i = 1, \dots, M$, which allows us to write $\mathcal{N} = \{\hat{\mathbf{x}}_1, \dots, \hat{\mathbf{x}}_M\}$.

Proposition 6.1. *The dimension of the local function space associated with the physical (mapped) element is the same as the master element*

$$\dim \mathcal{Y} = \dim \mathcal{Y}_\square = M. \quad (6.100)$$

Furthermore, \mathcal{B} is a nodal basis of \mathcal{Y} corresponding to the node set \mathcal{N} .

Proof. To establish this proposition, we need to prove two statements: (1) \mathcal{B} is a basis of \mathcal{Y} and (2) $\{\phi_1, \dots, \phi_M\}$ possess the nodal property with respect to the node set \mathcal{N} . Because \mathcal{B} contains M vectors, $\dim \mathcal{Y} = M$ will follow from (1) (\mathcal{B} basis of \mathcal{Y}). We consider these separately.

- First we prove \mathcal{B} is a basis of \mathcal{Y} . Suppose there exists $\alpha_1, \dots, \alpha_M \in \mathbb{R}$ such that $\sum_{i=1}^M \alpha_i \phi_i(\mathbf{x}) = 0$ for all $\mathbf{x} \in K$. Then

$$0 = \sum_{i=1}^M \alpha_i \phi_i(\mathbf{x}) = \sum_{i=1}^M \alpha_i \psi_i(\mathcal{G}^{-1}(\mathbf{x})) = \sum_{i=1}^M \alpha_i \psi_i(\boldsymbol{\xi}), \quad (6.101)$$

where we used the definition of ϕ_i (6.98) and defined $\boldsymbol{\xi} = \mathcal{G}^{-1}(\mathbf{x}) \in \Omega_\square$. From the fact that \mathcal{B}_\square is a basis of \mathcal{Y}_\square , the above condition implies $\alpha_1 = \dots = \alpha_M = 0$. Thus, \mathcal{B} is linearly independent. Now take any $f \in \mathcal{Y}$. From the defintion of \mathcal{Y} (6.96), there must exist $h \in \mathcal{Y}_\square$ such that for any $\mathbf{x} \in K$, $f(\mathbf{x}) = h(\mathcal{G}^{-1}(\mathbf{x}))$. Because $h \in \mathcal{Y}_\square$, we can expand it in the basis \mathcal{B}_\square as $h = \sum_{i=1}^M \alpha_i \psi_i$. Then

$$f(\mathbf{x}) = h(\mathcal{G}^{-1}(\mathbf{x})) = \sum_{i=1}^M \alpha_i \psi_i(\mathcal{G}^{-1}(\mathbf{x})) = \sum_{i=1}^M \alpha_i \phi_i(\mathbf{x}), \quad (6.102)$$

which establishes $\mathcal{Y} \subset \text{span } \mathcal{B}$. We can easily see that $\text{span } \mathcal{B} \subset \mathcal{Y}$ by following this procedure in reverese. Therefore $\mathcal{Y} = \text{span } \mathcal{B}$. Because \mathcal{B} is linearly independent and spans \mathcal{Y} , it is a basis of \mathcal{Y} and therefore the dimension of \mathcal{Y} is the number of vectors in \mathcal{B} : $\dim \mathcal{Y} = M$.

- To establish the nodal property, we have

$$\phi_i(\hat{\mathbf{x}}_j) = \psi_i(\mathcal{G}^{-1}(\hat{\mathbf{x}}_j)) = \psi_i(\mathcal{G}^{-1}(\mathcal{G}(\hat{\xi}_j))) = \psi_i(\hat{\xi}_j) = \delta_{ij}, \quad (6.103)$$

where the first two equalities follow from the definition of ϕ_i and $\hat{\mathbf{x}}_j$, the third equality follows from the fact that the compositon of a map with its inverse is the identity map, and the last equality follows from the nodal property of ϕ_i .

□

Example 6.20: Mapped \mathcal{P}^1 triangle element

We construct a physical (mapped) \mathcal{P}^1 triangle element by mapping the \mathcal{P}^1 master triangle element from

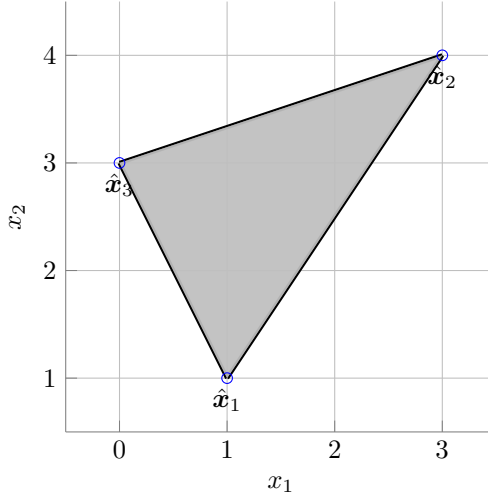


Figure 6.14: Element domain of the \mathcal{P}^1 physical (mapped) triangle element under the affine transformation (6.104).

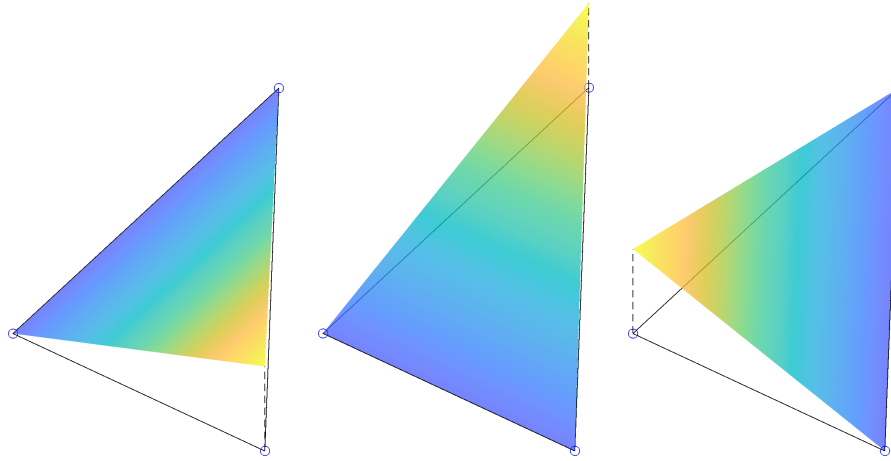


Figure 6.15: Nodal basis functions of \mathcal{P}^1 physical triangle element defined by mapping the \mathcal{P}^1 master triangle using the affine mapping (6.104).

Section 6.2.4 using the affine mapping

$$\mathcal{G}(\xi) = \begin{bmatrix} 1 + 2\xi_1 - \xi_2 \\ 1 + 3\xi_1 + 2\xi_2 \end{bmatrix}, \quad \mathcal{G}^{-1}(x) = \frac{1}{7} \begin{bmatrix} 2(x_1 - 1) + (x_2 - 1) \\ -3(x_1 - 1) + 2(x_2 - 1) \end{bmatrix}. \quad (6.104)$$

The physical element domain is shown in Figure 6.14 and the nodes of the mapped element are given by

$$\hat{x}_1 = \mathcal{G}(\hat{z}_1) = \begin{bmatrix} 1 \\ 1 \end{bmatrix}, \quad \hat{x}_2 = \mathcal{G}(\hat{z}_2) = \begin{bmatrix} 3 \\ 4 \end{bmatrix}, \quad \hat{x}_3 = \mathcal{G}(\hat{z}_3) = \begin{bmatrix} 0 \\ 3 \end{bmatrix}, \quad (6.105)$$

where $\hat{z}_1, \hat{z}_2, \hat{z}_3$ are the nodes of the master \mathcal{P}^1 triangle element (Section 6.2.4). The local function space is $\mathcal{P}^1(\Omega_\square) \circ \mathcal{G}^{-1}$; the nodal basis functions given by (6.98) are shown in Figure 6.15.

While this definition of mapped element is sufficiently abstract to encapsulate the finite elements of interest in this course, it does not answer how to construct the mapping \mathcal{G} in a practical setting. Recall that \mathcal{G} is a *vector-valued* function (d components) over the master element domain Ω_\square and \mathcal{G} can be any bijection. It turns out to be particularly convenient to use the local element to define \mathcal{G} ; however, it need not be the *same* local function space that will be used to approximate the solution of the

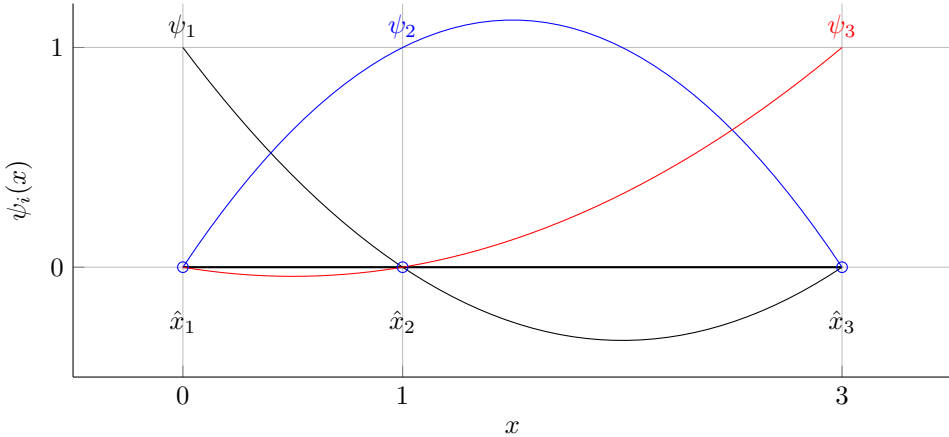


Figure 6.16: Element geometry and nodal basis functions of \mathcal{P}^2 physical line element defined by mapping the \mathcal{P}^2 master line element using the local function space of the master element; the nodes in (6.107) define the mapping according to (6.106).

PDE. In this course, we will use the same local function space for the mapping and solution approximation; this is called an *isoparametric* element. In this setting, we represent the mapping (componentwise) using the local function space $\mathcal{G} \in [\mathcal{V}_\square]^d$, which can be expanded in the nodal basis \mathcal{B}_\square as

$$\mathcal{G} = \sum_{i=1}^M \mathcal{G}(\hat{\xi}_i) \psi_i = \sum_{i=1}^M \hat{\mathbf{x}}_i \psi_i. \quad (6.106)$$

From this we see that \mathcal{G} is *completely defined* from the coordinates of the transformed reference nodes $\hat{\mathbf{x}}_i$; thus, to completely specify the mapping, we only need to define the positions to which the master nodes \mathcal{N}_\square are mapped (must simpler than explicitly prescribing a vector-valued function).

Example 6.21: \mathcal{P}^2 line element

We consider a \mathcal{P}^2 line element defined by a \mathcal{P}^2 mapping of the \mathcal{P}^2 master line element. Let $(\Omega_\square, \mathcal{Y}_\square, \mathcal{N}_\square)$ be the \mathcal{P}^2 master line element introduced in Section 6.2.2. In addition, let $\mathcal{N} = \{\hat{x}_1, \hat{x}_2, \hat{x}_3\}$ be the nodes of the physical element (Figure 6.16)

$$\hat{x}_1 = 0, \quad \hat{x}_2 = 1, \quad \hat{x}_3 = 3. \quad (6.107)$$

Then the geometry mapping is given by

$$\mathcal{G}(\xi) = \sum_{i=1}^3 \hat{x}_i \psi_i(\xi) = \psi_2(\xi) + 3\psi_3(\xi), \quad (6.108)$$

which leads to the element domain $K = \mathcal{G}(\Omega_\square)$ (Figure 6.16). Furthermore, the basis functions are defined according to (6.98) (Figure 6.16).

Example 6.22: \mathcal{Q}^2 quadrilateral element

We consider a \mathcal{Q}^2 quadrilateral element defined by a \mathcal{Q}^2 mapping of the \mathcal{Q}^2 master quadrilateral element. Let $(\Omega_\square, \mathcal{Y}_\square, \mathcal{N}_\square)$ be the \mathcal{Q}^2 master quadrilateral element introduced in Section 6.2.3. In addition, let

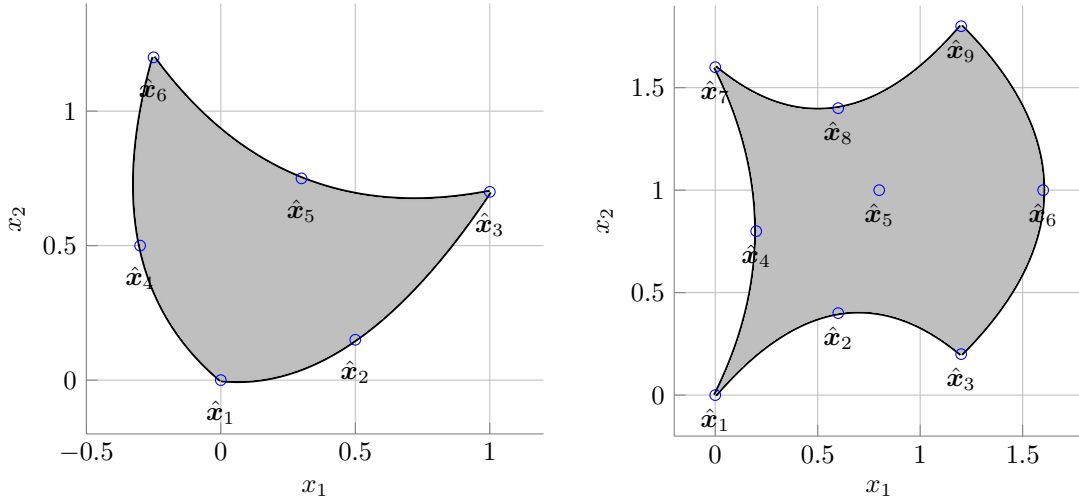


Figure 6.17: Mapped \mathcal{P}^2 triangle and \mathcal{Q}^2 quadrilateral elements from Examples 6.22-6.23.

$\mathcal{N} = \{\hat{x}_1, \dots, \hat{x}_9\}$ be the nodes of the physical element (Figure 6.17)

$$\begin{aligned}\hat{x}_1 &= \begin{bmatrix} 0.0 \\ 0.0 \end{bmatrix}, & \hat{x}_2 &= \begin{bmatrix} 0.6 \\ 0.4 \end{bmatrix}, & \hat{x}_3 &= \begin{bmatrix} 1.2 \\ 0.2 \end{bmatrix}, \\ \hat{x}_4 &= \begin{bmatrix} 0.2 \\ 0.8 \end{bmatrix}, & \hat{x}_5 &= \begin{bmatrix} 0.8 \\ 1.0 \end{bmatrix}, & \hat{x}_6 &= \begin{bmatrix} 1.6 \\ 1.0 \end{bmatrix}, \\ \hat{x}_7 &= \begin{bmatrix} 0.0 \\ 1.6 \end{bmatrix}, & \hat{x}_8 &= \begin{bmatrix} 0.6 \\ 1.4 \end{bmatrix}, & \hat{x}_9 &= \begin{bmatrix} 1.2 \\ 1.8 \end{bmatrix}.\end{aligned}\quad (6.109)$$

Then the geometry mapping is given by

$$\mathcal{G}(\xi) = \sum_{i=1}^9 \hat{x}_i \psi_i(\xi), \quad (6.110)$$

which leads to the element domain $K = \mathcal{G}(\Omega_\square)$ (Figure 6.17). Furthermore, the basis functions are defined according to (6.98) (Figure 6.18).

Example 6.23: \mathcal{P}^2 triangle elements

We consider a \mathcal{P}^2 triangle element defined by a \mathcal{P}^2 mapping of the \mathcal{P}^2 master triangle element. Let $(\Omega_\square, \mathcal{Y}_\square, \mathcal{N}_\square)$ be the \mathcal{P}^2 master triangle element introduced in Section 6.2.4. In addition, let $\mathcal{N} = \{\hat{x}_1, \dots, \hat{x}_6\}$ be the nodes of the physical element (Figure 6.17)

$$\begin{aligned}\hat{x}_1 &= \begin{bmatrix} 0.0 \\ 0.0 \end{bmatrix}, & \hat{x}_2 &= \begin{bmatrix} 0.5 \\ 0.15 \end{bmatrix}, & \hat{x}_3 &= \begin{bmatrix} 1.0 \\ 0.7 \end{bmatrix} \\ \hat{x}_4 &= \begin{bmatrix} -0.3 \\ 0.5 \end{bmatrix}, & \hat{x}_5 &= \begin{bmatrix} 0.3 \\ 0.75 \end{bmatrix}, & \hat{x}_6 &= \begin{bmatrix} -0.25 \\ 1.2 \end{bmatrix}.\end{aligned}\quad (6.111)$$

Then the geometry mapping is given by

$$\mathcal{G}(\xi) = \sum_{i=1}^6 \hat{x}_i \psi_i(\xi), \quad (6.112)$$

which leads to the element domain $K = \mathcal{G}(\Omega_\square)$ (Figure 6.17). Furthermore, the basis functions are defined according to (6.98) (Figure 6.19).

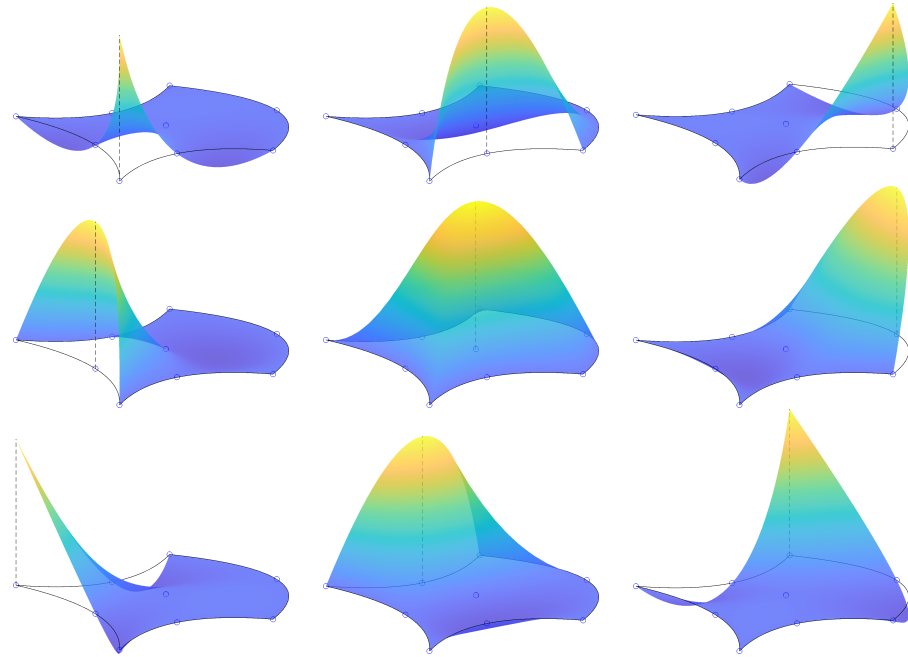


Figure 6.18: Nodal basis functions of \mathcal{Q}^2 mapped quadrilateral element from Example 6.22.

In the remainder of this section, we discuss the implications that mapped formulation has on the evaluation of derivatives and integrals. For convenience in the following sections, we introduce the mapping deformation gradient $\mathbf{G} : \Omega_\square \rightarrow M_{d,d}(\mathbb{R})$ and Jacobian $g : \Omega_\square \rightarrow \mathbb{R}$ defined as

$$\mathbf{G} := \frac{\partial \mathcal{G}}{\partial \xi}, \quad g := \det \mathbf{G}. \quad (6.113)$$

6.3.2 Derivatives with respect to mapped coordinates

As we saw in Chapter 4, the finite element equations require the (spatial) derivatives of the basis functions. In the present setting this translates to the derivatives of $\phi_i(\mathbf{x})$. To generalize the discussion, consider any $f \in \mathcal{F}_{K \rightarrow \mathbb{R}}$ where $f = h \circ \mathcal{G}^{-1}$ for some $h \in \mathcal{F}_{\Omega_\square \rightarrow \mathbb{R}}$. Then, by the chain rule, we have

$$\frac{\partial f}{\partial x_j}(\mathbf{x}) = \sum_{k=1}^d \frac{\partial h}{\partial \xi_k}(\mathcal{G}^{-1}(\mathbf{x})) \frac{\partial [\mathcal{G}^{-1}]_k}{\partial x_j}(\mathbf{x}). \quad (6.114)$$

To simplify the second term in the product, we use the inverse function theorem that gives the following identity

$$\left[\frac{\partial \mathcal{G}}{\partial \xi}(\boldsymbol{\xi}) \right]^{-1} = \frac{\partial [\mathcal{G}^{-1}]}{\partial \mathbf{x}}(\mathcal{G}(\boldsymbol{\xi})). \quad (6.115)$$

Therefore we can reduce the complicated expression for the derivative in (6.114) to

$$\frac{\partial f}{\partial x_j}(\mathbf{x}) = \sum_{k=1}^d \frac{\partial h}{\partial \xi_k}(\mathcal{G}^{-1}(\mathbf{x})) [G^{-1}(\boldsymbol{\xi})]_{kj}, \quad (6.116)$$

where $\mathbf{G}^{-1}(\boldsymbol{\xi}) = [\mathbf{G}(\boldsymbol{\xi})]^{-1}$ is the inverse of the mapping deformation gradient. Applying this expression to the mapped nodal basis functions we have

$$\frac{\partial \phi_i}{\partial x_j}(\mathbf{x}) = \sum_{k=1}^d \frac{\partial \psi_i}{\partial \xi_k}(\mathcal{G}^{-1}(\mathbf{x})) [G^{-1}(\boldsymbol{\xi})]_{kj}. \quad (6.117)$$

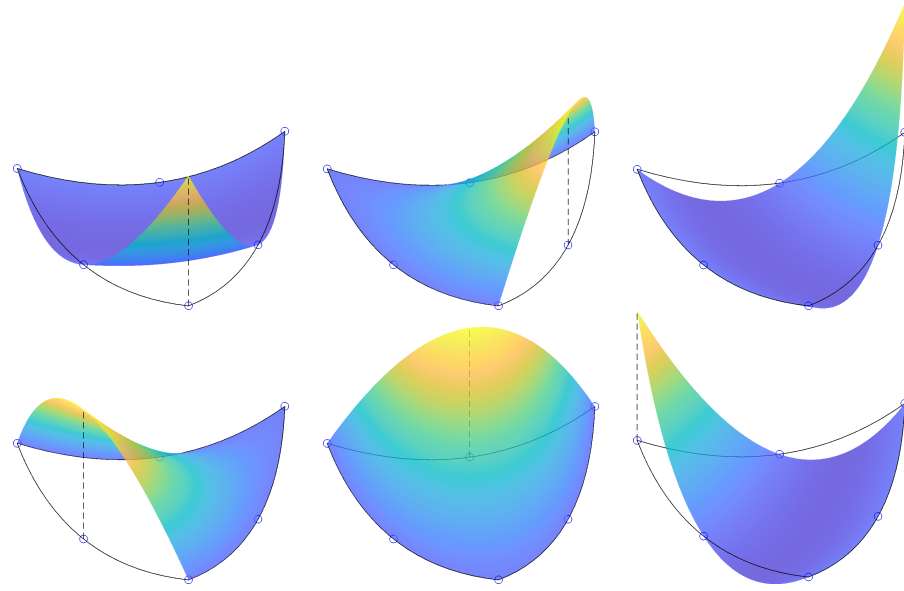


Figure 6.19: Nodal basis functions of \mathcal{P}^2 mapped triangle element from Example 6.23.

6.3.3 Volume integrals over mapped domain

Given that volume integrals are fundamental to the finite element method, we consider how the use of mapped finite elements will impact the development. Consider the integral of any function $\theta \in \mathcal{F}_{K \rightarrow \mathbb{R}}$ over the mapped element domain $K = \mathcal{G}(\Omega_\square)$

$$I_v = \int_K \theta(\mathbf{x}) d\mathbf{x}. \quad (6.118)$$

The change of variables formula of integration gives

$$I_v = \int_{\Omega_\square} \theta(\mathcal{G}(\boldsymbol{\xi})) g(\boldsymbol{\xi}) d\boldsymbol{\xi} \quad (6.119)$$

where $g := \det \mathbf{G}$ is the mapping Jacobian. This shows that any integral over the physical domain K can be conveniently re-written as an integral over the master domain Ω_\square . Furthermore, if the function can be written as a function $\pi \in \mathcal{F}_{\Omega_\square \rightarrow \mathbb{R}}$ composed with the inverse mapping, i.e., $\theta = \pi \circ \mathcal{G}^{-1}$, this reduces to an integral of π over Ω_\square

$$I_v = \int_{\Omega_\square} \theta(\mathcal{G}(\boldsymbol{\xi})) g(\boldsymbol{\xi}) d\boldsymbol{\xi} = \int_{\Omega_\square} \pi(\mathcal{G}^{-1}((\mathcal{G}(\boldsymbol{\xi}))) g(\boldsymbol{\xi}) d\boldsymbol{\xi}, = \int_{\Omega_\square} \pi(\boldsymbol{\xi}) g(\boldsymbol{\xi}) d\boldsymbol{\xi}. \quad (6.120)$$

Example 6.24: Integrals in one-dimension

Consider the special case of $d = 1$. In this case, $K = [a, b] \subset \mathbb{R}$ is an arbitrary interval and $\Omega_\square = [-1, 1]$. Let $\mathcal{G} : \Omega_\square \rightarrow [a, b]$ be any bijective mapping. Then (6.119) reduces to

$$I_v = \int_a^b \theta(x) dx = \int_{\Omega_\square} \theta(\mathcal{G}(\xi)) \mathcal{G}'(\xi) d\xi, \quad (6.121)$$

which is the familiar change of variables formula for one-dimensional integrals.

Example 6.25: Volume integral over mapped triangle

Suppose we wish to compute the volume and centroid of mapped triangle in Example 6.20. The volume

and centroid are given by

$$V = \int_K d\mathbf{x}, \quad \mathbf{c} = \frac{1}{V} \int_k \mathbf{x} d\mathbf{x}, \quad (6.122)$$

which fit the form of (6.118) with $\theta(\mathbf{x}) = 1$ for the volume and $\theta(\mathbf{x}) = \mathbf{x}$ for the centroid. First, we must compute the deformation gradient and Jacobian of the mapping, which are both constant in this case because the mapping is affine

$$\mathbf{G}(\xi) = \begin{bmatrix} 2 & -1 \\ 3 & 2 \end{bmatrix}, \quad g(\xi) = 7. \quad (6.123)$$

Then the change of variable formula gives

$$V = g \int_{\Omega_\square} d\xi, \quad \mathbf{c} = \frac{g}{V} \int_{\Omega_\square} \mathcal{G}(\xi) d\xi. \quad (6.124)$$

We can easily see the volume is simply $V = 7/2$ because the transformed integral is just the volume of the reference element ($= 1/2$). The centroid reduces to

$$c_1 = 2 \int_{\Omega_\square} (1 + 2\xi_1 - \xi_2) d\xi, \quad c_2 = 2 \int_{\Omega_\square} (1 + 3\xi_1 + 2\xi_2) d\xi, \quad (6.125)$$

where the expression for $\mathcal{G}(\xi)$ in (6.104) was used. Since these integrals are manageable (integrals over unit right triangle), we compute them directly to get: $c_1 = 4/3$, $c_2 = 8/3$.

6.3.4 Surface integrals over mapped domain

In addition to volume integrals, surface integrals frequently arise in the finite element method when considering non-homogeneous natural boundary conditions. Consider the surface integral

$$I_b = \int_{\partial K_f} \theta ds, \quad (6.126)$$

where $\theta \in \mathcal{F}_{K \rightarrow \mathbb{R}}$, $K = \mathcal{G}(\Omega_\square)$ is the mapped element, and ∂K_f is the f th face of the mapped element, i.e., the mapping \mathcal{G} applied to the f th face of Ω_\square

$$\partial K_f := \mathcal{G}(\partial \Omega_{\square,f}) := \{\mathcal{G}(\xi) \mid \xi \in \partial \Omega_{\square,f}\}. \quad (6.127)$$

Before continuing, we observe that ∂K_f is a $(d-1)$ -dimensional surface embedded in \mathbb{R}^d . To re-write the integral I_b in a computable form, we introduce a *parametrization* of ∂K_f . To begin, we introduce a $(d-1)$ -dimensional reference domain $\Gamma_\square \subset \mathbb{R}^{d-1}$ and a mapping from Γ_\square to each face of the master element domain, i.e.,

$$\gamma_f : \Gamma_\square \rightarrow \partial \Omega_{\square,f}. \quad (6.128)$$

We assume only one face reference domain is required to parametrize all faces of the master element; this is true for *regular* polytopes where all each face has the same geometry, e.g., simplices (each face is a simplex in \mathbb{R}^{d-1}) and hypercubes (each face is a hypercube in \mathbb{R}^{d-1}). More general constructions are straightforward, but tedious.

Example 6.26: Boundary parametrization of master element

- Recall the two-dimensional hypercube (quadrilateral) in Figure 6.1 with the face numbering discussed in Section 6.2.3. The boundary parametrizations of the master quadrilateral is

$$\gamma_1(r) = (-1, r), \quad \gamma_2(r) = (r, -1), \quad \gamma_3(r) = (1, r), \quad \gamma_4(r) = (r, 1) \quad (6.129)$$

for $r \in \Gamma_\square = [-1, 1]$ (master hypercube in $d = 1$).

- Recall the two-dimensional simplex (triangle) in Figure 6.1 with the face numbering discussed in Section 6.2.4. The boundary parametrizations of the master triangle is

$$\gamma_1(r) = (0, r), \quad \gamma_2(r) = (r, 0), \quad \gamma_3(r) = (r, 1-r) \quad (6.130)$$

for $r \in \Gamma_{\square} = [0, 1]$ (master simplex in $d = 1$).

- Recall the d -dimensional hypercube with face numbering discussed in Section 6.2.5. The boundary parametrizations of the master hypercube is

$$\begin{aligned}\gamma_1(\mathbf{r}) &= (-1, r_1, r_2, \dots, r_{d-1}) \\ \gamma_2(\mathbf{r}) &= (r_1, -1, r_2, \dots, r_{d-1}) \\ &\dots \\ \gamma_d(\mathbf{r}) &= (r_1, r_2, \dots, r_{d-1}, -1) \\ \gamma_{d+1}(\mathbf{r}) &= (1, r_1, r_2, \dots, r_{d-1}) \\ \gamma_{d+2}(\mathbf{r}) &= (r_1, 1, r_2, \dots, r_{d-1}) \\ &\dots \\ \gamma_{2d}(\mathbf{r}) &= (r_1, r_2, \dots, r_{d-1}, 1)\end{aligned}\tag{6.131}$$

for $\mathbf{r} \in \Gamma_{\square}$ (master hypercube in \mathbb{R}^{d-1}).

- Recall the d -dimensional simplex with face numbering discussed in Section 6.2.6. The boundary parametrizations of the master simplex is

$$\begin{aligned}\gamma_1(\mathbf{r}) &= (0, r_1, r_2, \dots, r_{d-1}) \\ \gamma_2(\mathbf{r}) &= (r_1, 0, r_2, \dots, r_{d-1}) \\ &\dots \\ \gamma_d(\mathbf{r}) &= (r_1, r_2, \dots, r_{d-1}, 0) \\ \gamma_{d+1}(\mathbf{r}) &= (r_1, r_2, \dots, r_{d-1}, 1 - \sum_{i=1}^{d-1} r_i)\end{aligned}\tag{6.132}$$

for $\mathbf{r} \in \Gamma_{\square}$ (master simplex in \mathbb{R}^{d-1}).

With this notion of a parametrization of the faces of the master element $\partial\Omega_{square,f}$, a parametrization of the faces of the physical element ∂K_f can be defined as a composition of master face parametrization γ_f and the domain mapping $\mathcal{G}: \mathcal{H}_f : \Gamma_{\square} \rightarrow \partial K_f$, i.e.,

$$\mathcal{H}_f = \mathcal{G} \circ \gamma_f.\tag{6.133}$$

The deformation gradient of this face mapping is a function $\mathbf{H}_f : \Gamma_{\square} \rightarrow M_{d,d-1}(\mathbb{R})$

$$\mathbf{H}_f(\mathbf{r}) := \frac{\partial \mathcal{H}_f}{\partial \mathbf{r}}(\mathbf{r}) = \frac{\partial \mathcal{G}}{\partial \boldsymbol{\xi}}(\gamma_f(\mathbf{r})) \frac{\partial \gamma_f}{\partial \mathbf{r}}(\mathbf{r}) = \mathbf{G}(\gamma_f(\mathbf{r})) \frac{\partial \gamma_f}{\partial \mathbf{r}}(\mathbf{r})\tag{6.134}$$

for $\mathbf{r} \in \Gamma_{\square}$. Furthermore, the surface element $\sigma_f : \Gamma_{\square} \rightarrow \mathbb{R}$, used to transform surface integrals, is defined as

$$\sigma_f(\mathbf{r}) := \sqrt{\mathbf{H}(\mathbf{r})^T \mathbf{H}(\mathbf{r})}\tag{6.135}$$

for $\mathbf{r} \in \Gamma_{\square}$. Now the surface integral I_b can be re-written as a standard integral over Γ_{\square} as

$$I_b = \int_{\Gamma_{\square}} \theta(\mathcal{H}_f(\mathbf{r})) \sigma_f(\mathbf{r}) d\mathbf{r}.\tag{6.136}$$

This shows that any suface integral over the physical element face ∂K_f can be conveniently re-written as a standard integral over the reference domain Γ_{\square} . Notice that in the case of $d = 2$, this agrees with the well-known definition of a *line integral* because $\sigma_f(r) = \|\mathcal{H}'_f(r)\|$ and $\Gamma_{\square} = [a, b] \subset \mathbb{R}$ (a and b depend on whether considering simplex or hypercube). Finally, consider the case where the integrand can be written as a function $\pi \in \mathcal{F}_{\Omega_{\square} \rightarrow \mathbb{R}}$ composed with the inverse mapping, i.e., $\theta = \pi \circ \mathcal{G}^{-1}$; the above integral reduces to

$$I_b = \int_{\Gamma_{\square}} \theta(\mathcal{H}_f(\mathbf{r})) \sigma_f(\mathbf{r}) d\mathbf{r} = \int_{\Gamma_{\square}} \pi(\mathcal{G}^{-1}(\mathcal{G}(\gamma_f(\mathbf{r})))) \sigma_f(\mathbf{r}) d\mathbf{r} = \int_{\Gamma_{\square}} \pi(\gamma_f(\mathbf{r})) \sigma_f(\mathbf{r}) d\mathbf{r}.\tag{6.137}$$

Example 6.27: Surface integral over mapped triangle

Let us return to Example 6.20 and compute the following surface integral

$$I_b = \int_{\partial K_2} \sin(x_1) \cos(x_2) \, ds, \quad (6.138)$$

which clearly fits the form of (6.126). From Example 6.26, we see the boundary parametrization of $\partial\Omega_{\square,f}$ (master triangle) is $\gamma_2(r) = (r, 0)$. Combining this boundary parametrization with the mapping \mathcal{G} from Example 6.20, we see that

$$\mathcal{H}_2(r) = \mathcal{G}(\gamma_2(r)) = \begin{bmatrix} 1+2r \\ 1+3r \end{bmatrix}, \quad \mathbf{H}_2(r) = \begin{bmatrix} 2 \\ 3 \end{bmatrix}, \quad \sigma_2(r) = \sqrt{13}. \quad (6.139)$$

Finally, this leads to the transformed integral

$$I_b = \sqrt{13} \int_0^1 \sin(1+2r) \cos(1+3r) \, dr = \frac{\sqrt{13}}{10} [5 \cos(r) - \cos(5r+2)]_0^1 \approx -1.2506, \quad (6.140)$$

where we used the reference $(d-1)$ -dimensional simplex $\Gamma_\square = [0, 1]$.

6.4. Mesh

With the notions of master and physical (mapped) elements established, we can provide a complete description of a finite element mesh. Consider a domain $\Omega \subset \mathbb{R}^d$ with boundary $\partial\Omega$ partitioned into N_b non-overlapping portions $\partial\Omega_1, \dots, \partial\Omega_{N_b}$

$$\partial\Omega = \bigcup_{s=1}^{N_b} \overline{\partial\Omega_s}, \quad \partial\Omega_s \cap \partial\Omega_{s'} = \emptyset \quad (s \neq s'). \quad (6.141)$$

Example 6.28: Domains and boundaries

A few examples of domains and their boundaries in one- and two-dimensions are:

- One-dimensional domain and boundaries (Figure 6.20)

$$\Omega = (a, b), \quad \partial\Omega_1 = \{a\}, \quad \partial\Omega_2 = \{b\} \quad (6.142)$$

- Two-dimensional square domain (Figure 6.20)

$$\Omega = (a_1, b_1) \times (a_2, b_2) \quad (6.143)$$

with boundaries

$$\begin{aligned} \partial\Omega_1 &= \{a_1\} \times (a_2, b_2) \\ \partial\Omega_2 &= (a_1, b_1) \times \{a_2\} \\ \partial\Omega_3 &= \{b_1\} \times (a_2, b_2) \\ \partial\Omega_4 &= (a_1, b_1) \times \{b_2\} \end{aligned} \quad (6.144)$$

- Batman domain (Figure 6.21) with three boundaries $\partial\Omega_1, \partial\Omega_2$, and $\partial\Omega_3 := \partial\Omega \setminus (\partial\Omega_1 \cup \partial\Omega_2)$
- Notre Dame domain (Figure 6.21) with three boundaries $\partial\Omega_1, \partial\Omega_2$, and $\partial\Omega_3 := \partial\Omega \setminus (\partial\Omega_1 \cup \partial\Omega_2)$.

The partitioning of the boundary $\partial\Omega$ into pieces $\partial\Omega_i$ was arbitrary. Usually the boundary is partitioned into pieces such that boundary conditions can be conveniently specified.

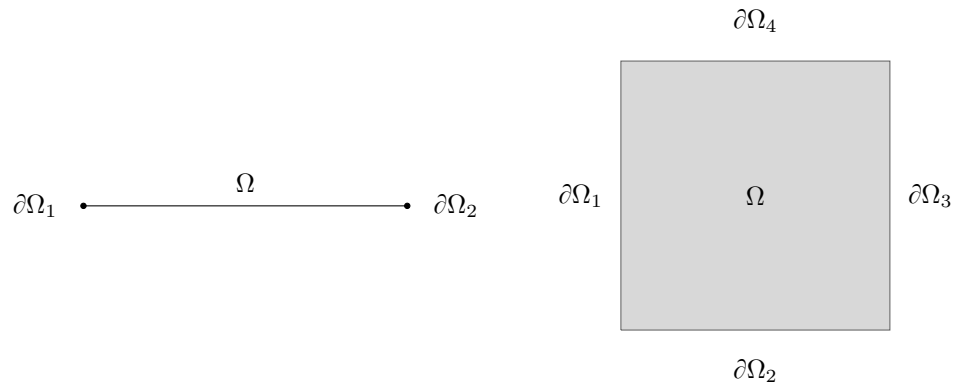


Figure 6.20: One-dimensional domain and two-dimensional square domain and their boundaries.

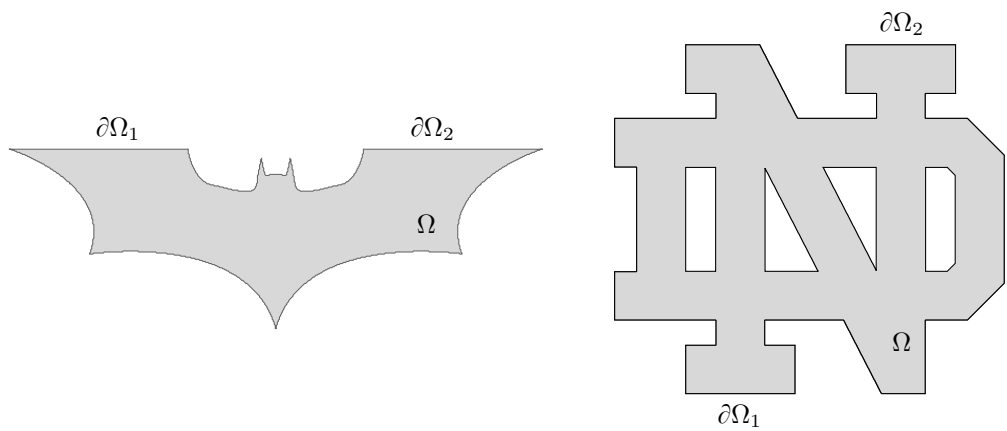


Figure 6.21: Batman and Notre Dame domains and their boundaries.

A mesh \mathcal{E}_h of Ω is an ordered collection of N_{el} non-overlapping elements (open sets) $\Omega_e \subset \Omega$, $e = 1, \dots, N_e$ that cover the domain, that is,

$$\mathcal{E}_h := \{\Omega_e\}_{e=1}^{N_{\text{el}}}, \quad \Omega = \bigcup_{e=1}^{N_e} \overline{\Omega}_e, \quad \Omega_e \cap \Omega_{e'} = \emptyset \quad (e \neq e'). \quad (6.145)$$

In practice, the elements are usually generalized polytopes (polygons if $d = 2$, polyhedra if $d = 3$) consisting of smooth surfaces (faces) connected at their boundaries to form smooth curves (edges) and sharp corners (vertices). Often the elements are *straight-sided*, i.e., the faces are planes and the edges are straight lines. Generalized polytopes are usually generated by applying a transformation to a standard (straight-sided) polytope, i.e., the mapped master elements (Section 6.3.1). For the remainder, we assume the elements are generalized polytope for concreteness (the finite element method can be formulated for more general elements). Furthermore, we assume all elements of the mesh are the same generalized *regular* polytope. Regular polytopes are the most highly symmetrical: all face are the same generalized polytope in $d - 1$ dimensions, e.g., simplices and hypercubes. This turns out to be a rather restrictive assumption since it limits the elements that can be used for $d > 2$; however, having elements where all faces have the same geometry substantially simplifies the implementation of the finite element method. The assumption that all elements are the same polytope implies all elements have the same number of faces, edges, and vertices, which also turns out to be convenient from an implementation viewpoint.

Example 6.29: Meshes

Meshes consisting of straight-sided simplex elements (triangles for $d = 2$, and tetrahedra for $d = 3$) of complex domains are shown in Figures 6.22-6.23.

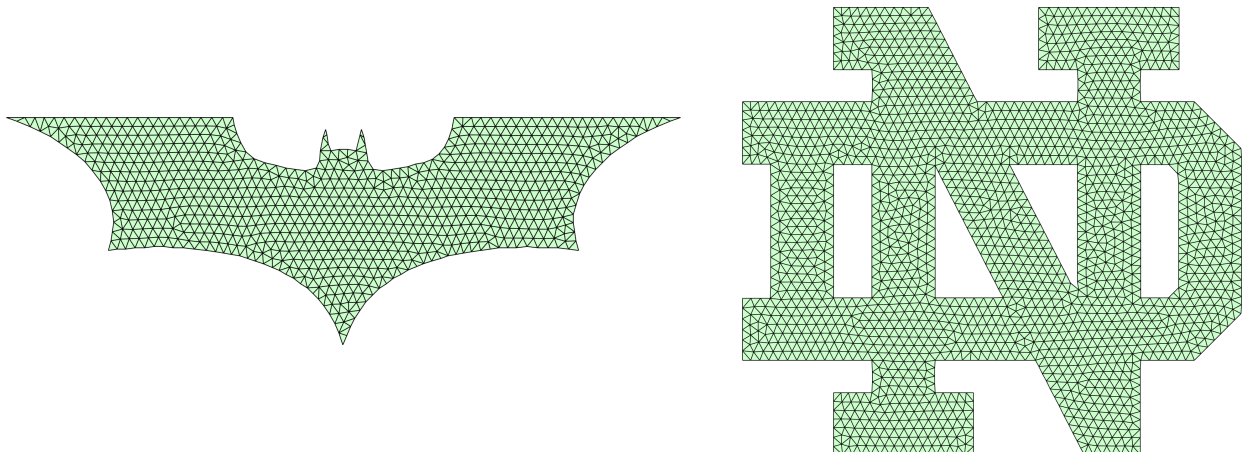


Figure 6.22: Simplicial mesh ($d = 2$) of the batman symbol and Notre Dame logo.

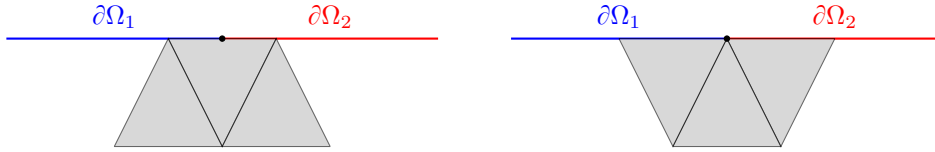


Figure 6.24: *Left:* Inadmissible mesh because the interior of an element face touches two boundaries. *Right:* An admissible mesh because, even though a single element touches multiple boundaries, the interior of a face does not.

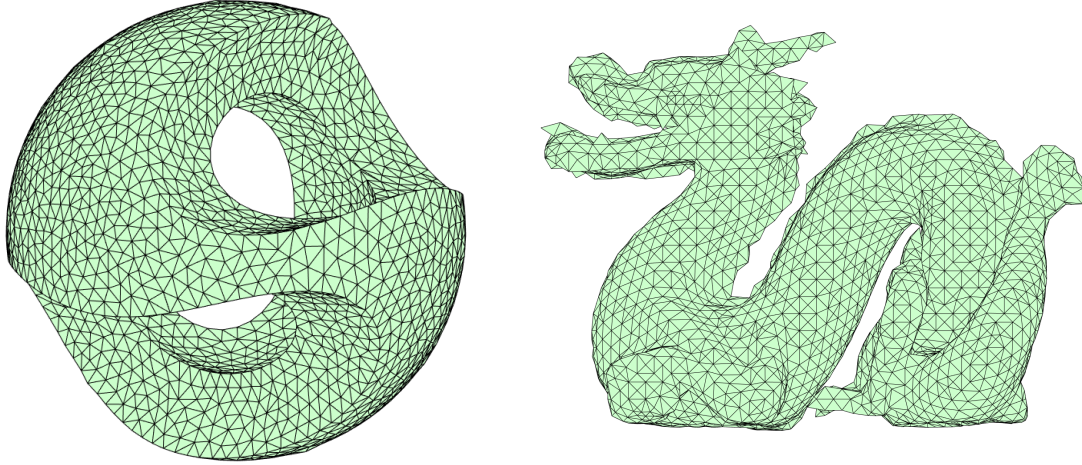


Figure 6.23: Simplicial mesh ($d = 3$) of a sculpture and dragon.

Let $N_{\text{fc}}^{\text{el}}$ denote the number of faces per element and \mathcal{F}_h^e the ordered collection of faces of element Ω_e , i.e., $\partial\Omega_{ef} \subset \partial\Omega_e$ for $f = 1, \dots, N_{\text{fc}}^{\text{el}}$

$$\mathcal{F}_h^e := \{\partial\Omega_{ef}\}_{f=1}^{N_{\text{fc}}^{\text{el}}}, \quad \partial\Omega_e = \bigcup_{f=1}^{N_{\text{fc}}^{\text{el}}} \overline{\partial\Omega}_{ef}. \quad (6.146)$$

Recall that element faces intersect at element edges or vertices. One final assumption we make for implementation convenience is that each element face interior intersects *at most one* domain boundary (Figure 6.24).

The diameter of an element Ω_e is the supremum distance between pairs of points, i.e.,

$$\text{diam}(\Omega_e) := \sup_{x,y \in \Omega_e} \|x - y\|. \quad (6.147)$$

The diameter of a triangle is the length of the longest edge, while the diameter of a quadrilateral is the length of the longest diagonal.

The finite element subspace can be defined abstractly in terms of only elements; however, given our restriction to *nodal* finite elements, we require the concept of nodes. For each element $\Omega_e \in \mathcal{E}_h$, let \mathcal{N}_h^e be an ordered collection of $N_{\text{nd}}^{\text{el}}$ points $\{\hat{x}_1^e, \dots, \hat{x}_{N_{\text{nd}}^{\text{el}}}^e\} \subset \Omega_e$ called *nodes* or vertices; we say x_i^e is the i (local) node of element Ω_e . A thorough discussion of how nodes are distributed throughout a master element and transformed to a physical element is provided in Section 6.2. We denote the union of all element nodes as

$$\mathcal{N}_h = \bigcup_{e=1}^{N_{\text{el}}} \mathcal{N}_h^e \quad (6.148)$$

and endow this set of $N_{\text{nd}} := |\mathcal{N}_h|$ nodes with an ordering called the global node numbering; we say $\hat{x}_i \in \mathcal{N}_h$ is the i th global node. Similar to Chapter 4, we describe the relationship between the global and local node

Table 6.1: Mesh data structure xcg (*left*) and e2vcg (*right*) corresponding to the \mathcal{P}^1 mesh of the unit circle in Figure 6.25.

node			element	node 1	node 2	node 3
	x_1	x_2		4	5	7
1	-0.97	0.26	2	4	6	1
2	-0.88	-0.5	3	7	6	4
3	-0.50	0.87	4	12	7	10
4	-0.37	-0.21	5	7	5	10
5	-0.26	-0.97	6	1	6	3
6	-0.22	0.37	7	3	6	8
7	0.21	-0.37	8	9	11	8
8	0.26	0.97	9	8	6	9
9	0.37	0.22	10	9	6	7
10	0.50	-0.87	11	9	7	12
11	0.87	0.50	12	12	11	9
12	0.97	-0.26	13	2	4	1
			14	5	4	2

numbering using the *connectivity* matrix $\Theta \in M_{N_{\text{nd}}^{\text{el}}, N_{\text{el}}}(\mathbb{N})$. This leads to the following relationship between local and global nodes

$$\hat{\mathbf{x}}_i^e = \hat{\mathbf{x}}_{\Theta_{ie}}. \quad (6.149)$$

For convenience, we also introduce the set of nodes that lie on the domain boundary $\partial\Omega_i$

$$\mathcal{N}_h^{\partial_i} := \mathcal{N}_h \cap \partial\Omega_i. \quad (6.150)$$

To encode a mesh that satisfies our assumptions (homogeneous regular polytopes), we use three arrays: xcg , e2vcg , e2bnd . The first array xcg has size $d \times N_{\text{nd}}$ and encodes the positions of the global nodes; the i th column is the position of the i th global node. The second array e2vcg , size $N_{\text{nd}}^{\text{el}} \times N_{\text{el}}$ encodes how the nodes are connected to form elements; the (i, e) entry contains the global node number of the i th local node of element e , i.e., $\text{e2vcg}(i, e) = \Theta_{ie}$. Notice that if we did not choose all elements to be of the same type, this data structure would be more complex because there could be a different number of nodes associated with each element. The last array e2bnd , size $N_{\text{fc}}^{\text{el}} \times N_{\text{el}}$, encodes which faces lie on which boundary, i.e., $\text{e2bnd}(f, e) = i$ if face f of element e lies on boundary $\partial\Omega_i$. Notice that without the assumption that all element faces (interiors) intersect exactly one boundary, this data structure would be more complex.

Example 6.30: Mesh data structures

Figure 6.25 shows two meshes of the unit circle. For the mesh consisting of \mathcal{P}^1 triangular elements, the data structure xcg and e2vcg are shown in Table 6.1.

This completes our definition of a mesh. Notice that we have only introduced the concept of a mesh and how to store it on a computer. We have made no attempt to discuss how to *generate* a mesh of a general domain as this can be quite difficult depending requirements on the mesh, most importantly, the desired element geometry. Mesh generation is largely considered a *solved* problem when using straight-sided simplicial elements; however, it is very much an open problem for curved meshes or other types of element geometries, e.g., hypercubes. In this class, we will use the popular open-source mesh generation software written MATLAB known as DistMesh.

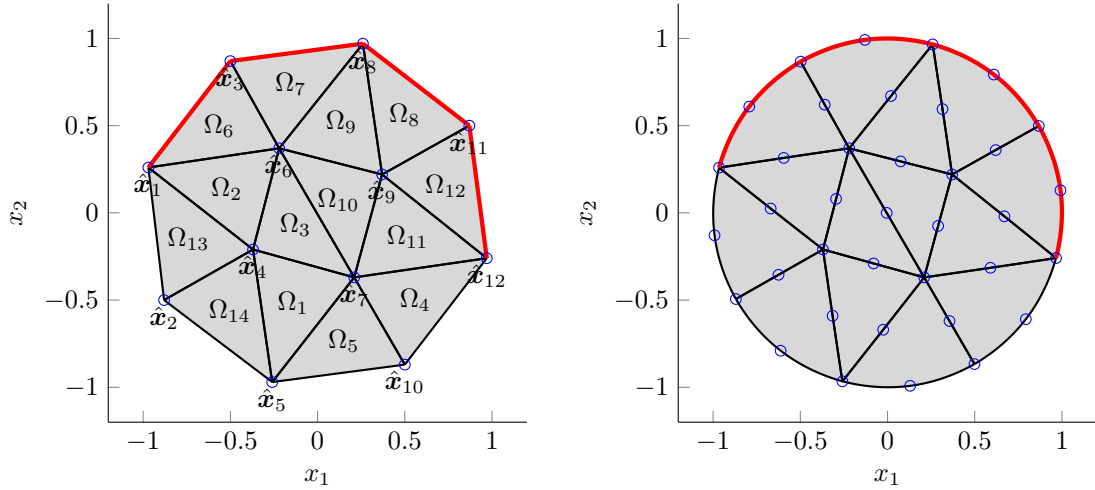


Figure 6.25: Mesh of the unit circle using $N_{\text{el}} = 14$ \mathcal{P}^1 (left) and \mathcal{P}^2 (right) triangular elements. Nodes are shown with blue circles and element faces/edges are indicated with black lines. The node and element numbers are included on the \mathcal{P}^1 mesh but omitted on the \mathcal{P}^2 mesh for clarity. The faces of the mesh on which the essential boundary condition is applied is indicated with a thick red line.

6.5. Finite element formulation

Consider a domain $\Omega \subset \mathbb{R}^d$ with boundary $\partial\Omega$ partitioned as $\partial\Omega = \overline{\partial\Omega_D} \cup \overline{\partial\Omega_N}$ and the following abstract variational problem:

$$\text{find } u \in \mathcal{V} \text{ such that } B(w, u) = \ell(w) \text{ for all } w \in \mathcal{V}^0, \quad (6.151)$$

where $B : H^1(\Omega) \times H^1(\Omega) \rightarrow \mathbb{R}$ is a bilinear form, $\ell : H^1(\Omega) \rightarrow \mathbb{R}$ is a linear functional, and $\mathcal{V}, \mathcal{V}^0 \subset H^1(\Omega)$ are the following subsets

$$\mathcal{V} := \{f \in H^1(\Omega) \mid f|_{\partial\Omega_D} = g\}, \quad \mathcal{V}^0 := \{f \in H^1(\Omega) \mid f|_{\partial\Omega_D} = 0\}. \quad (6.152)$$

The function $g \in L^2(\partial\Omega)$ is the prescribed essential boundary condition, \mathcal{V} is an affine subspace, and \mathcal{V}^0 is a linear subspace. Since \mathcal{V} is affine, it can be written as $\mathcal{V} = \varphi + \mathcal{V}^0$ for any $\varphi \in \mathcal{V}$. Following the procedure in Chapter 5, the variational problem can be converted to a bilinear form with the same test and trial space:

$$\text{find } \bar{u} \in \mathcal{V}^0 \text{ such that } B(w, \bar{u}) = \bar{\ell}(w) := \ell(w) - B(w, \varphi) \text{ for all } w \in \mathcal{V}^0. \quad (6.153)$$

We assume the bilinear form B is continuous and coercive on \mathcal{V}^0 and the linear functional $\bar{\ell}$ is continuous on \mathcal{V}^0 . Then the Lax-Milgram theorem guarantees (6.153) (and therefore (6.151)) possesses a unique solution.

The finite element method introduces a finite-dimensional linear subspace $\mathcal{V}_h^0 \subset \mathcal{V}^0$, which leads to the variational Galerkin formulation:

$$\text{find } u_h \in \mathcal{V}_h \text{ such that } B(w_h, u_h) = \ell(w_h) \text{ for all } w_h \in \mathcal{V}_h^0, \quad (6.154)$$

where $\mathcal{V}_h := \varphi + \mathcal{V}_h^0$ for any $\varphi \in \mathcal{V}$. The FE variational problem possesses a unique solution (Lax-Milgram theorem) since the properties of the bilinear form (continuity, coercivity) and linear functional (continuity) are inherited by virtue of \mathcal{V}_h^0 being a linear subspace of \mathcal{V}^0 . Similar to Chapter 4, the finite element subspace is defined by partitioning the domain into elements and introducing a local, finite-dimensional function space over each element.

Consider a mesh of Ω with elements $\{\Omega_e\}_{e=1}^{N_{\text{el}}}$ and nodes $\mathcal{N} = \{\hat{x}_1, \dots, \hat{x}_{N_{\text{nd}}}\}$, which we use to define a collection of finite elements $(\Omega_e, \mathcal{Y}_e, \mathcal{N}_e)$. The local function space, $\mathcal{Y}_e \subset \mathcal{C}^0(\Omega_e)$, is constructed by mapping a master finite element (Section 6.2) and $\mathcal{N}_e = \{\hat{x}_1^e, \dots, \hat{x}_{N_{\text{nd}}^e}\} \subset \mathcal{N}$ are the nodes associated with element Ω_e . Then we define the finite element subspace $\mathcal{V}_h^0 \subset \mathcal{V}^0$ as

$$\mathcal{V}_h^0 := \{f \in H^1(\Omega) \mid f|_{\Omega_e} \in \mathcal{Y}(\Omega_e) \forall \Omega_e \in \mathcal{E}_h, f|_{\partial\Omega_D} = 0\}. \quad (6.155)$$

It can be shown (Example 5.1) that any $f \in \mathcal{V}_h^0$ is *continuous*, i.e., $\mathcal{V}_h^0 \subset \mathcal{C}^0(\Omega)$; in the following sections, when we construct the finite element space, special attention will be given to enforcing this continuity requirement. Furthermore, $\mathcal{V}_h^0 \subset \mathcal{V}^0$ is a finite-dimensional linear subspace ($\bar{N}_{\text{dof}} := \dim \mathcal{V}_h^0$).

Let $\{\Phi_1, \dots, \Phi_{\bar{N}_{\text{dof}}}\}$ be a basis for \mathcal{V}_h^0 , then any $u \in \mathcal{V}_h$ can be written as

$$u = \varphi + \sum_{I=1}^{\bar{N}_{\text{dof}}} \hat{u}_I^u \Phi_I. \quad (6.156)$$

In finite-dimensional setting, the variational problem (6.151) is equivalent to

$$\text{find } u_h \in \mathcal{V}_h \text{ such that } B(\Phi_I, u_h) = \ell(\Phi_I) \text{ for } I = 1, \dots, \bar{N}_{\text{dof}} \quad (6.157)$$

by Proposition 3.1, which reduces to

$$\sum_{J=1}^{\bar{N}_{\text{dof}}} B(\Phi_I, \Phi_J) \hat{u}_J = \ell(\Phi_I) - B(\Phi_I, \varphi). \quad (6.158)$$

This can be written compactly as a linear system of equations

$$\hat{\mathbf{K}}^{uu} \hat{\mathbf{u}}^u = \hat{\mathbf{b}}^u, \quad (6.159)$$

where we defined $\hat{\mathbf{K}}^{uu} \in M_{\bar{N}_{\text{dof}}, \bar{N}_{\text{dof}}}(\mathbb{R})$ and $\hat{\mathbf{b}}^u \in \mathbb{R}^{\bar{N}_{\text{dof}}}$ as

$$\hat{K}_{IJ}^{uu} := B(\Phi_I, \Phi_J), \quad \hat{f}_I^u := \ell(\Phi_I), \quad \hat{b}_I^u := \hat{f}_I^u - B(\Phi_I, \varphi) \quad (6.160)$$

for $I, J = 1, \dots, \bar{N}_{\text{dof}}$. In the next section, we provide a concrete construction of the finite element subspace \mathcal{V}_h^0 and a nodal basis from the finite elements.

6.6. Construction of finite element subspace

Following the approach in Chapter 4, we first construct a collection of function $\{\Psi_1, \dots, \Psi_{N_{\text{nd}}}\}$, called *shape functions*, whose span includes the finite element subspace \mathcal{V}_h^0 , i.e.,

$$\mathcal{V}_h^0 \subset \text{span}\{\Psi_1, \dots, \Psi_{N_{\text{nd}}}\}. \quad (6.161)$$

We require each shape function to be continuous, be a member of \mathcal{Y}_e when restricted to Ω_e , and possess the nodal property

$$\Psi_I \in \mathcal{C}^0(\Omega), \quad \Psi_I|_{\Omega_e} \in \mathcal{Y}_e, \quad \Psi_I(\hat{x}_J) = \delta_{IJ} \text{ for } J = 1, \dots, N_{\text{nd}} \quad (6.162)$$

for $I = 1, \dots, N_{\text{nd}}$. These properties are sufficient to establish the inclusion of \mathcal{V}_h^0 in the span of the shape functions (6.161). We construct the global shape function from the element level. Let $\{\phi_1^e, \dots, \phi_{N_{\text{el}}}^e\}$ be a nodal basis of \mathcal{Y}_e corresponding to the node set \mathcal{N}_e . Because we require $\Psi_I|_{\Omega_e} \in \mathcal{Y}_e$, we can expand $\Psi_I|_{\Omega_e} \in \mathcal{Y}_e$ in the nodal element basis as

$$\Psi_I|_{\Omega_e} = \sum_{i=1}^{N_{\text{nd}}} \alpha_{Ii}^e \phi_i^e. \quad (6.163)$$

The nodal property of the element basis implies

$$\Psi_I|_{\Omega_e}(\hat{x}_j^e) = \sum_{i=1}^{N_{\text{nd}}} \alpha_{Ii}^e \phi_i^e(\hat{x}_j^e) = \alpha_j^e \quad (6.164)$$

Observe that continuity within an element Ω_e follows directly from $\mathcal{Y}_e \subset \mathcal{C}^0(\Omega_e)$; however, continuity across elements is more delicate. In the case where \mathcal{Y}_e is a (mapped) polynomial space, continuity across elements will be guaranteed if the functions in abutting elements agree at enough points (determined by polynomial

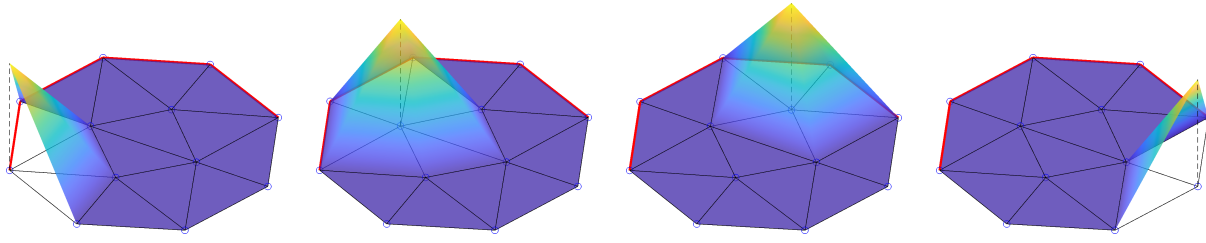


Figure 6.26: Global nodal basis functions Ψ_I (left-to-right: $I = 1, 6, 9, 10$) for various nodes in the \mathcal{P}^1 mesh in Figure 6.25.

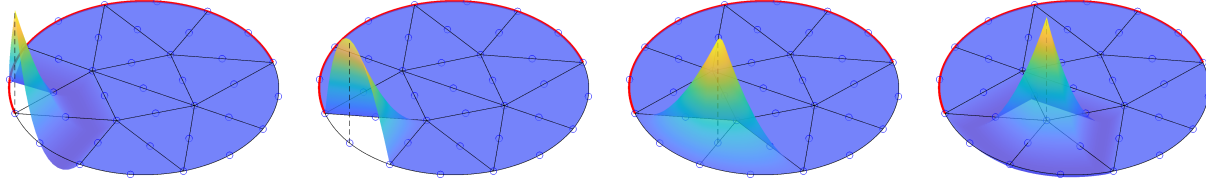


Figure 6.27: Global nodal basis functions Ψ_I for various nodes in the \mathcal{P}^2 mesh in Figure 6.25.

degree) on the shared surface (element face). This is precisely why in Section 6.2 we constructed master elements with enough nodes on each face such that a polynomial in $(d - 1)$ -dimensions is uniquely defined by the nodal values of the face. Therefore, the difficult issue of enforcing global continuity reduces to simply requiring any function $v \in \mathcal{V}_h^0$ is single-valued at every node in the mesh \mathcal{N} , which can be written compactly using the connectivity of the mesh

$$v(\hat{\mathbf{x}}_j^e) = v(\hat{\mathbf{x}}_{\Theta_{je}}). \quad (6.165)$$

Using this relationship to enforce global continuity and the nodal property of the shape functions, we arrive at

$$\Psi_I|_{\Omega_e}(\hat{\mathbf{x}}_j^e) = \Psi_I|_{\Omega_e}(\hat{\mathbf{x}}_{\Theta_{je}}) = \delta_{I\Theta_{je}}. \quad (6.166)$$

Combining (6.164) and (6.166), we arrive at the following compact representation of the expansion coefficients of the shape functions

$$\alpha_{Ij}^e = \delta_{I\Theta_{je}}, \quad (6.167)$$

which in turn leads to the following global basis functions in terms of the local ones

$$\Psi_I|_{\Omega_e} = \sum_{i=1}^{N_{\text{nd}}^{\text{el}}} \delta_{I\Theta_{ie}} \phi_i^e. \quad (6.168)$$

Remark 6.3. This procedure defines the global (nodal) shape functions by “patching together” nodal basis functions of the local function space \mathcal{Y}_e associated with the finite element $(\Omega_e, \mathcal{Y}_e, \mathcal{N}_e)$ in a manner that ensures global continuity. This is the analog to the approach taken in Chapter 4 to construct the piecewise linear hat functions.

Example 6.31: \mathcal{P}^1 and \mathcal{P}^2 shape functions on mesh of unit circle

The global shape functions for \mathcal{P}^1 and \mathcal{P}^2 triangle elements on the meshes in Figure 6.25 are shown in Figure 6.26 and 6.27, respectively. It is easy to see the basis functions are continuous and possess the nodal property. Furthermore, the \mathcal{P}^1 shape function in Figure 6.26 are linear when restricted to any element; the \mathcal{P}^2 shape functions in Figure 6.26 are mapped quadratic functions when restricted to any element. Also observe that any particular shape function Ψ_I is *only non-zero in elements that contain the node*, i.e., $\hat{\mathbf{x}}_I \in \mathcal{N}^e$.

Now we can construct a basis $\{\Phi_1, \dots, \Phi_{N_{\text{dof}}}\}$ of the finite element subspace \mathcal{V}_h from the shape functions $\{\Psi_1, \dots, \Psi_{N_{\text{nd}}}\}$. Since we have (6.161), the only property missing ingredient is the boundary condition. Let

$\mathcal{I}_c \subset \{1, \dots, N_{\text{nd}}\}$ be the (ordered) set of node numbers corresponding to nodes on the essential boundary $\partial\Omega_D$ (constrained), i.e.,

$$\mathcal{I}_c = \{i \in \mathbb{N} \mid \hat{\mathbf{x}}_i \in \mathcal{N}_D\} \quad (6.169)$$

and let $\mathcal{I}_u = \{1, \dots, N_{\text{nd}}\} \setminus \mathcal{I}_c$ be the remaining (unconstrained) nodes with cardinality $|\mathcal{I}_u| = \bar{N}_{\text{dof}}$. Now we claim the following definition of the global basis functions will ensure $\Phi_I|_{\partial\Omega_D} = 0$:

$$\Phi_I = \Psi_{\mathcal{I}_u(I)}, \quad I = 1, \dots, \bar{N}_{\text{dof}}. \quad (6.170)$$

This definition of Φ_I directly inherits continuity, $\Phi_I|_{\Omega_e} \in \mathcal{Y}_e$, and the nodal property from the complete set of shape function; we only need to verify the boundary condition. First we notice that all of the basis functions Φ_I , $I = 1, \dots, \bar{N}_{\text{dof}}$ are zero at any node on $\partial\Omega_D$, i.e., for any $J \in \mathcal{I}_c$ we have

$$\Phi_I(\hat{\mathbf{x}}_J) = \Psi_{\mathcal{I}_u(I)}(\hat{\mathbf{x}}_J) = 0 \quad (6.171)$$

due to the nodal property of Ψ and fact that $J \in \mathcal{I}_c \implies J \notin \mathcal{I}_u$. Due to our assumption that the interior of an element face touches at most one domain boundary, this implies Φ_I is zero at all nodes on all element faces lying on $\partial\Omega_D$, which in turn implies $\Phi_I(\mathbf{x}) = 0$ for any \mathbf{x} on those faces (at least for the elements introduced in Section 6.2).

Example 6.32: Partition of degrees of freedom for \mathcal{P}^1 mesh in Figure 6.25

By examining the \mathcal{P}^1 mesh of the unit circle in Figure 6.25 we can easily see that

$$\mathcal{I}_c = \{1, 3, 8, 11, 12\}, \quad \mathcal{I}_u = \{2, 4, 5, 6, 7, 9, 10\}. \quad (6.172)$$

Furthermore, from the basis functions shown in Figure 6.26, we see that for any non-boundary node I , the corresponding basis function is zero on the boundary, $\Psi_I(\mathbf{x}) = 0$ for $x \in \partial\Omega$. This show the choice of basis function in (6.170) satisfies the boundary condition, $\Phi_I|_{\partial\Omega_D} = 0$.

We can also use the shape functions to define the affine offset φ , defined as any function in \mathcal{V} such that $\varphi|_{\partial\Omega_D} = g$, as

$$\varphi = \sum_{I \in \mathcal{I}_c} g(\hat{\mathbf{x}}_I) \Psi_I. \quad (6.173)$$

Due to the nodal property of the shape functions, we clearly have $\varphi(\hat{\mathbf{x}}_I) = g(\hat{\mathbf{x}}_I)$; however, in general, away from nodes it is not guaranteed that $\varphi(\mathbf{x}) = g(\mathbf{x})$. Therefore this is a useful *approximation* to the affine offset that lies in our finite-dimensional space.

With the approximation in (6.173), the finite element solution u_h in (6.156) can be written as

$$u_h = \sum_{I \in \mathcal{I}_c} g(\hat{\mathbf{x}}_I) \Psi_I + \sum_{I=1}^{\bar{N}_{\text{dof}}} \hat{u}_I^u \Psi_{\mathcal{I}_u(I)}, = \sum_{I \in \mathcal{I}_c} g(\hat{\mathbf{x}}_I) \Psi_I + \sum_{I \in \mathcal{I}_u} \hat{u}_I \Psi_I = \sum_{I=1}^{N_{\text{nd}}} \hat{u}_I \Psi_I, \quad (6.174)$$

where we used (6.170) and the following definitions

$$\hat{u}_I^u = \hat{u}_{\mathcal{I}_u(I)}, \quad \text{for } I = 1, \dots, \bar{N}_{\text{dof}}, \quad \hat{u}_I^c = g(\hat{\mathbf{x}}_{\mathcal{I}_c(I)}), \quad \text{for } I = 1, \dots, N_{\text{nd}} - \bar{N}_{\text{dof}}. \quad (6.175)$$

Example 6.33: Essential boundary conditions for \mathcal{P}^1 mesh in Figure 6.25

Recall the \mathcal{P}^1 mesh of the unit circle in Figure 6.25 with the essential boundary condition applied on the red segments. Then the affine offset approximation on the mesh given in (6.173) is

$$\varphi = g(\hat{\mathbf{x}}_1)\Psi_1 + g(\hat{\mathbf{x}}_3)\Psi_3 + g(\hat{\mathbf{x}}_8)\Psi_8 + g(\hat{\mathbf{x}}_{11})\Psi_{11} + g(\hat{\mathbf{x}}_{12})\Psi_{12} \quad (6.176)$$

This approximation is shown in Figure 6.28 for the essential boundary condition $g(\mathbf{x}) = \sin(x_1) \cos(x_2)$ for both meshes.

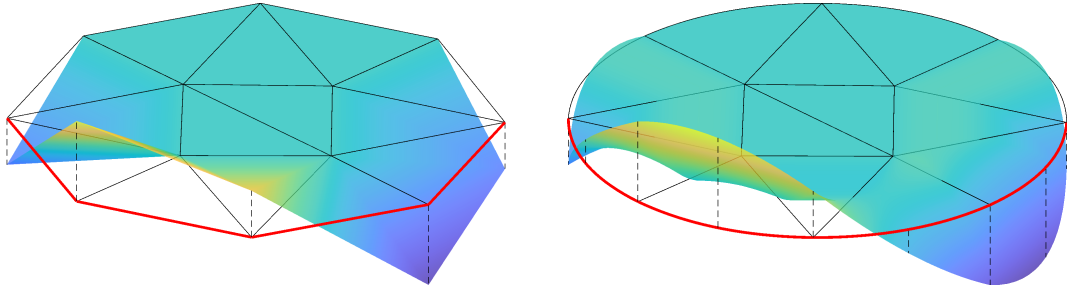


Figure 6.28: Approximation of the affine offset φ of the \mathcal{P}^1 and \mathcal{P}^2 meshes corresponding to the essential boundary condition $g(\mathbf{x}) = \sin(x_1) \cos(x_2)$.

6.7. Assembly of finite element matrices

Now we return to the finite element formulation in Section 6.5 to derive expressions for the terms in the global finite element system from *element quantities*. We begin by following the approach in Chapter 4 of breaking the bilinear weak formulation into a summation of element contributions

$$B(w, u) = \sum_{e=1}^{N_e} B_e(w, u), \quad \ell(w) = \sum_{e=1}^{N_e} \ell_e(w), \quad (6.177)$$

where $B_e : \mathcal{V}^0 \times \mathcal{V} \rightarrow \mathbb{R}$ is the restriction of the bilinear functional B to element $\Omega_e \in \mathcal{E}_h$ and $\ell_e : \mathcal{V}^0 \rightarrow \mathbb{R}$ is the restriction of ℓ to Ω_e ; the additive decomposition follows from the fact that the terms in weak formulation are volume/boundary integrals. Furthermore, the restricted bilinear form only depend on the value of the input functions *over the corresponding element*, i.e.,

$$B_e(w, u) = B_e(w|_{\Omega_e}, u|_{\Omega_e}), \quad \ell_e(w) = \ell_e(w|_{\Omega_e}) \quad (6.178)$$

for any $w \in \mathcal{V}^0$ and $u \in \mathcal{V}$, which again follows trivially from the fact these terms are integral over Ω_e and $\partial\Omega_e$.

Example 6.34: Additive decomposition of Poisson bilinear form

Recall the bilinear form of the Poisson equation from Chapter 5

$$B(w, u) := \int_{\Omega} w_{,i} u_{,i} dx, \quad \ell(w) := \int_{\Omega} wf dx + \int_{\partial\Omega_N} wh ds. \quad (6.179)$$

Both terms can be decomposed into the form of (6.177) as

$$B_e(w, u) := \int_{\Omega_e} w_{,i} u_{,i} dx, \quad \ell_e(w) := \int_{\Omega_e} wf dx + \int_{\partial\Omega_e \cap \partial\Omega_N} wh ds. \quad (6.180)$$

using the additive property of volume and surface integrals. From this decomposition, the property in (6.178) follows trivially since the integrals only depend on the functions in the element Ω_e .

Next we define the finite element stiffness matrix $\hat{\mathbf{K}} \in M_{N_{nd}, N_{nd}}(\mathbb{R})$ and load vector $\hat{\mathbf{f}} \in \mathbb{R}^{N_{nd}}$ as

$$\hat{K}_{IJ} := B(\Psi_I, \Psi_J), \quad \hat{f}_I := \ell(\Psi_I). \quad (6.181)$$

We can re-write these in terms of the *element basis functions* as

$$\hat{K}_{IJ} = \sum_{e=1}^{N_{el}} B_e(\Psi_I, \Psi_J) = \sum_{e=1}^{N_{el}} B_e(\Psi_I|_{\Omega_e}, \Psi_J|_{\Omega_e}) = \sum_{e=1}^{N_{el}} \sum_{i=1}^{N_{nd}^{el}} \sum_{j=1}^{N_{nd}^{el}} B_e(\phi_i^e, \phi_j^e) \delta_{I\Theta_{ie}} \delta_{J\Theta_{je}}, \quad (6.182)$$

and

$$\hat{f}_I = \sum_{e=1}^{N_{\text{el}}} \ell_e(\Psi_I) = \sum_{e=1}^{N_{\text{el}}} \ell_e(\Psi_I|_{\Omega_e}) = \sum_{e=1}^{N_{\text{el}}} \sum_{i=1}^{N_{\text{nd}}^{\text{el}}} \ell_e(\phi_i^e) \delta_{I\Theta_{ie}}, \quad (6.183)$$

which is a particularly useful form because it gives the explicit expression for the global quantities in terms of the element basis functions and the connectivity of the mesh. From these terms, we can extract the terms required to define the finite element system in (6.159) using the relationship between the global basis Φ_I and shape function Ψ_I in (6.170):

$$\begin{aligned} \hat{K}_{IJ}^{\text{uu}} &= B(\Phi_I, \Phi_J) = B(\Psi_{\mathcal{I}_u(I)}, \Psi_{\mathcal{I}_u(J)}) = \hat{K}_{\mathcal{I}_u(I), \mathcal{I}_u(J)} \\ \hat{f}_I^{\text{u}} &= \ell(\Phi_I) = \ell(\Psi_{\mathcal{I}_u(I)}) = \hat{f}_{\mathcal{I}_u(I)} \end{aligned} \quad (6.184)$$

for $I, J = 1, \dots, \bar{N}_{\text{dof}}$, where we used the definition in \hat{K}^{uu} and \hat{f}^{u} in (6.160). To complete the finite element system in (6.159), we consider the following term required to define the right-hand side

$$B(\Phi_I, \varphi) = B(\Psi_{\mathcal{I}_u(I)}, \sum_{J \in \mathcal{I}_c} g(\hat{x}_J) \Psi_J) = \sum_{J \in \mathcal{I}_c} B(\Psi_{\mathcal{I}_u(I)}, \Psi_J) g(\hat{x}_J) = \sum_{J=1}^{N_{\text{nd}} - \bar{N}_{\text{dof}}} \hat{K}_{IJ}^{\text{uc}} \hat{u}_J^{\text{c}}, \quad (6.185)$$

where we defined

$$\hat{K}_{IJ}^{\text{uc}} := B(\Psi_{\mathcal{I}_u(I)}, \Psi_{\mathcal{I}_c(J)}) = \hat{K}_{\mathcal{I}_u(I), \mathcal{I}_c(J)}, \quad \hat{u}_J^{\text{c}} := g(\hat{x}_{\mathcal{I}_c(J)}) \quad (6.186)$$

for $I = 1, \dots, \bar{N}_{\text{dof}}$ and $J = 1, \dots, N_{\text{nd}} - \bar{N}_{\text{dof}}$. Notice that this is exactly the static condensation approach introduced in Chapter 1 whereby the degrees of freedom are partitioned into those that are constrained and unconstrained and a reduced system for the unconstrained degrees of freedom is extracted.

Example 6.35: Finite element system for \mathcal{P}^1 mesh in Figure 6.25

The \mathcal{P}^1 triangle mesh of the unit circle in Figure 6.25 has $N_{\text{nd}} = 12$ nodes with an essential boundary condition prescribed on $\bar{N}_{\text{dof}} = 5$ of them (recall the constrained and unconstrained degrees of freedom in (6.172)). Then terms of the final finite element system are ($\hat{\mathbf{K}}$ is the 12×12 stiffness matrix that depends on the particular weak formulation):

$$\hat{\mathbf{K}}^{\text{uu}} = \begin{bmatrix} \hat{K}_{2,2} & \hat{K}_{2,4} & \hat{K}_{2,5} & \hat{K}_{2,6} & \hat{K}_{2,7} & \hat{K}_{2,9} & \hat{K}_{2,10} \\ \hat{K}_{4,2} & \hat{K}_{4,4} & \hat{K}_{4,5} & \hat{K}_{4,6} & \hat{K}_{4,7} & \hat{K}_{4,9} & \hat{K}_{4,10} \\ \hat{K}_{5,2} & \hat{K}_{5,4} & \hat{K}_{5,5} & \hat{K}_{5,6} & \hat{K}_{5,7} & \hat{K}_{5,9} & \hat{K}_{5,10} \\ \hat{K}_{6,2} & \hat{K}_{6,4} & \hat{K}_{6,5} & \hat{K}_{6,6} & \hat{K}_{6,7} & \hat{K}_{6,9} & \hat{K}_{6,10} \\ \hat{K}_{7,2} & \hat{K}_{7,4} & \hat{K}_{7,5} & \hat{K}_{7,6} & \hat{K}_{7,7} & \hat{K}_{7,9} & \hat{K}_{7,10} \\ \hat{K}_{9,2} & \hat{K}_{9,4} & \hat{K}_{9,5} & \hat{K}_{9,6} & \hat{K}_{9,7} & \hat{K}_{9,9} & \hat{K}_{9,10} \\ \hat{K}_{10,2} & \hat{K}_{10,4} & \hat{K}_{10,5} & \hat{K}_{10,6} & \hat{K}_{10,7} & \hat{K}_{10,9} & \hat{K}_{10,10} \end{bmatrix}, \quad \hat{\mathbf{f}}^{\text{u}} = \begin{bmatrix} \hat{f}_2 \\ \hat{f}_4 \\ \hat{f}_5 \\ \hat{f}_6 \\ \hat{f}_7 \\ \hat{f}_6 \\ \hat{f}_{10} \end{bmatrix} \quad (6.187)$$

and

$$\hat{\mathbf{K}}^{\text{uc}} = \begin{bmatrix} \hat{K}_{2,1} & \hat{K}_{2,3} & \hat{K}_{2,8} & \hat{K}_{2,11} & \hat{K}_{2,12} \\ \hat{K}_{4,1} & \hat{K}_{4,3} & \hat{K}_{4,8} & \hat{K}_{4,11} & \hat{K}_{4,12} \\ \hat{K}_{5,1} & \hat{K}_{5,3} & \hat{K}_{5,8} & \hat{K}_{5,11} & \hat{K}_{5,12} \\ \hat{K}_{6,1} & \hat{K}_{6,3} & \hat{K}_{6,8} & \hat{K}_{6,11} & \hat{K}_{6,12} \\ \hat{K}_{7,1} & \hat{K}_{7,3} & \hat{K}_{7,8} & \hat{K}_{7,11} & \hat{K}_{7,12} \\ \hat{K}_{9,1} & \hat{K}_{9,3} & \hat{K}_{9,8} & \hat{K}_{9,11} & \hat{K}_{9,12} \\ \hat{K}_{10,1} & \hat{K}_{10,3} & \hat{K}_{10,8} & \hat{K}_{10,11} & \hat{K}_{10,12} \end{bmatrix}, \quad \hat{\mathbf{u}}^{\text{c}} = \begin{bmatrix} g(\hat{x}_1) \\ g(\hat{x}_3) \\ g(\hat{x}_8) \\ g(\hat{x}_{11}) \\ g(\hat{x}_{12}) \end{bmatrix}. \quad (6.188)$$

6.8. Sparse storage of global stiffness matrix

At this point we have extensively covered the procedure to assemble the global stiffness matrix $\hat{\mathbf{K}}$ from element stiffness matrices \mathbf{K}^e and connectivity Θ using (6.182). However, we have only briefly mentioned a

particularly critical property of the stiffness matrix that makes the FEM competitive for difficult problems where meshes with many elements are required: its *sparsity*.

A sparse matrix is one in which many of its entries are zero. In such a situation, it is wasteful to ignore the sparsity of a matrix and simply store and operate on it as though it were dense: this requires storing and performing (potentially many) operations with 0. Substantial savings can be realized by *only* storing the non-zero entries of the matrix along with information needed to map the non-zeros to the appropriate position in the matrix. A number of different *sparsity* structures exist, each with their own advantages and disadvantages (regarding the efficiency with which data is stored/access/operated), for only storing the non-zero values of the matrix. Examples include *coordinate* or triplet format, *compressed sparse column/row* (CSC/CSR), skyline matrix storage, and block variants of most of these options.

The simplest sparsity structure is known as coordinate (COO) or triplet format and the only one we will discuss in this course. Let $\mathbf{A} \in M_{n \times n}(\mathbb{R})$ be a square matrix (square not required) and let n_z denote the number of non-zeros in the matrix. The COO format stores three arrays of size n_z : the nonzeros of the matrix, $\mathbf{v} \in \mathbb{R}^{n_z}$, the row number of each entry in \mathbf{v} , $\mathbf{r} \in \mathbb{N}^{n_z}$, and the column number of each entry in \mathbf{v} , $\mathbf{c} \in \mathbb{N}^{n_z}$. The cost of directly storing \mathbf{A} is n^2 while the cost of storing \mathbf{A} using COO format is $3n_z$ (actually less if you account for that $2n_z$ entries that must be stored are natural numbers, rather than real numbers). Therefore, if we are only concerned about storage (not the cost of accessing entries or operating with them), it pays off to use COO format if

$$n_z \leq \frac{n^2}{3}. \quad (6.189)$$

Example 6.36: Sparse matrix in COO

Consider the matrix

$$\mathbf{A} = \begin{bmatrix} 10 & 0 & 0 & 7 \\ 3 & 9 & 0 & 0 \\ 0 & 7 & 8 & 0 \\ 7 & 0 & 2 & 7 \end{bmatrix}. \quad (6.190)$$

There are $n_z = 9$ non-zeros in this matrix. The COO format is

$$\mathbf{v} = \begin{bmatrix} 10 \\ 3 \\ 7 \\ 9 \\ 7 \\ 8 \\ 2 \\ 7 \\ 7 \end{bmatrix}, \quad \mathbf{r} = \begin{bmatrix} 1 \\ 2 \\ 4 \\ 2 \\ 3 \\ 3 \\ 4 \\ 1 \\ 4 \end{bmatrix}, \quad \mathbf{c} = \begin{bmatrix} 1 \\ 1 \\ 1 \\ 2 \\ 2 \\ 3 \\ 3 \\ 4 \\ 4 \end{bmatrix}. \quad (6.191)$$

In Example 6.8, we ordered the arrays columnwise. While this is not required for the COO format, it can significantly reduce the time required to, e.g., find A_{ij} , which requires a search through these three vectors. While COO is the simplest sparsity structure to understand, it is not the most efficient in terms of storage or performing operations; however, storing the data in a meaningful order can help minimize the impact of these inefficiencies.

Example 6.37: Sparsity structure of FE stiffness matrices

To demonstrate that FE stiffness matrices are extremely sparse, we consider a second-order, scalar PDE discretized on various meshes without essential boundary conditions:

- Square mesh ($p = 1$): This mesh consists of 16 nodes and 9 \mathcal{Q}^1 quadrilateral elements; mesh and stiffness sparsity structure shown in Figure 6.29.
- Square mesh ($p = 2$): This mesh consists of 49 nodes and 9 \mathcal{Q}^2 quadrilateral elements; mesh and stiffness sparsity structure shown in Figure 6.29.
- Staypuft ($p = 1$): This mesh consists of 27000 nodes and 102392 \mathcal{P}^1 tetrahedra elements; mesh

and stiffness sparsity structure shown in Figure 6.29. The ratio of entries in the matrix to non-zero entries is $n^2/n_z = 2260 \gg 3$ and there is a clear benefit to using sparse storage. Dense storage requires roughly 5.8GB, while COO sparse storage only requires 7MB. This is the most dramatic example we have seen and clearly sparse storage is a necessity, not an option for a mesh of this size.

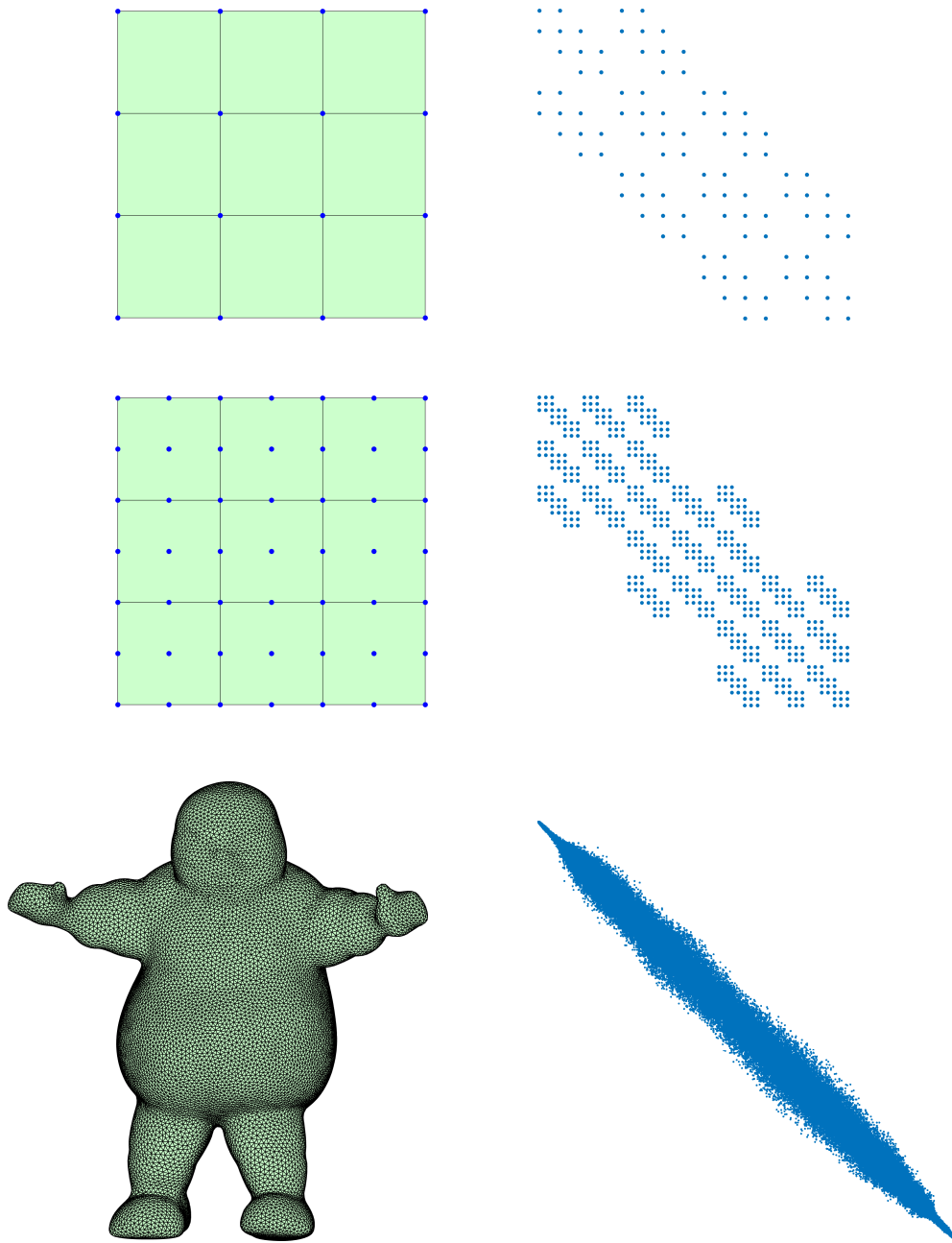


Figure 6.29: Mesh and sparsity structure for several domains (scalar PDE).

6.9. Numerical quadrature

As we have seen to this point in the course, integration is central to the FEM; however, as the complexity of our PDE and our FE basis increase, it quickly becomes impractical to analytically compute the integrals that arise. Therefore we turn to numerical integration or *quadrature* to approximate the integrals that arise

in the element stiffness matrix and load vector.

Suppose we wish to integrate a function $f \in \mathcal{F}_{\Omega \rightarrow \mathbb{R}}$, where $\mathcal{R} \subset \mathbb{R}^d$. A quadrature rule is a collection of quadrature nodes $\mathbf{z}_1, \dots, \mathbf{z}_{N_{\text{qd}}} \subset \mathcal{R}$ and weights $w_1, \dots, w_{N_{\text{qd}}}$ such that

$$I = \int_{\mathcal{R}} f \, dV \approx \sum_{k=1}^{N_{\text{qd}}} w_k f(\mathbf{z}_k). \quad (6.192)$$

A major computational cost of a finite element simulation comes from integrating the element terms, which drives us to seek *optimal* quadrature rules, i.e., quadrature rules that are as accurate as possible for a fixed number of quadrature points. We measure the accuracy of a quadrature by the *highest degree polynomial it can integrate exactly*.

6.9.1 Quadrature in one dimension

First, notice the integral of f over an arbitrary line segment $[a, b]$ can be transformed to an integral over the interval $[-1, 1]$ as

$$\int_a^b f(x) \, dx = \frac{b-a}{2} \int_{-1}^1 h(z) \, dz, \quad (6.193)$$

where $h(z) = f(b(z+1)/2 - a(z-1)/2)$. If f is polynomial, h is a polynomial of the same degree so this transformation does not alter our notion of accuracy of a quadrature rule. Therefore, without loss of generality, we can consider quadrature rules for the integral in (6.192) over the interval $\mathcal{R} = [-1, 1]$.

Newton-Cotes formulas

The Newton-Cotes formulas are a collection of quadrature rules that utilize *equally spaced* quadrature nodes and are a staple of any numerical analysis class. They are derived by fitting a polynomial of degree q to the function f using its value at the n_{qd} equally spaced quadrature nodes and integrating the resulting polynomial. This implies $q = n_{\text{qd}} - 1$ and the resulting quadrature rule will be exact for polynomials of degree q ($n_{\text{qd}} = q + 1$ quadrature points). While simple, these quadrature rules are *not* optimal and therefore not desired if the function is expensive to evaluate.

Example 6.38: Trapezoidal rule

The trapezoidal rule

$$w_1 = w_2 = 1, \quad z_1 = -1, \quad z_2 = 1 \quad (6.194)$$

is the Newton-Cotes formula with $n_{\text{qd}} = 2$

$$I \approx w_1 f(z_1) + w_2 f(z_2) = f(-1) + f(1), \quad (6.195)$$

which is clearly the area of the trapezoid with base $[-1, 1]$ and sides $f(-1)$ and $f(1)$. It exactly integrates any linear function.

Example 6.39: Simpson's rule

Simpson's rule

$$w_1 = \frac{1}{3}, \quad w_2 = \frac{4}{3}, \quad w_3 = \frac{1}{3}, \quad z_1 = -1, \quad z_2 = 0, \quad z_3 = 1 \quad (6.196)$$

is the Newton-Cotes formula with $n_{\text{qd}} = 3$

$$I \approx w_1 f(z_1) + w_2 f(z_2) + w_3 f(z_3) = \frac{1}{3} (f(-1) + 4f(0) + f(1)). \quad (6.197)$$

It exactly integrates any quadratic function.

Consider a quadrature rule with n_{qd} points $\{(w_i, z_i)\}_{i=1}^{n_{\text{qd}}}$ and the corresponding approximation of I (6.192)

$$I \approx \sum_{k=1}^{n_{\text{qd}}} w_k f(z_k). \quad (6.198)$$

It should be clear that there are $2n_{\text{qd}}$ tunable parameters, the n_{qd} quadrature nodes and weights, that can be used to fit a polynomial to f . However, the Newton-Cotes formula require the quadrature nodes be equally spaced which reduces the tunable parameters to n_{qd} (weights only). Therefore it comes as no surprise that we can only integrate polynomials of degree $q = n_{\text{nd}} - 1$ exactly.

Gaussian quadrature

The Gaussian quadrature rules remove the restriction that the nodes be equally spaced and the construction proceeds as follows. Consider a polynomial $P \in \mathcal{P}^q([-1, 1])$ that we wish to integrate *exactly*. We expand P as

$$P(z) = a_0 + a_1 z + \cdots + a_q z^q \quad (6.199)$$

and require

$$\int_{-1}^1 P(z) dz = \sum_{k=1}^{n_{\text{qd}}} w_k P(z_k), \quad (6.200)$$

i.e., the condition for the quadrature rule to integrate P exactly. Using the expansion of $P(z)$ on each side of the equality, we arrive at

$$\int_{-1}^1 (a_0 + a_1 z + \cdots + a_q z^q) dz = \sum_{k=1}^{n_{\text{qd}}} w_k (a_0 + a_1 z_k + \cdots + a_q z_k^q). \quad (6.201)$$

Since the left side of the equality is a (definite) integral of a polynomial, we can reduce this to

$$\left[a_0 z + \frac{a_1}{2} z^2 + \cdots + \frac{a_q}{q+1} z^{q+1} \right]_{-1}^1 = \sum_{k=1}^{n_{\text{qd}}} w_k (a_0 + a_1 z_k + \cdots + a_q z_k^q). \quad (6.202)$$

Moving all terms to the same side of the equation and compressing in summation form, we have

$$\sum_{i=0}^q a_i \left(\left[\frac{z^{i+1}}{i+1} \right]_{-1}^1 - \sum_{k=1}^{n_{\text{qd}}} w_k z_k^i \right) = 0. \quad (6.203)$$

Because we require the quadrature rule be exact for *any* polynomial of degree q , the coefficients a_0, \dots, a_q are arbitrary, which means the equation will only be true if each term is equal to zero, i.e.,

$$\left[\frac{z^{i+1}}{i+1} \right]_{-1}^1 = \sum_{k=1}^{n_{\text{qd}}} w_k z_k^i \quad (6.204)$$

for $i = 0, \dots, q$. After evaluating the expression on the left-hand side, we arrive at the following nonlinear system of equations for w_k and z_k

$$\sum_{k=1}^{n_q} w_k z_k^i = \begin{cases} \frac{2}{i+1} & i \text{ even} \\ 0 & i \text{ odd} \end{cases} \quad (6.205)$$

for $i = 0, \dots, q$. This is a system of $q+1$ nonlinear equations in $2n_{\text{qd}}$ unknowns, which can be solved using nonlinear iterations (Chapter 7); a unique solution requires $q = 2n_{\text{qd}} - 1$. This means a polynomial of degree $q = 2n_{\text{qd}} - 1$ can be integrated *exactly* with n_{qd} quadrature points. Because Gaussian quadrature rules depend on the solution of this nonlinear system, they are usually tabulated.

Table 6.2: Gaussian quadrature rules for $[-1, 1]$

q	n_{qd}	w	z_k
1	1	2.0000000000000000	0.0000000000000000
3	2	1.0000000000000000	-0.577350269189626
		1.0000000000000000	0.577350269189626
5	3	0.5555555555555556	-0.77459669241483
		0.8888888888888889	0.0000000000000000
		0.5555555555555556	0.77459669241483
7	4	0.347854845137454	-0.861136311594053
		0.652145154862546	-0.339981043584856
		0.652145154862546	0.339981043584856
		0.347854845137454	0.861136311594053
9	5	0.236926885056189	-0.906179845938664
		0.478628670499366	-0.538469310105683
		0.5688888888888889	0.0000000000000000
		0.478628670499366	0.538469310105683
		0.236926885056189	0.906179845938664

Example 6.40: Gaussian quadrature over $[-1, 1]$

The one-point Gaussian quadrature rule is the midpoint rule: $w_1 = 2$, $z_1 = 0$ (midpoint rule). The two-point Gaussian quadrature rule is: $w_1 = w_2 = 1$, $z_1 = -1/\sqrt{3}$, $z_2 = 1/\sqrt{3}$. These and higher order quadrature rules are listed in Table 6.2 and Figure 6.30. Notice that the endpoints of the interval $\{-1, 1\}$ are not quadrature nodes; this is usually the case for optimal quadrature rules.

6.9.2 Quadrature over $[-1, 1]^d$

In the special case where the integration domain is $\mathcal{R} = [-1, 1]^d$, or more generally, a tensor product of one-dimensional domains, a quadrature rule for \mathcal{R} can be constructed from tensor products of one-dimensional quadrature rules. To see this, we first consider the case $d = 2$ and let $\{(\tilde{w}_i, \tilde{s}_i)\}_{i=1}^{n_{\text{qd},1}}$ be the quadrature rule associated with the one-dimensional domain $[-1, 1]$. Then we have

$$\int_{[-1,1]^2} f(\mathbf{z}) d\mathbf{z} = \int_{-1}^1 \int_{-1}^1 f(z_1, z_2) dz_1 dz_2 \approx \int_{-1}^1 \sum_{j=1}^{n_{\text{qd},1}} \tilde{w}_j f(\tilde{s}_j, z_2) dz_2 \approx \sum_{k=1}^{n_{\text{qd},1}} \sum_{j=1}^{n_{\text{qd},1}} \tilde{w}_j \tilde{w}_k f(\tilde{s}_j, \tilde{s}_k). \quad (6.206)$$

Since the one-dimensional quadrature rule integrates polynomials of degree $q = 2n_{\text{qd}} - 1$ exactly, it is easy to see this procedure will integrate any $f \in \mathcal{Q}^q([-1, 1]^2)$ exactly (the \approx in the above equation would be replaced with $=$ because any $f \in \mathcal{Q}^q([-1, 1]^d)$, it is a polynomial of degree at most q in each component).

To make a stronger connection to the form of a quadrature rule in (6.192) (single summation), we introduce $\{(w_k, \mathbf{z}_k)\}_{k=1}^{n_{\text{qd}}}$ where $n_{\text{qd}} = n_{\text{qd},1}^2$ and require

$$\sum_{i=1}^{n_{\text{qd}}} w_i f(\mathbf{z}_i) = \sum_{k=1}^{n_{\text{qd},1}} \sum_{j=1}^{n_{\text{qd},1}} \tilde{w}_j \tilde{w}_k f(\tilde{s}_j, \tilde{s}_k). \quad (6.207)$$

This is clearly satisfied if we take

$$w_i = \tilde{w}_{\mathcal{I}(i)} \tilde{w}_{\mathcal{J}(i)}, \quad \mathbf{z}_i = \begin{bmatrix} \tilde{s}_{\mathcal{I}(i)} \\ \tilde{s}_{\mathcal{J}(i)} \end{bmatrix}, \quad (6.208)$$

where

$$\mathcal{I} : \{1, \dots, n_{\text{qd},1}^2\} \rightarrow \{1, \dots, n_{\text{qd},1}\}, \quad \mathcal{J} : \{1, \dots, n_{\text{qd},1}^2\} \rightarrow \{1, \dots, n_{\text{qd},1}\} \quad (6.209)$$

map between the overall quadrature node number to the quadrature node in the z_1 -direction (\mathcal{I}) and z_2 -direction (\mathcal{J}). Since the order in which the quadrature nodes are traversed is unimportant (sum over all in

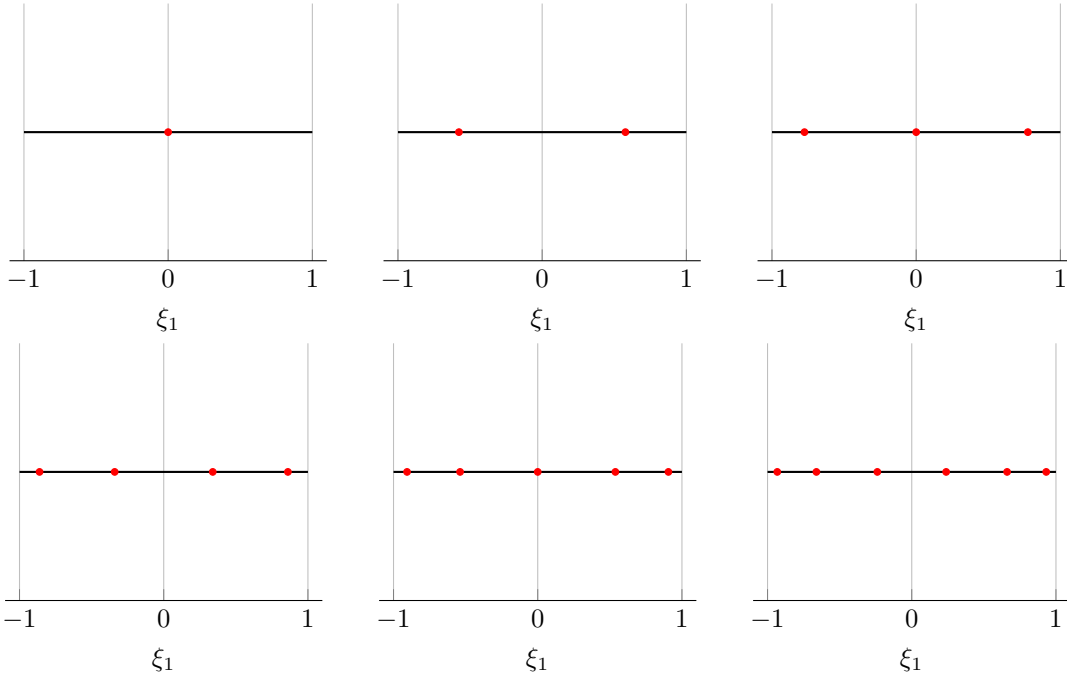


Figure 6.30: Gaussian quadrature nodes over the interval $[-1, 1]$.

the end), there is some flexibility in defining these mappings; however, for consistency with Section 6.2.3, we choose

$$\mathcal{I}(k) := 1 + [(k - 1)\%n_{\text{qd},1}], \quad \mathcal{J}(k) := 1 + \left\lfloor \frac{k - 1}{n_{\text{qd},1}} \right\rfloor. \quad (6.210)$$

This procedure easily generalized to higher dimensions; however, we omit the details.

Remark 6.4. Since we chose the master hypercube element Ω_\square to be the bi-unit hypercube $[-1, 1]^d$, these quadrature rules are all one needs if solely considering hypercube elements. By using the mapped element approach, all integrals get converted to the master hypercube $\Omega_\square = [-1, 1]^d$. Simplices or master elements with other geometries require more general quadrature rules, which we consider in the next section.

Example 6.41: Gaussian quadrature over $[-1, 1]^2$

The one-point Gaussian quadrature rule is: $w_1 = 2, z_1 = (0, 0)$ (midpoint rule). The four-point Gaussian quadrature rule is: $w_1 = w_2 = w_3 = w_4 = 1, z_1 = (-1/\sqrt{3}, -1/\sqrt{3}), z_2 = (1/\sqrt{3}, -1/\sqrt{3}), z_3 = (-1/\sqrt{3}, 1/\sqrt{3}), z_4 = (1/\sqrt{3}, 1/\sqrt{3})$. These Gaussian quadrature rules and higher order ones are shown in Figure 6.31.

6.9.3 Quadrature in multiple dimensions

For more general domains, it is more difficult to derive optimal quadrature rules. In this section we consider a general, systematic procedure to construct quadrature rules from a quadrature rule of $[-1, 1]^d$. While this procedure will be general, it is by no means optimal. Suppose we wish to construct a quadrature rule for the domain $\mathcal{R} \subset \mathbb{R}^d$ and suppose there exists a mapping $\mathcal{G} : [-1, 1]^d \rightarrow \mathcal{R}$. Then the integral over \mathcal{R} can be transferred to an integral over $[-1, 1]^d$ using the change of variables formula

$$\int_{\mathcal{R}} f(z) dz = \int_{[-1,1]^d} f(\mathcal{G}(\tilde{z})) \det \mathcal{G}(\tilde{z}) d\tilde{z}. \quad (6.211)$$

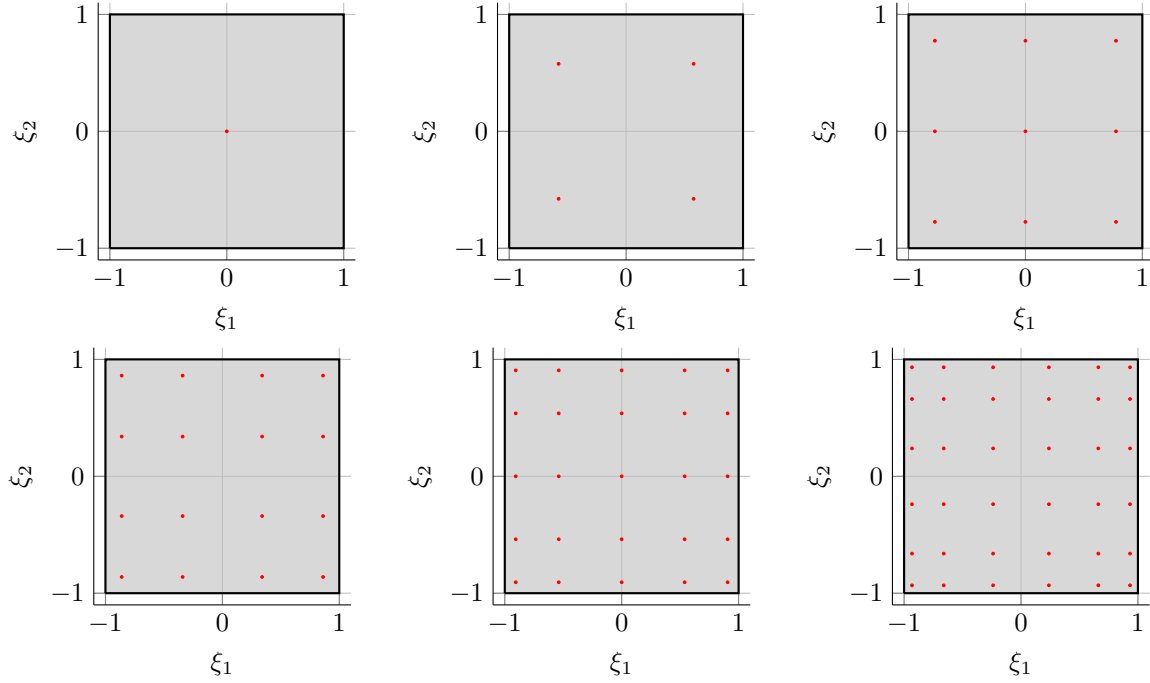


Figure 6.31: Gaussian quadrature nodes over the domain $[-1, 1]^2$.

Furthermore, let $\{(\tilde{w}_k, \tilde{z}_k)\}_{k=1}^{n_{\text{qd}}}$ be a quadrature rule associated with the bi-unit box $[-1, 1]^d$. Then we can approximate the above integral as

$$\int_{\mathcal{R}} f(z) dz = \int_{[-1,1]^d} f(\mathcal{G}(\tilde{z})) \det \mathcal{G}(\tilde{z}) d\tilde{z} \approx \sum_{k=1}^{n_{\text{qd}}} \tilde{w}_k f(\mathcal{G}(\tilde{z}_k)) \det \mathcal{G}(\tilde{z}_k) = \sum_{k=1}^{n_{\text{qd}}} w_k f(z_k), \quad (6.212)$$

where

$$w_k := \tilde{w}_k \det \mathcal{G}(\tilde{z}_k), \quad z_k := \mathcal{G}(\tilde{z}_k). \quad (6.213)$$

Thus $\{(w_k, z_k)\}_{k=1}^{n_{\text{qd}}}$ is a quadrature rule for the region \mathcal{R} .

Remark 6.5. The quadrature rule is *suboptimal* because, even if the original quadrature rule $\{(\tilde{w}_k, \tilde{z}_k)\}_{k=1}^{n_{\text{qd}}}$ could exactly integrate a polynomial of degree q , the new quadrature rule $\{(w_k, z_k)\}_{k=1}^{n_{\text{qd}}}$ would not be able to exactly integrate it exactly because the integrand to which the original quadrature rule is applied is $(f \circ \mathcal{G}) \det \mathcal{G}$, which is only a polynomial if \mathcal{G} is also a polynomial, but will have much higher degree than f (unless \mathcal{G} is linear).

Example 6.42: Gaussian quadrature rule for master triangle

Consider the master triangle in Section 6.2.4. It is easy to see the following mapping

$$\mathcal{G}(\tilde{z}_1, \tilde{z}_2) = \frac{1}{4} \begin{bmatrix} 2(1 + \tilde{z}_1) \\ (1 + \tilde{z}_2)(1 - \tilde{z}_1) \end{bmatrix} \quad (6.214)$$

transforms the master hypercube $[-1, 1]^d$ into the master triangle (6.40). The Jacobian of the mapping is

$$\det \mathcal{G}(\tilde{z}_1, \tilde{z}_2) = (1 - \tilde{z}_1)/4. \quad (6.215)$$

From these two quantities, any quadrature rule for $[-1, 1]^2$ can be transformed into a quadrature rule for the master triangle using (6.214) (Figure 6.32). A similar procedure can be used in higher dimensions to obtain a quadrature rule for a general simplex from the quadrature rule of $[-1, 1]^d$.

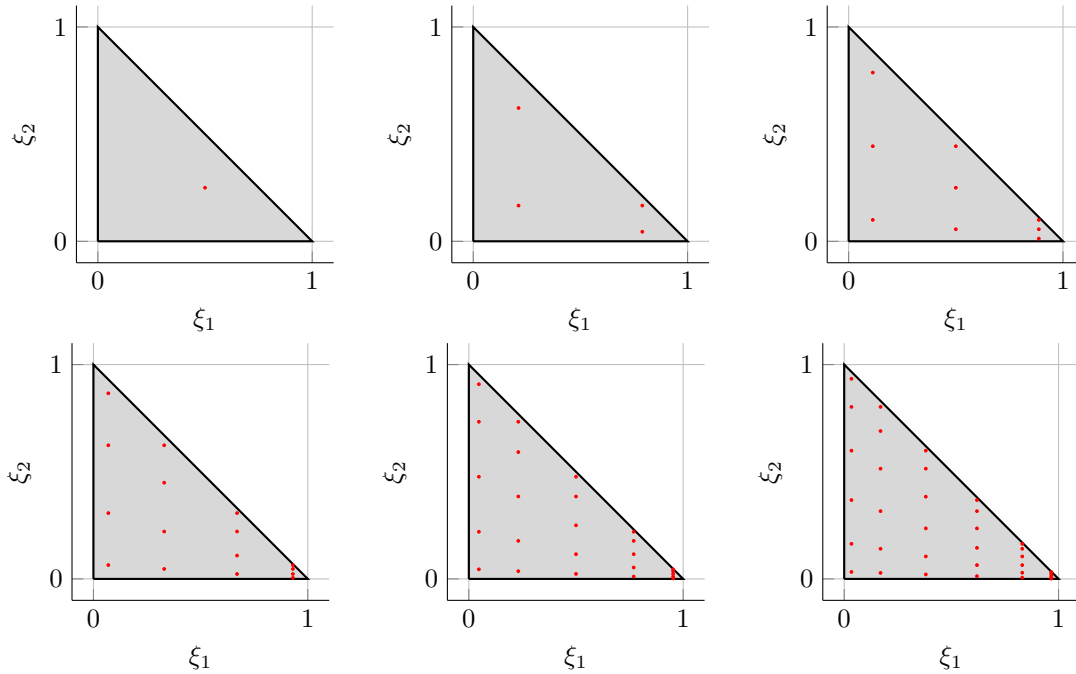


Figure 6.32: Gaussian quadrature nodes over the right unit triangle using the transformation of the Gaussian quadrature rule of $[-1, 1]^2$ (Figure ??) in (6.213). Notice that the nodes bunch up near the point where the edge as collapsed.

6.10. Summary

This chapter introduced the finite element method in d -dimensions for linear, scalar-valued partial differential equations:

- The concept of a *finite element* was introduced and a number of master elements (line, quadrilateral, triangle, d -hypercube, d -simplex) with fixed idealized domain were introduced along with the local function space and distribution of the nodes throughout the element. We also detailed a construction of nodal basis functions for each elements (and local function space).
- The concept of a *physical* or *mapped* finite element was introduced as a (bijective) mapping applied to a master element, which is used to generate all elements of a mesh and allows for a general class of elements (including those with curved boundaries).
- A finite element mesh was introduced as a collection of mapped elements and the associated nodes. The concept of element boundaries/faces was introduced and restrictions placed on the mesh to facilitate a convenient implementation.
- The finite element formulation in this setting largely follows the procedure from Chapter 4 and leads to familiar expressions for the global basis functions in terms of element ones and the concept of assembling the global stiffness matrix and load vector from element contributions. Application of essential boundary condition leads to a form of static condensation (Chapter 1).
- The practical issue of storing the FE stiffness matrix in a sparse format to significantly reduce the memory burden was introduced and the significance was demonstrated on a number of FE meshes.
- Finally, we introduced the concept of numerical quadrature which will be helpful in reducing the integrals that arise in the weak and Galerkin forms to a weighted summation of the integrand evaluated at a number of (quadrature) points. The Gaussian quadrature rules were constructed and shown to be optimal in one-dimension and for tensor products of one-dimensional domains.